# Measurement of neutron yields in the Xe+CsI reaction by the Highly Granular time-of-flight Neutron Detector prototype in the BM@N experiment

A. Zubankov on behalf of the HGND group

14.05.2025

# Introduction

- The Highly Granular Neutron Detector (HGND) at the BM@N experiment is under development for measuring the energy of neutrons up to 4 GeV produced in nucleus-nucleus collisions.
- Neutron measurements are necessary to obtain robust information on the symmetry energy of the Equation of State for high baryon density matter.
- A compact HGND prototype has already been designed and constructed to validate the concept of the full-scale HGND.
- For the first time, small prototype of the HGND was used in $^{124}$Xe+CsI at 3.8A GeV run at the BM@N.
- The neutron yields in the HGND prototype acceptance were evaluated with model-estimated efficiencies for central and semi-central collisions and for electromagnetic dissociation (EMD) of $^{124}$Xe.

# Outline

- Design of **H**ighly **G**ranular **N**eutron **D**etector prototype
- EMD in RELDIS model
- UrQMD-AMC vs DCM-QGSM-SMM models
- HGND prototype efficiencies and acceptances
- Neutron yields and cross sections
- Background problem at 27° position

# HGND prototype design

- Scint. layer **Veto** 120x120x25 (мм)
- 1st (electromagnetic) part:
  **5 layers**: **Pb (8mm)** + Scint. (25mm)
  + PCB + air
- 2nd (hadronic) part:
  **9 layers**: **Cu (30mm)** + Scint. (25mm)
  + PCB + air

Scint. cell – 40 x 40 x 25 $mm^3$
Total number of cells – 135
Total size – 12 x 12 x 82.5 $cm^3$
Total length ~ 2.5 $\lambda_{int}$

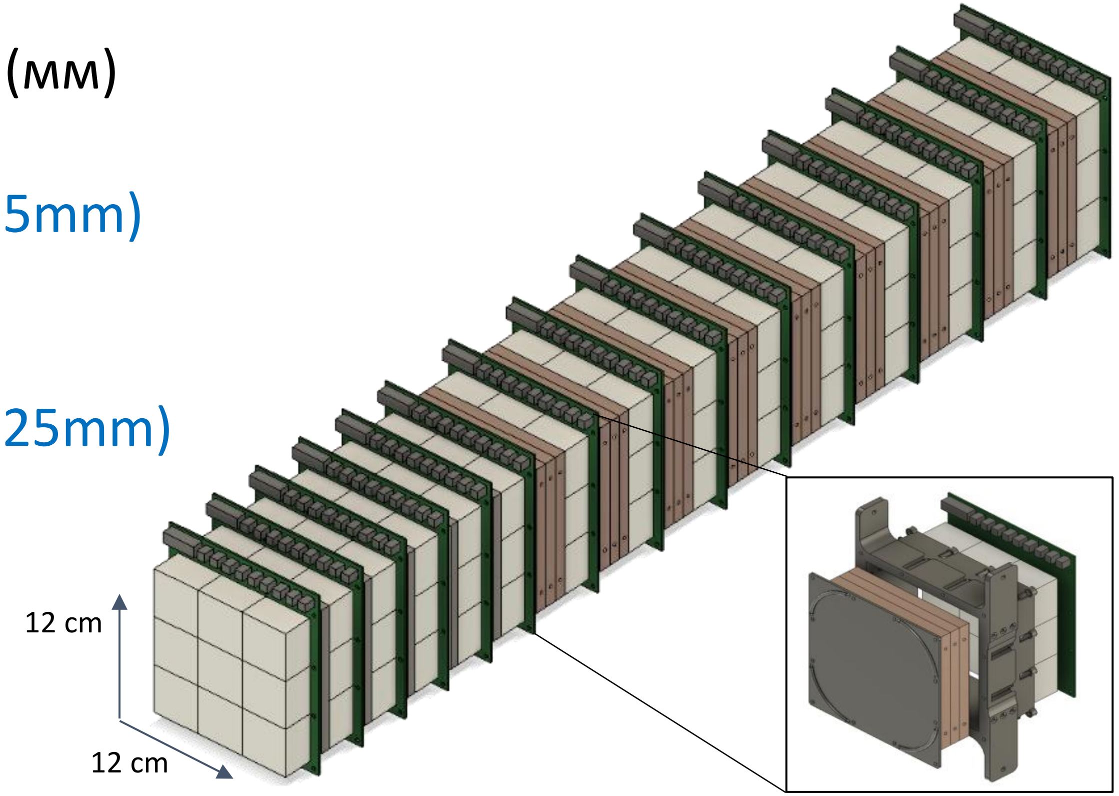


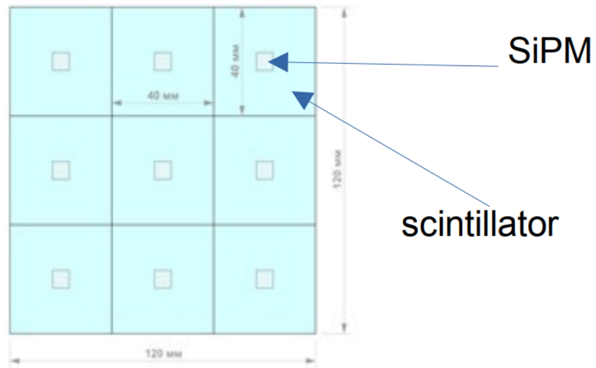


Hamamatsu S13360- 6050PE
Photosensitive area – 6x6 $mm^2$
Number of pixels – 14400
Pixel size – 50 µm
Gain – $1.7x10^6$
PDE – 40%

Time resolution of cell ~200 ps*,
+ with light collection heterogeneity ~240 ps,
+ with other factors (such as trigger time resolution) ~270 ps

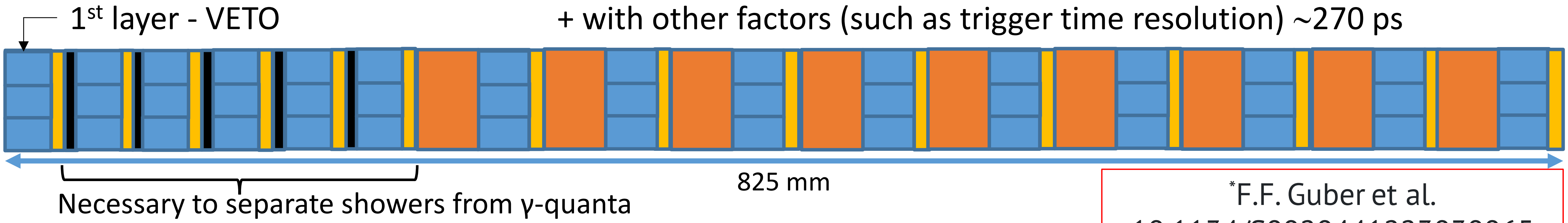


*F.F. Guber et al.
10.1134/S0020441223030065

# HGND prototype in the Xe+CsI@3.8A GeV run of BM@N

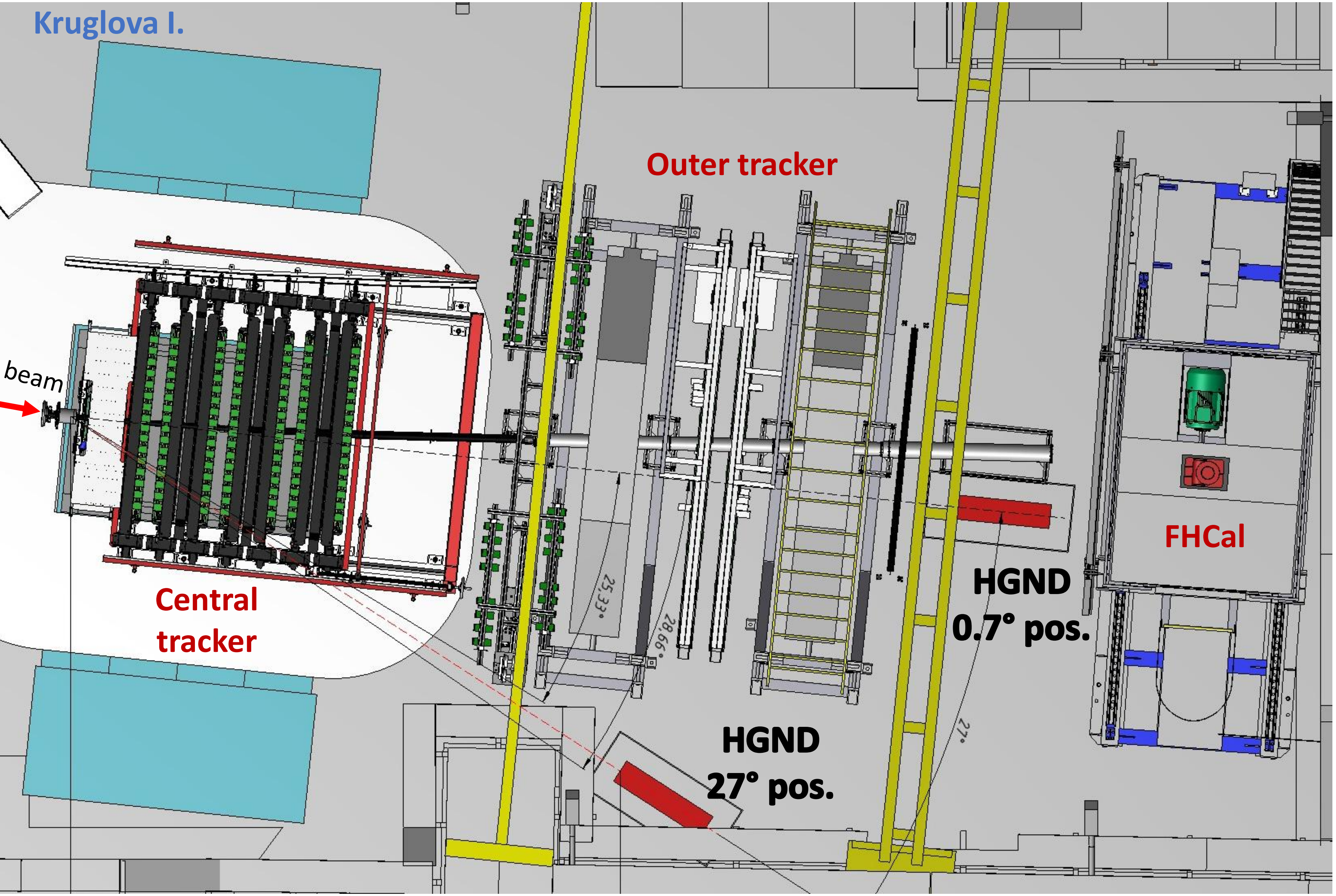


**27° position:**

Measurements of the neutron spectrum at ~ midrapidity.

**0° position:**

Test and calibration with known neutron energy (energy of a beam of spectator neutrons)

**EMD:**

In most cases, EMD of a heavy nucleus results in the emission of a single or just few neutrons with the production of a single residual nucleus

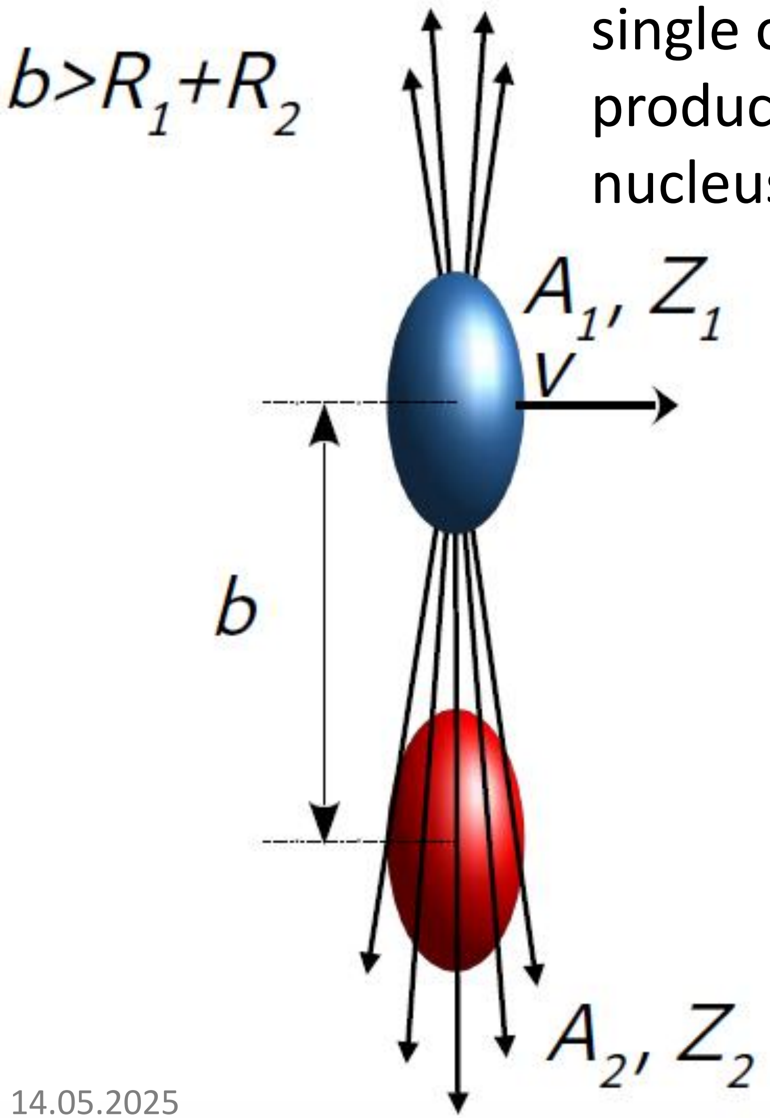


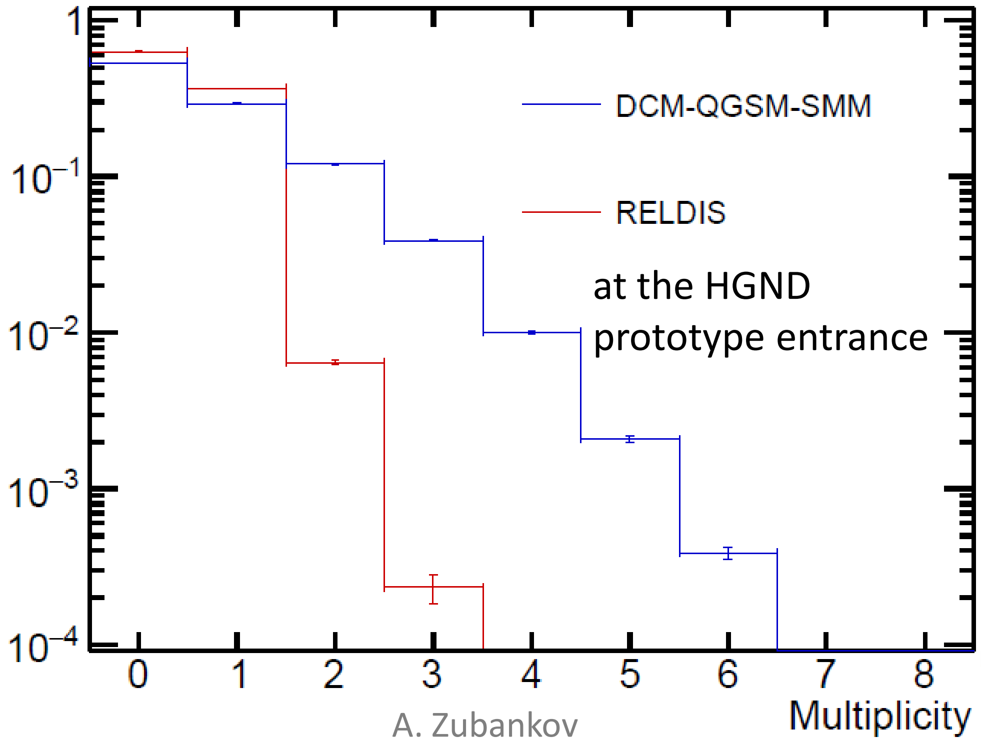


**Hadronic interactions:**

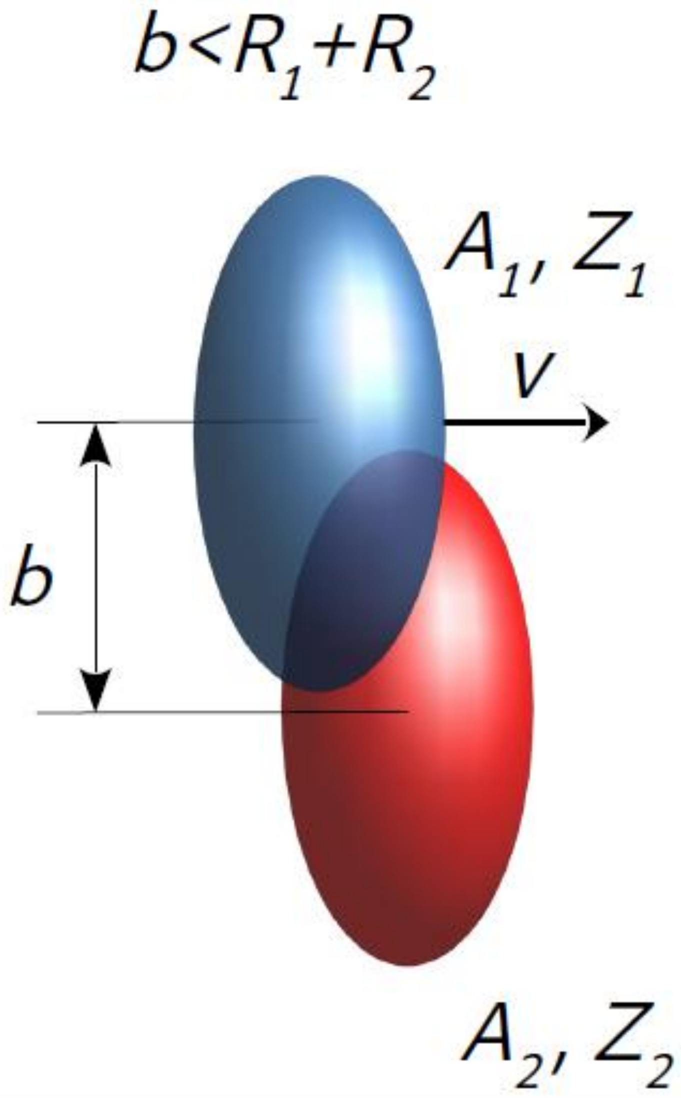

# Criteria for selecting events with spectator neutrons

Only single Xe ion in target

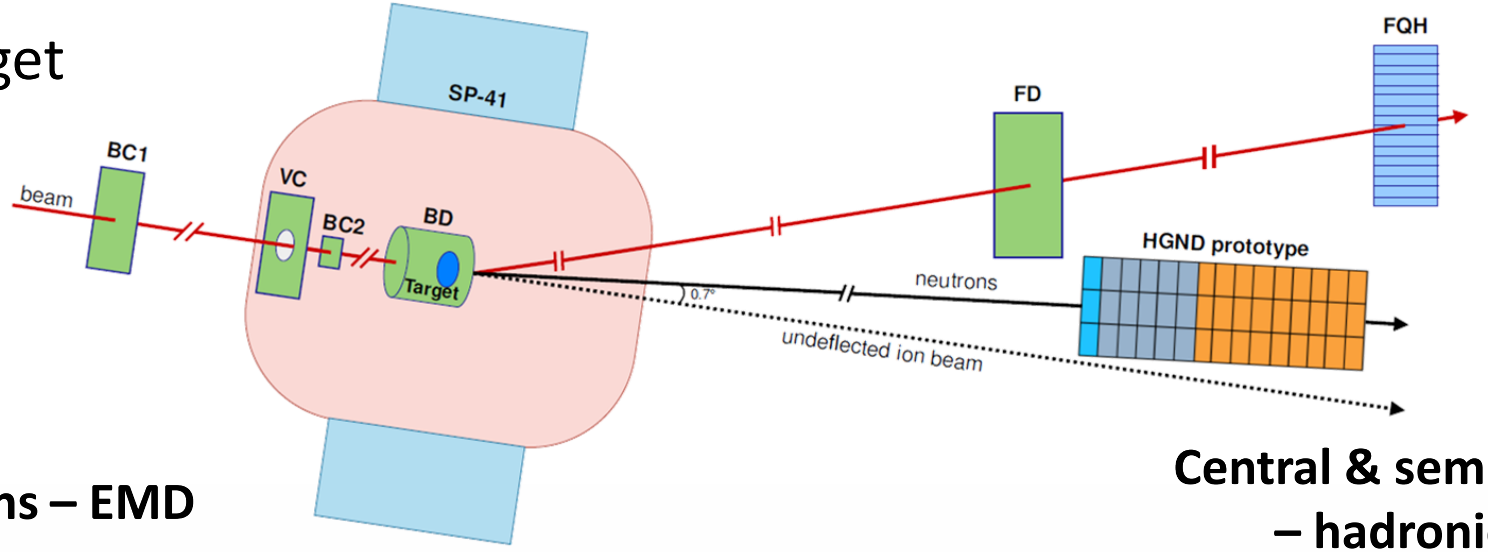


**Ultra-peripheral collisions – EMD**

**Central & semi-central collisions – hadronic interactions**

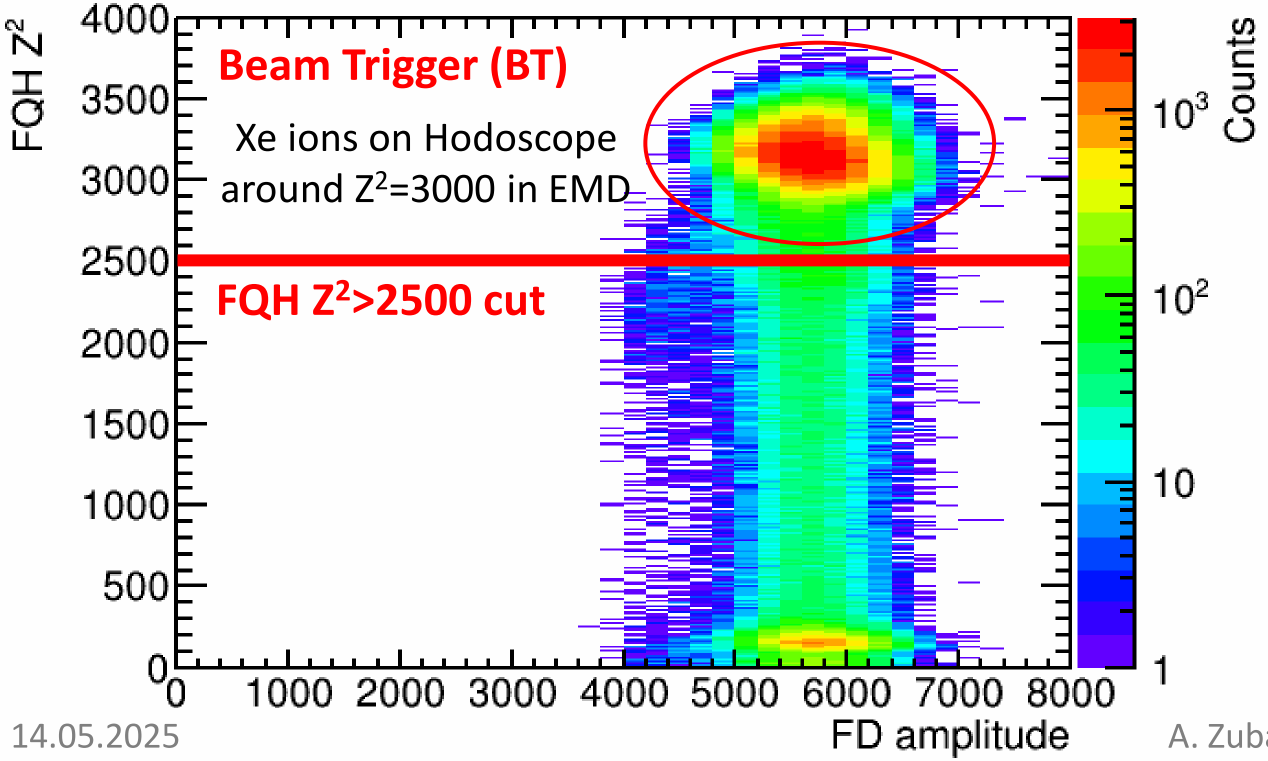


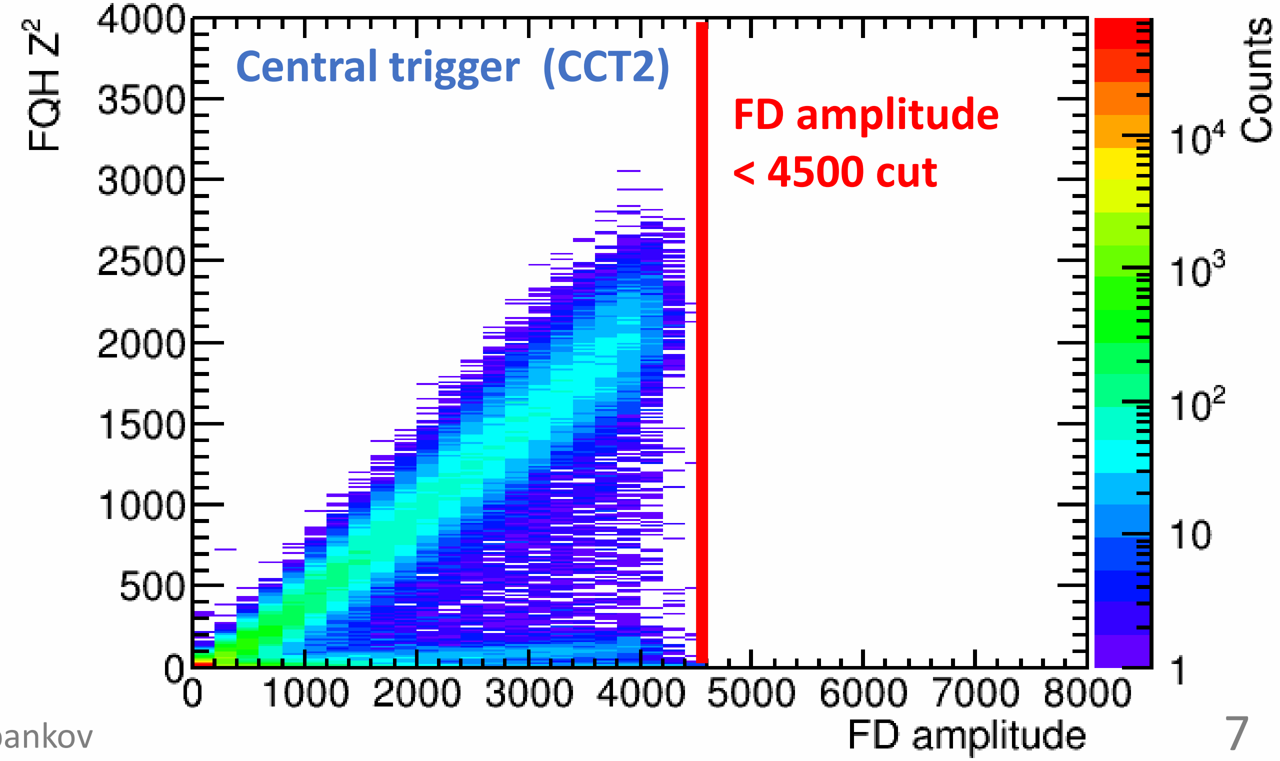

# Criteria for selecting events with spectator neutrons

- Selection of events without charged particles, ToF cut, γ-cut (1.55 $X_0$ or 0.11 $\lambda_{int}$)
- Reconstruction of energy by maximum velocity
- Scaled by incident ion beam rate

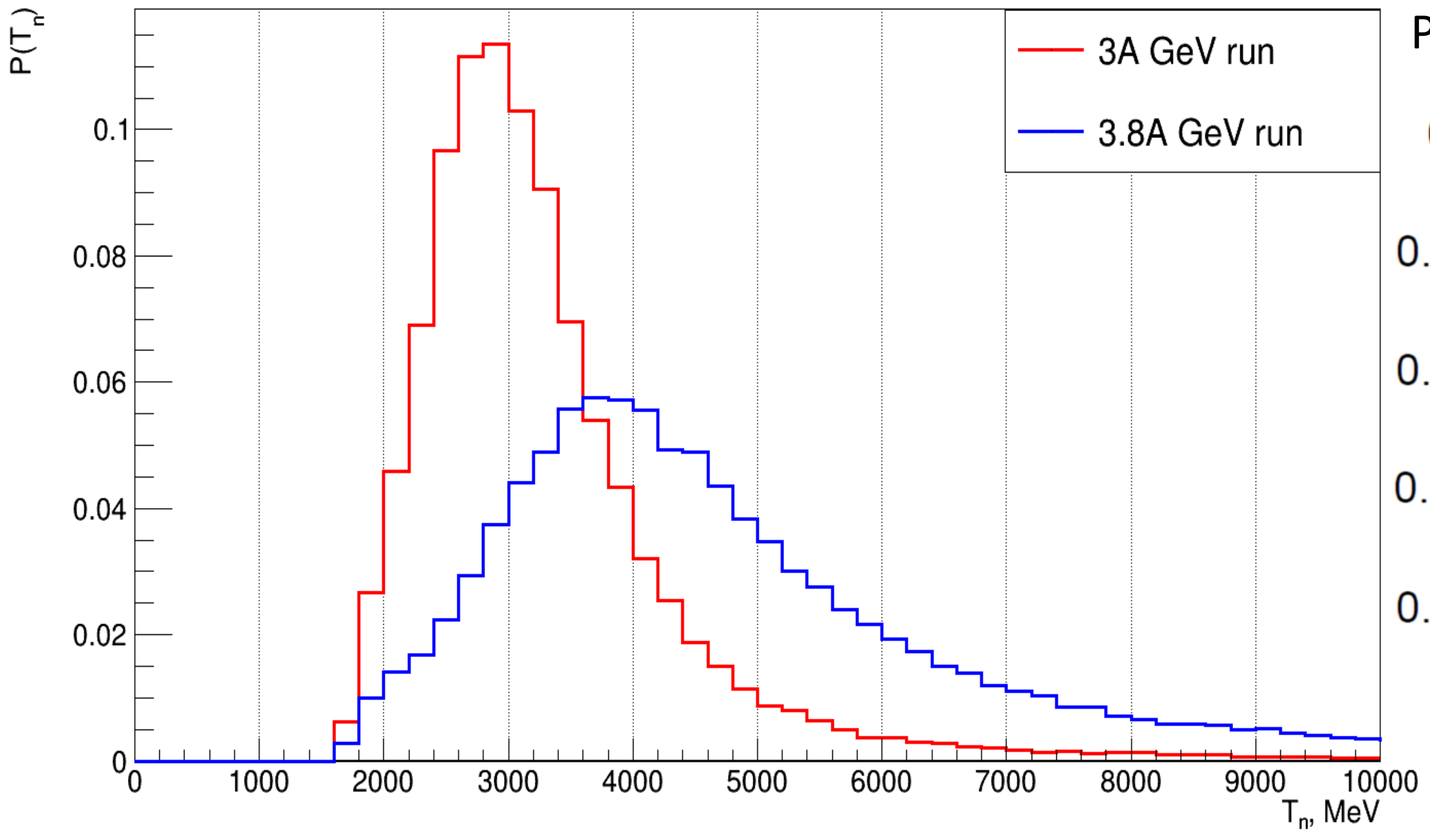


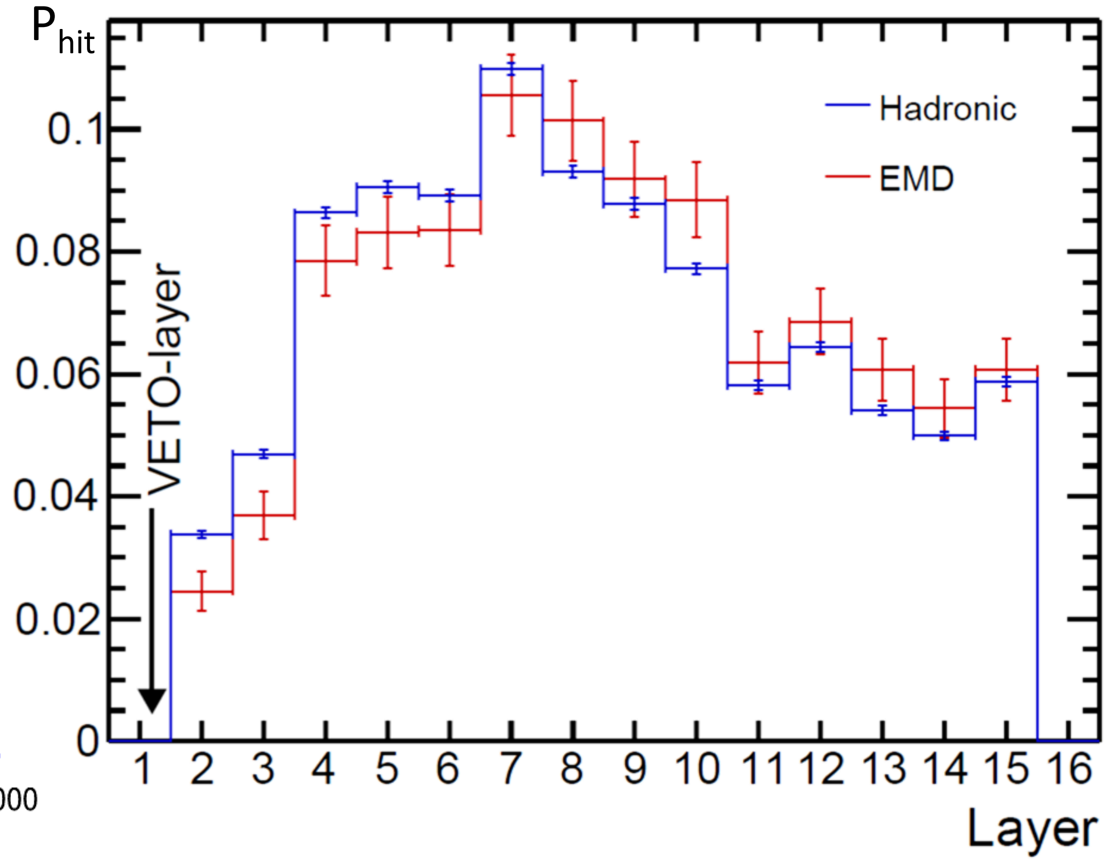

# Criteria for selecting events with spectator neutrons

- Selection of events without charged particles, ToF cut, γ-cut (1.55 $X_0$ or 0.11 $\lambda_{int}$)
- Reconstruction of energy by maximum velocity
- Scaled by incident ion beam rate

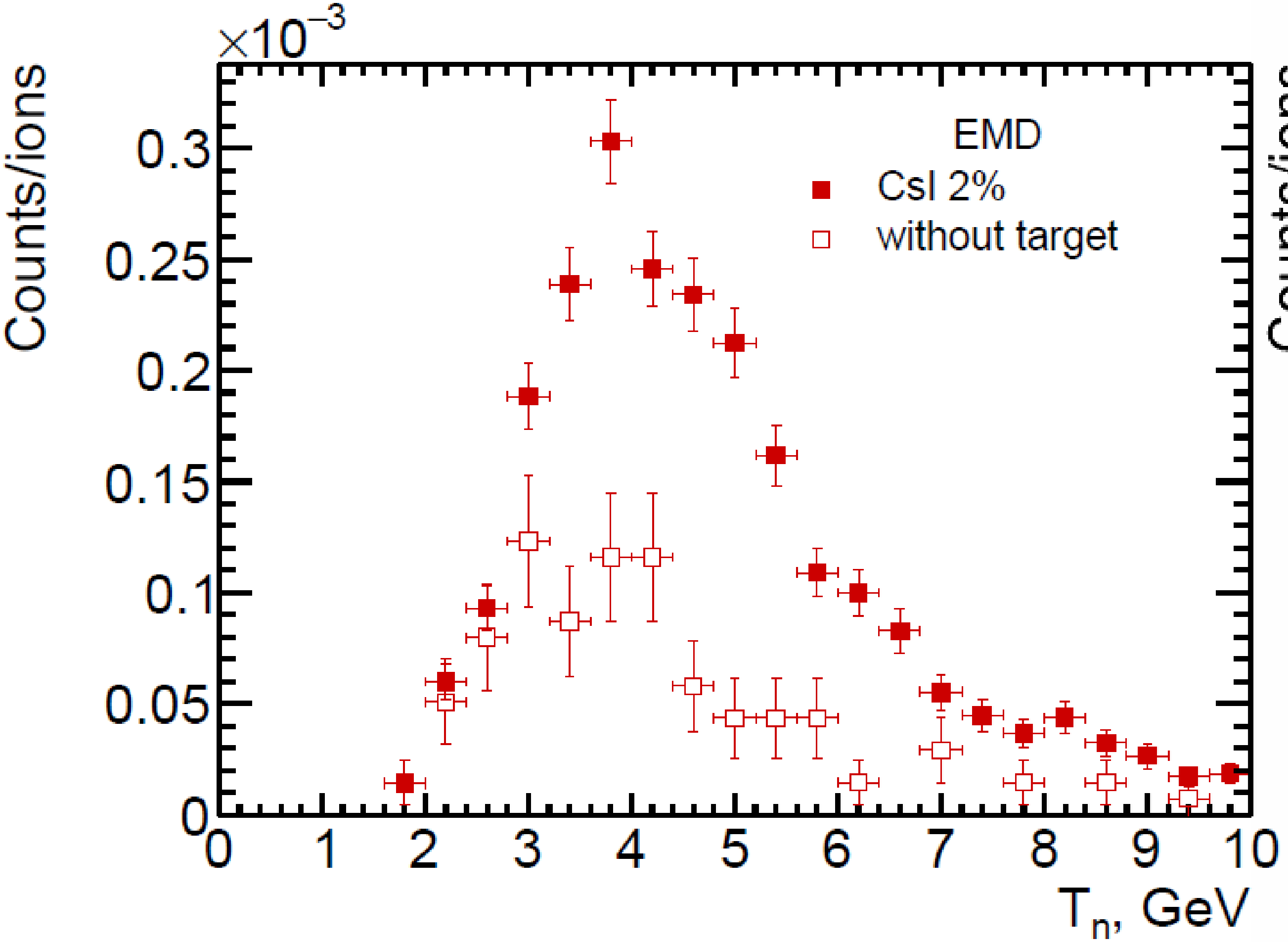


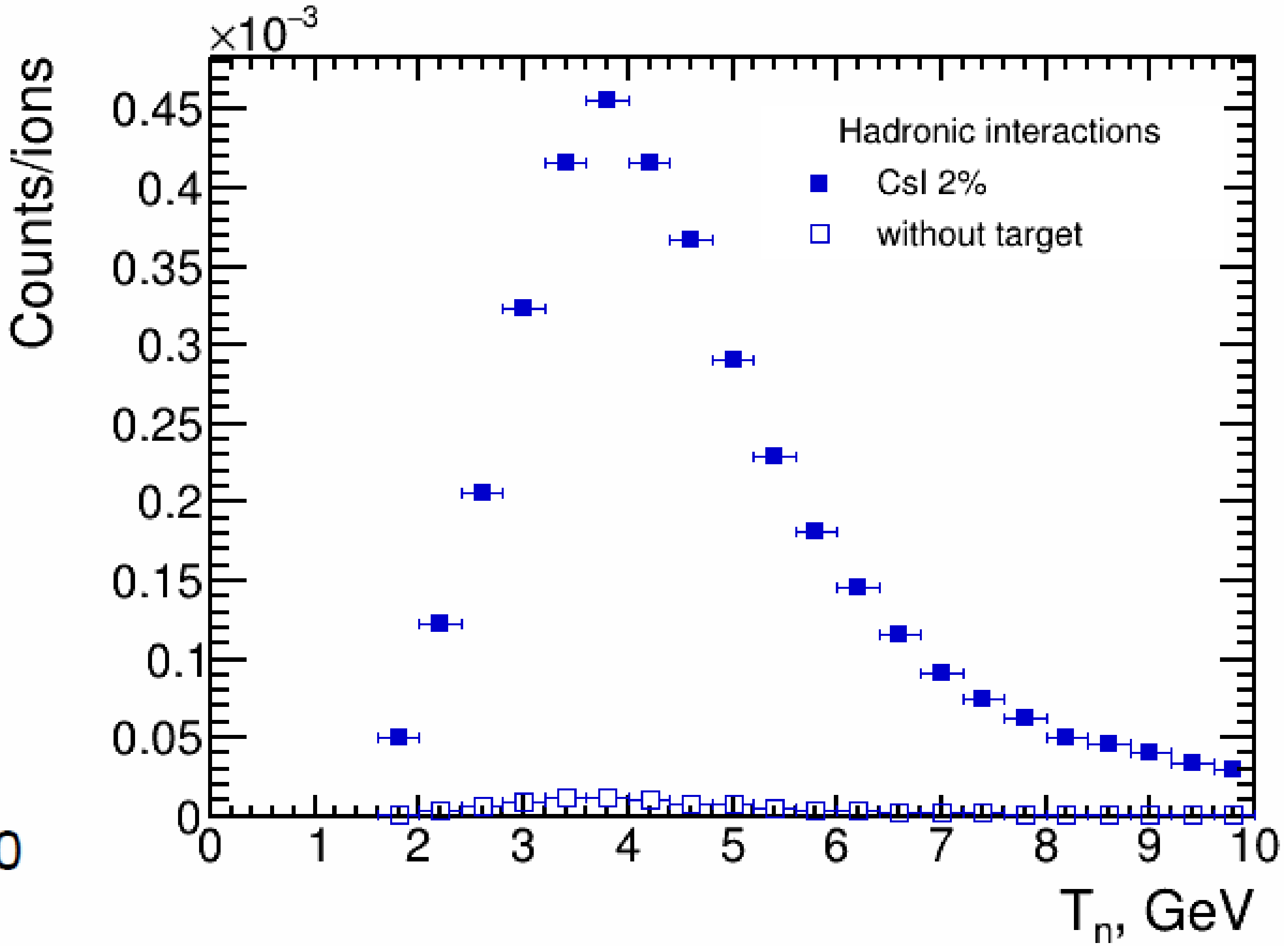

# Run with CsI 1% target

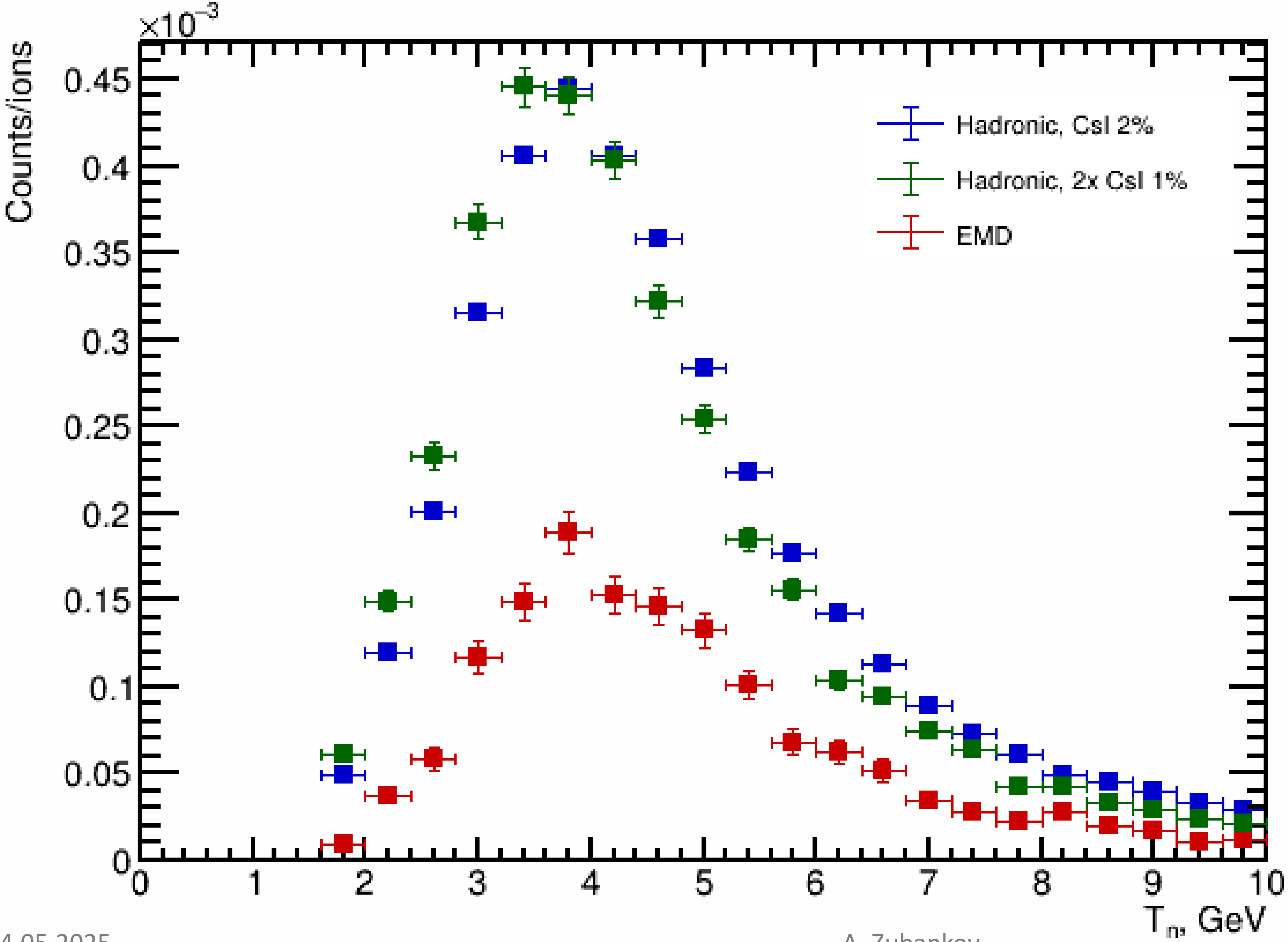


After subtracting events from empty target

# HGND prototype efficiency for neutrons

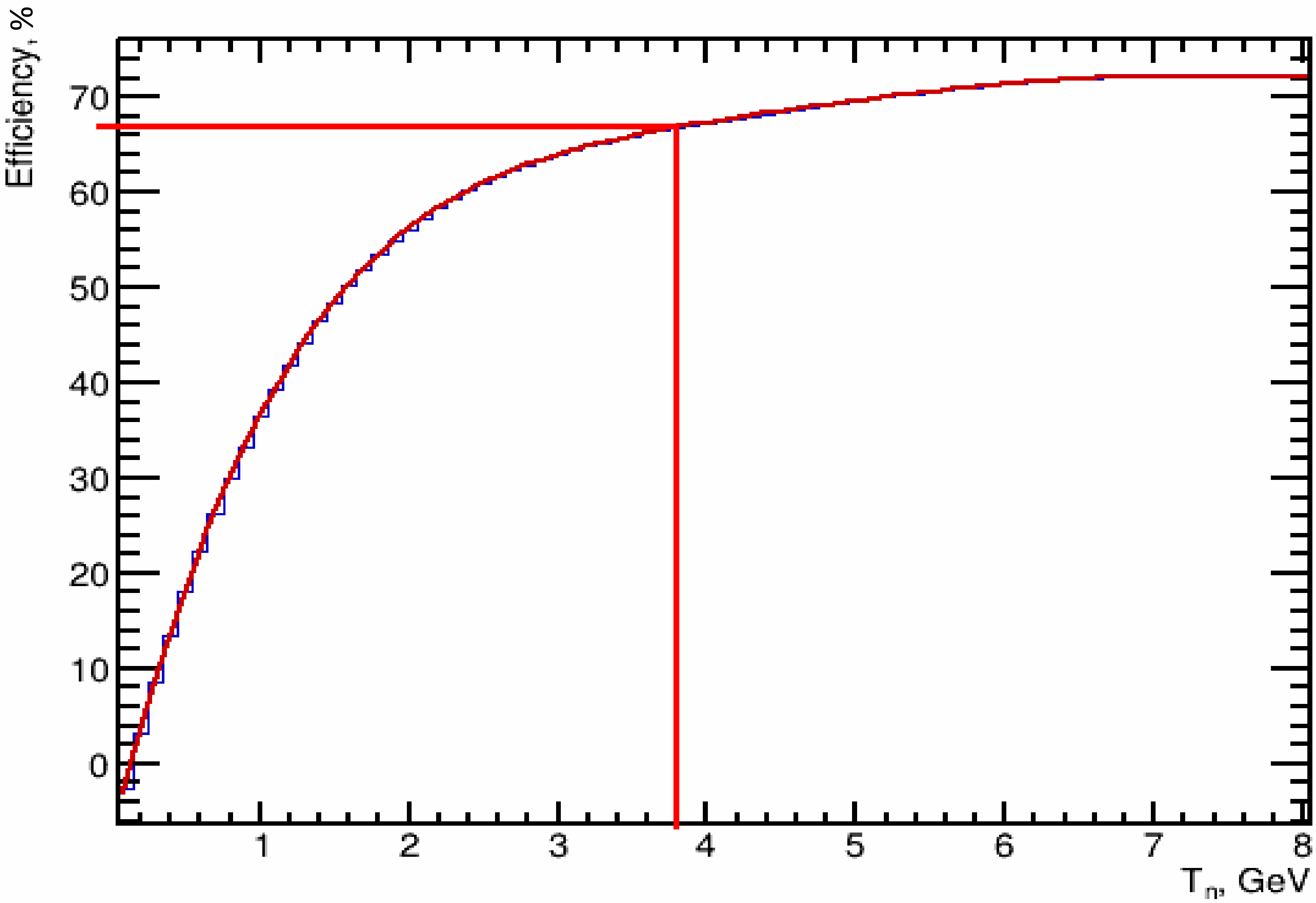


Geant4 simulation:

Box generator, only neutrons

- VETO-cut
- $\gamma$-cut
- ToF cut

We use the DCM-QGSM-SMM* and UrQMD-AMC models to estimate the detector efficiency for hadronic interactions, and RELDIS** for EMD

*M. Baznat et al., Monte-Carlo Generator of Heavy Ion Collisions DCM-SMM, *Phys. Part. Nucl. Lett.* **2020**, 17, 303.

**I. Pshenichnov, Electromagnetic Excitation and Fragmentation of Ultrarelativistic Nuclei. *Phys. Part. Nucl.* **2011**, 42 (2), 215-250.

# RELDIS – EMD in simulation

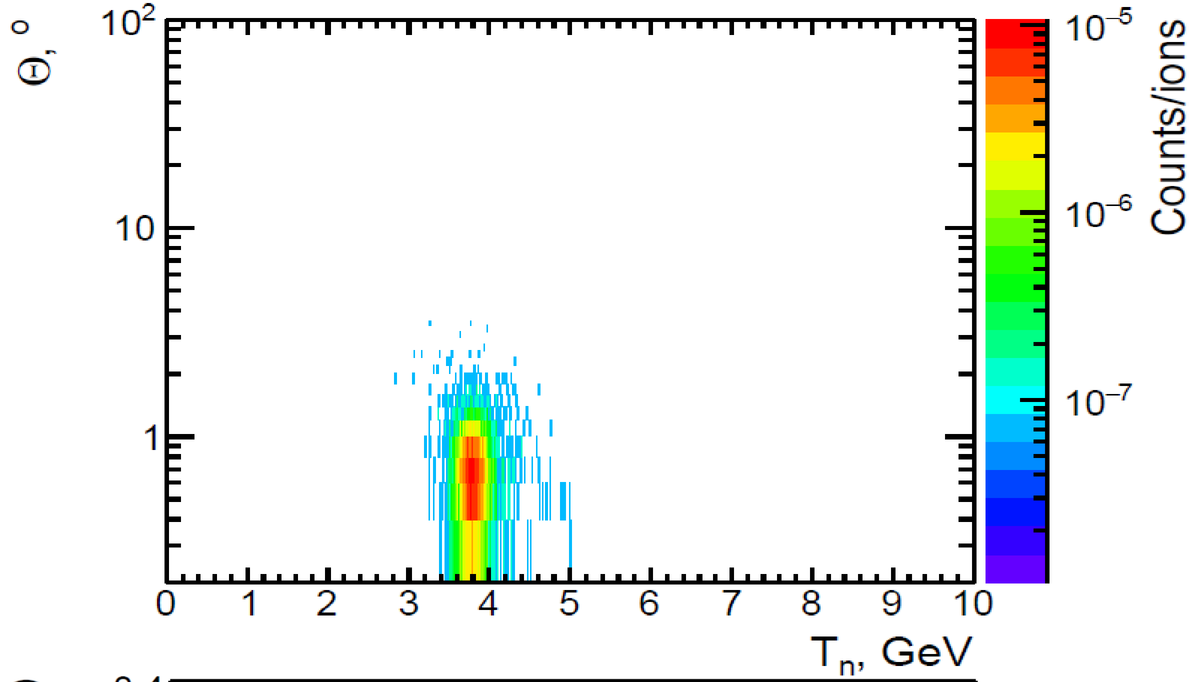


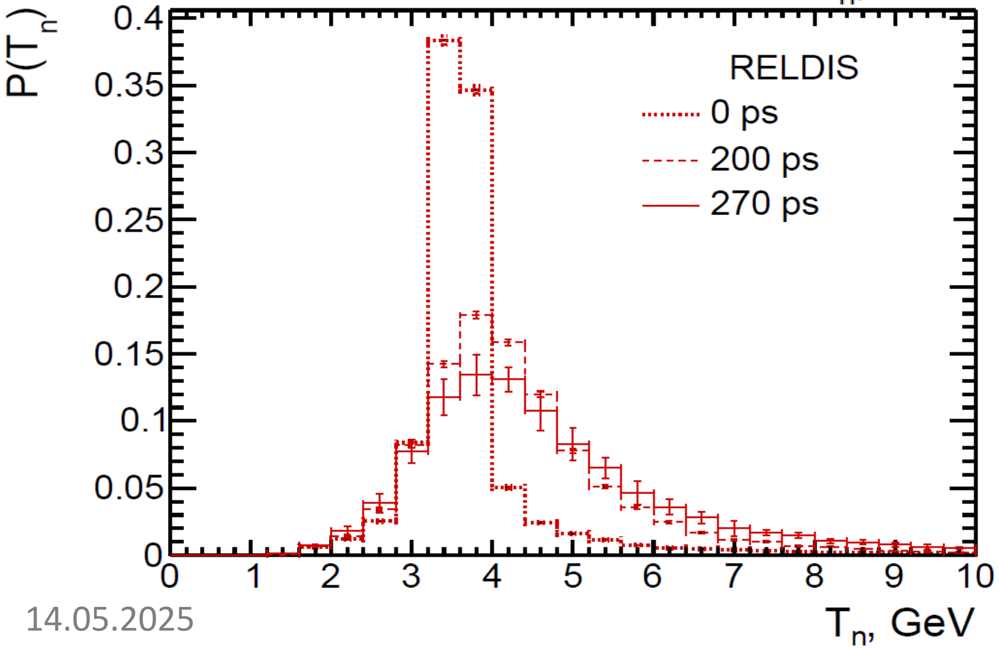


## RELDIS

$^{124}Xe + ^{130}Xe$ @ 3.8A GeV

Neutron multiplicity – **1.05**

Neutron multiplicity on the surface – **1.02**

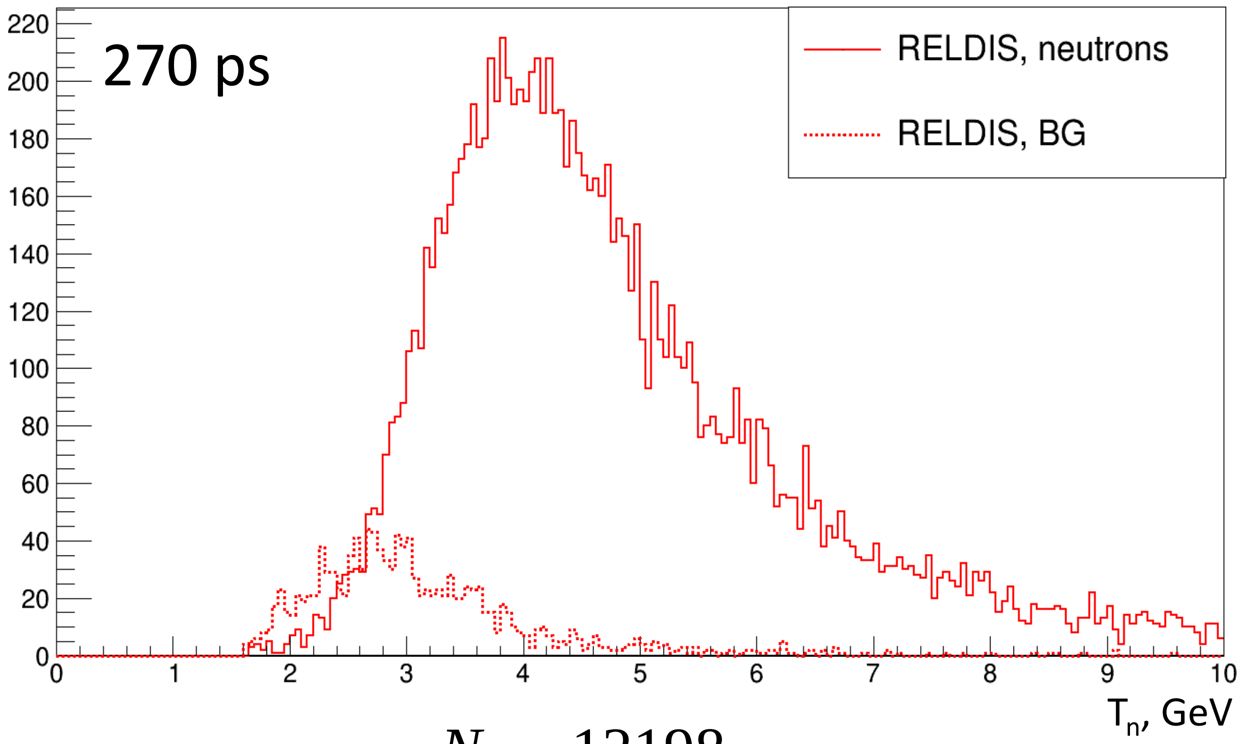


$$\frac{N}{BG} = \frac{12198}{1292} = 9.44$$

# RELDIS – EMD in simulation

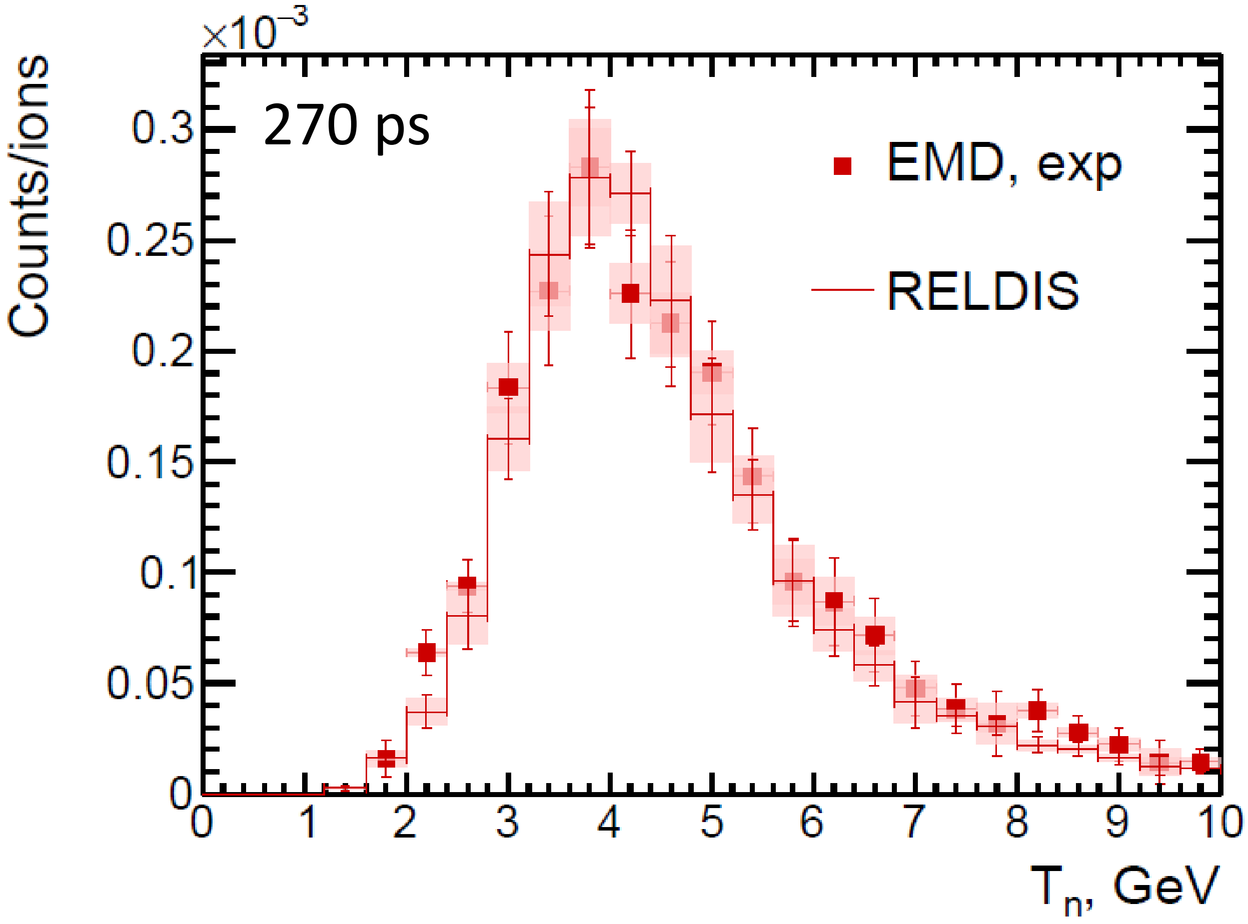


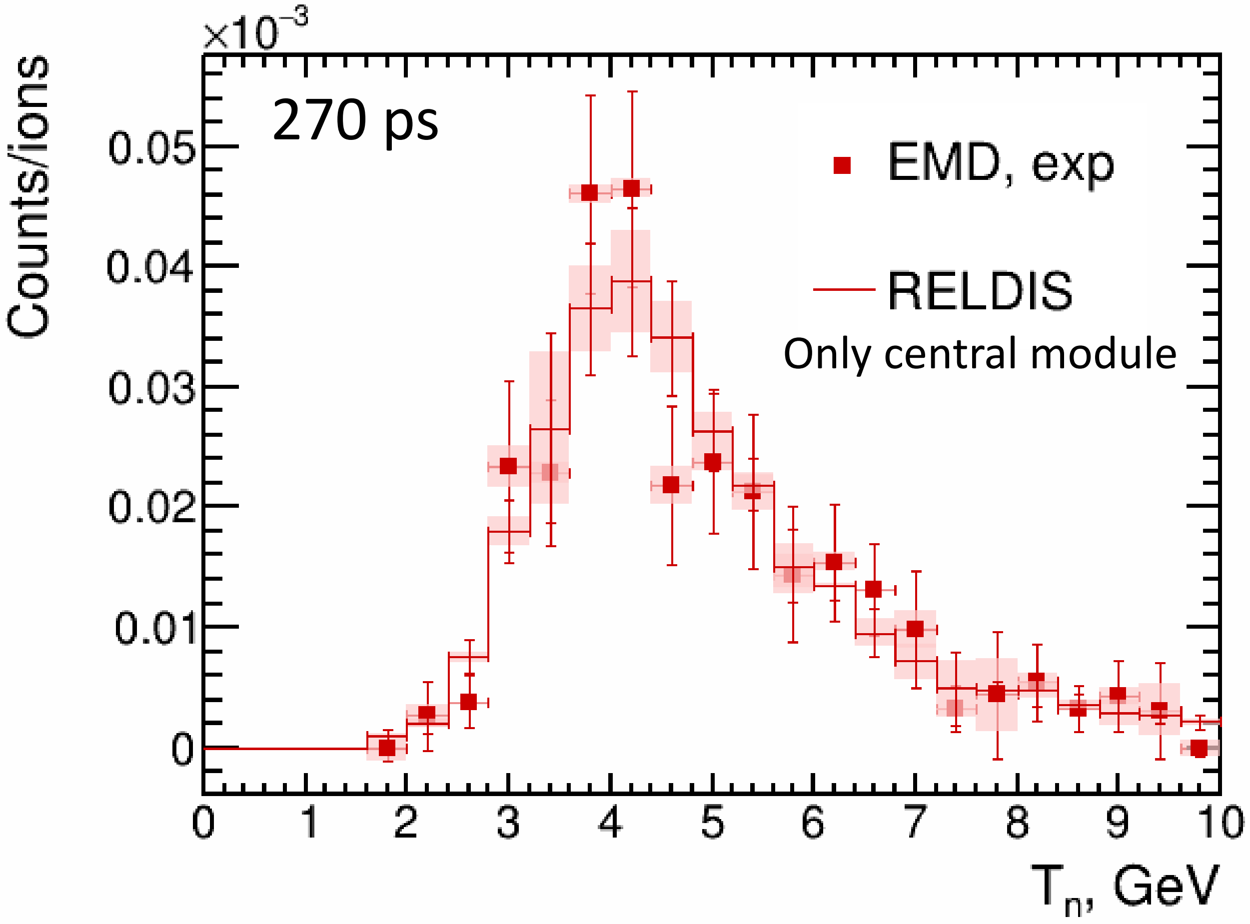


$$acc = \frac{N_{hit}}{N_{gen}} \qquad \varepsilon = \frac{N_{rec}}{N_{hit}}$$

| Model | *acc*, % | *ε*, % | *acc* x *ε*, % |
|---|---|---|---|
| **RELDIS** | **36.77 ± 0.27** | **55.77 ± 0.41** | **20.51 ± 0.15** |
| RELDIS (1 mod.) | 8.15 ± 0.14 | 36.80 ± 0.65 | 3.00 ± 0.05 |

# UrQMD-AMC vs DCM-QGSM-SMM

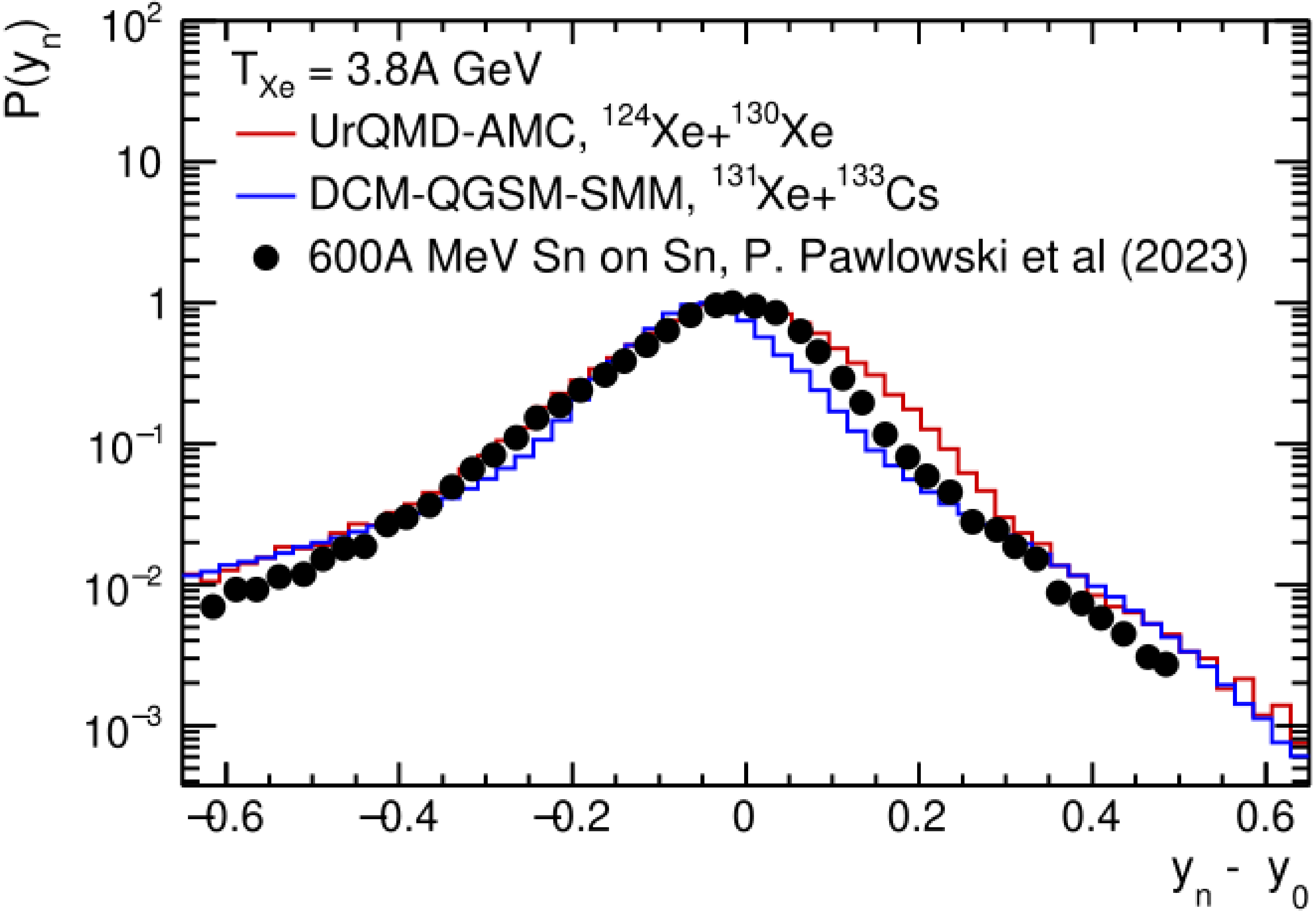


DCM-QGSM-SMM and UrQMD-AMC describe the experiment well in the rapidity region $y_n$-$y_0$<0.

In the region $y_n$-$y_0$>0, DCM-QGSM-SMM underestimates the data whereas UrQMD-AMC overestimates.

For DCM-QGSM-SMM, there is a shift in the rapidity relative to the beam rapidity.

# UrQMD-AMC vs DCM-QGSM-SMM for BM@N

## UrQMD-AMC
3.8A GeV $^{124}Xe + {}^{130}Xe$

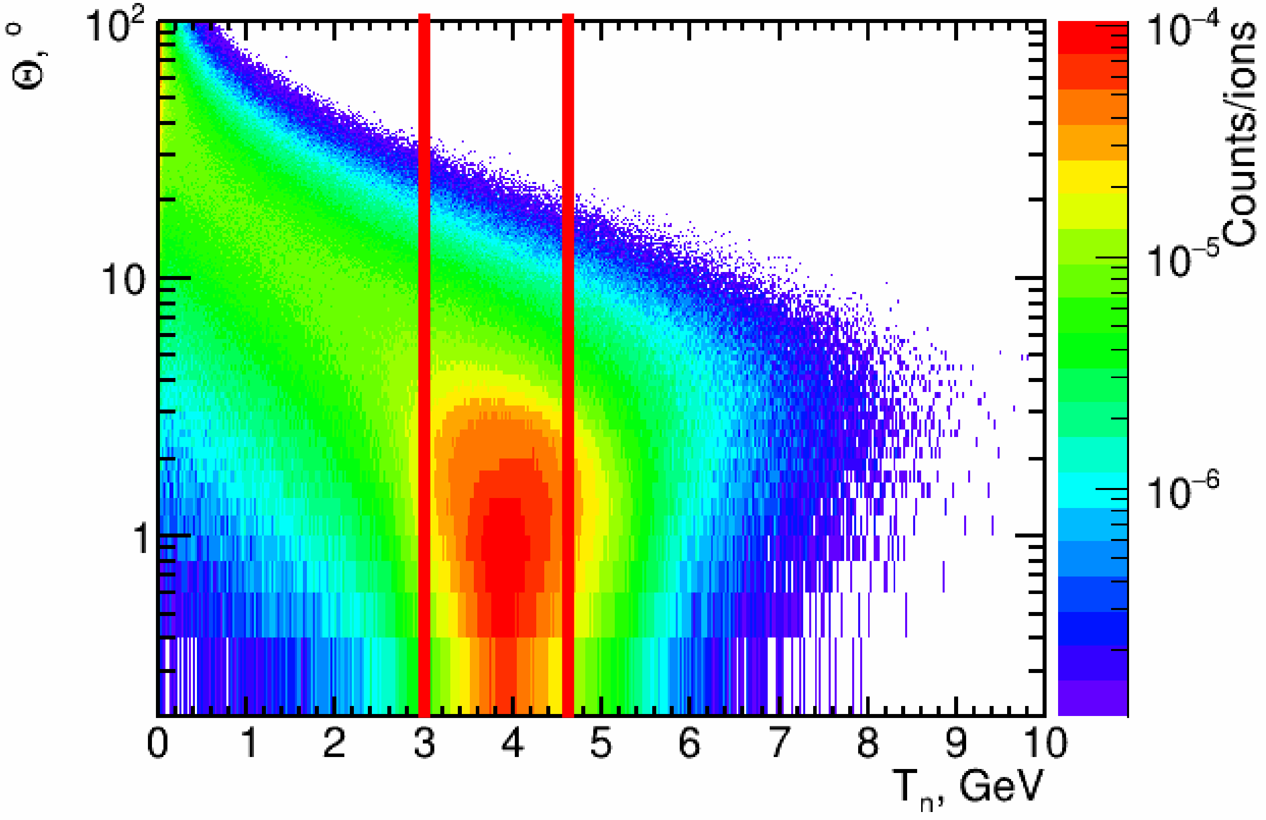


Spectator neutron multiplicity – **17.70**

## DCM-QGSM-SMM
3.8A GeV $^{131}Xe + {}^{133}Cs$

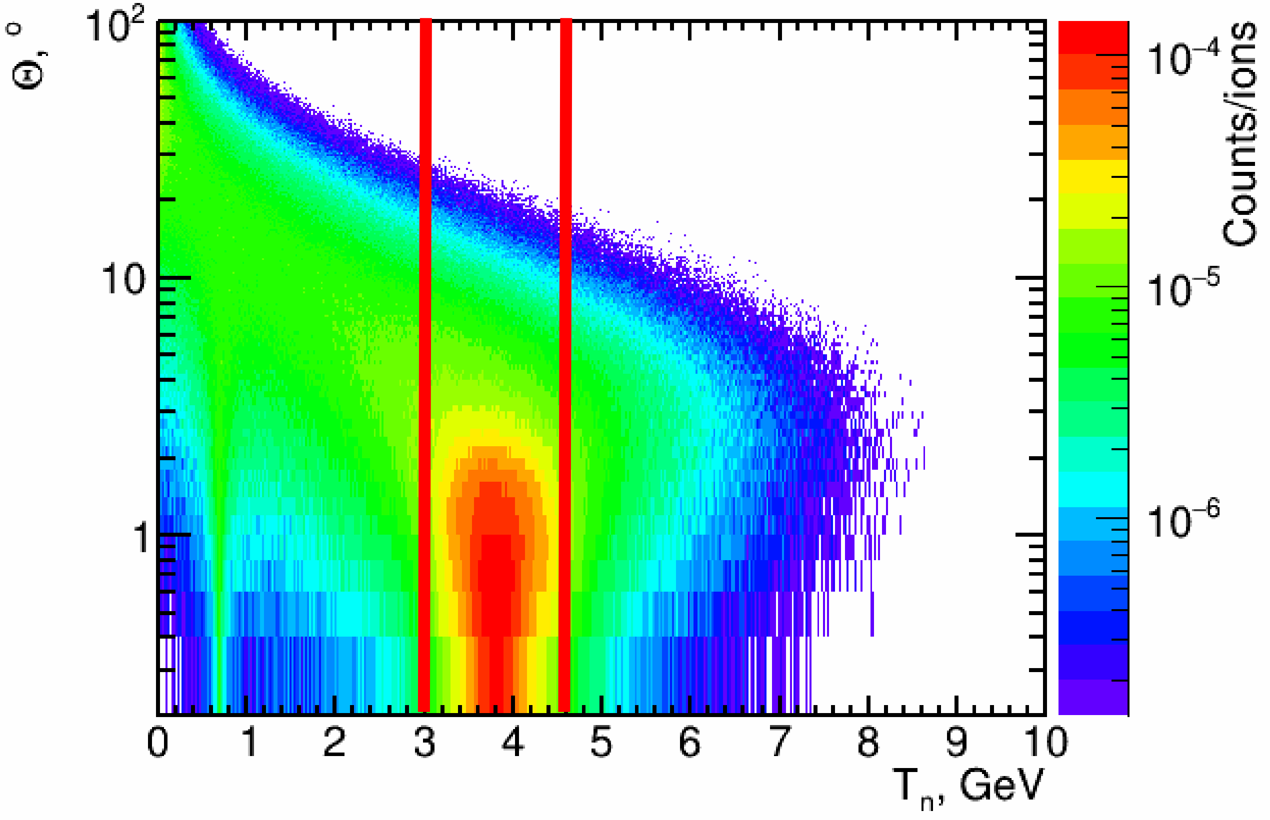


Spectator neutron multiplicity – **16.01**

# Spectator neutrons on the surface of the HGND prototype

with trigger efficiency correction from V. Plotnikov

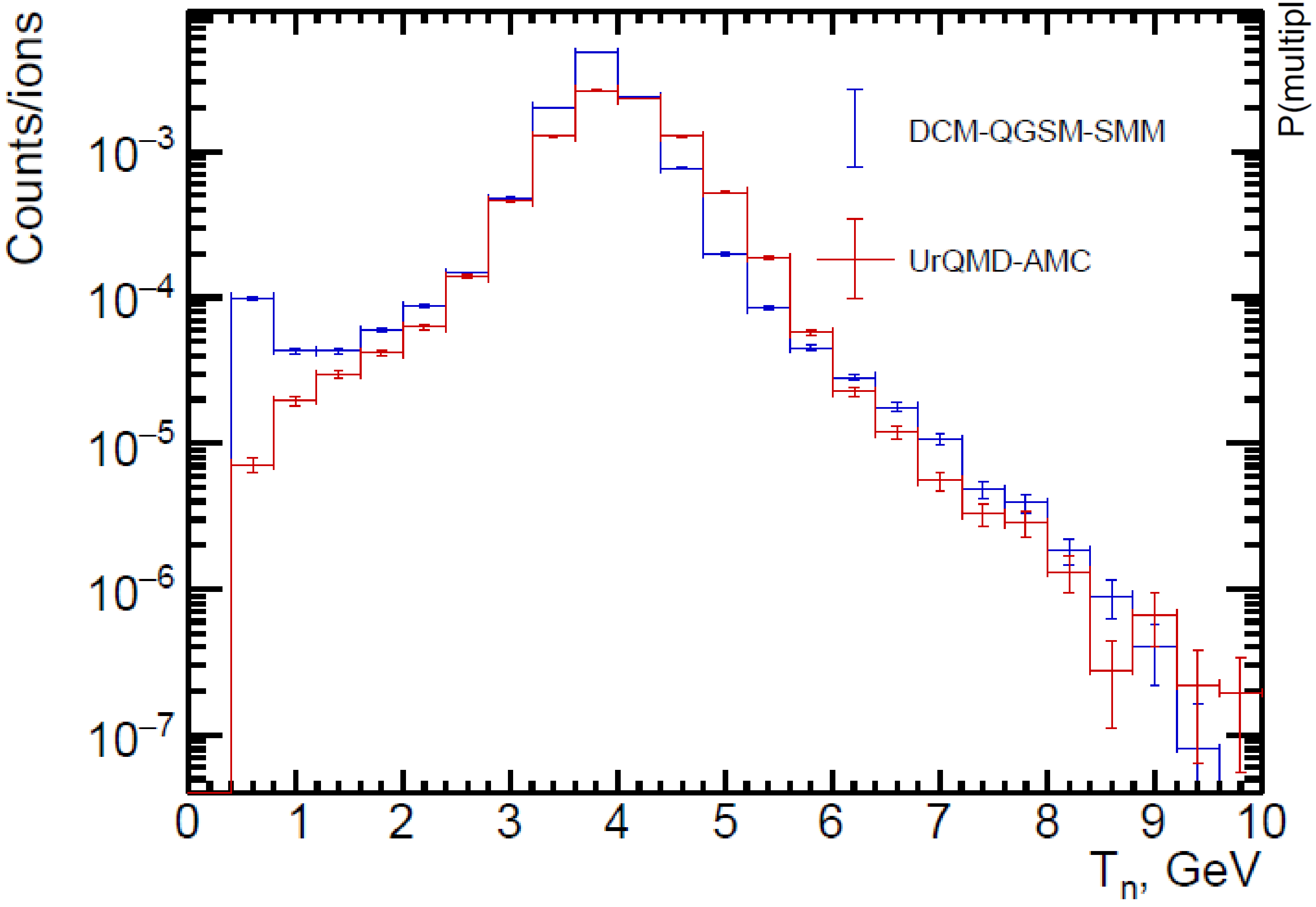


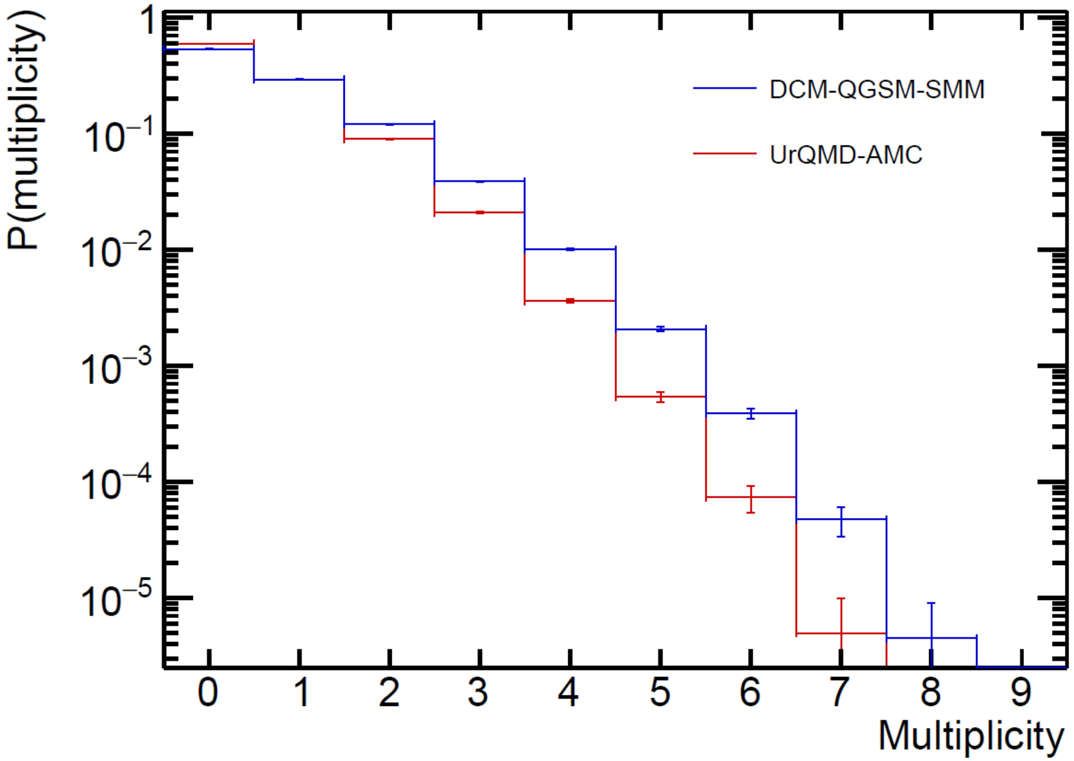


Neutron multiplicity on the surface of the HGND prototype
– **1.36** for **UrQMD-AMC**
– **1.51** for **DCM-QGSM-SMM**

# Backgrounds & time resolution

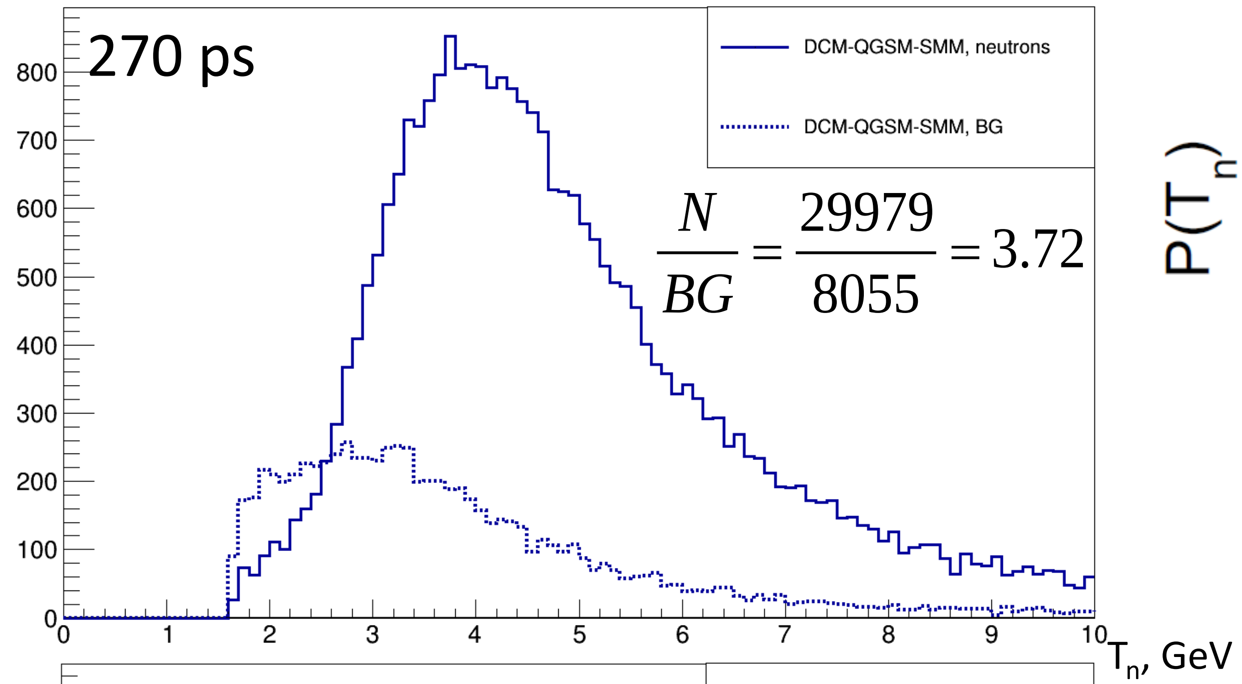


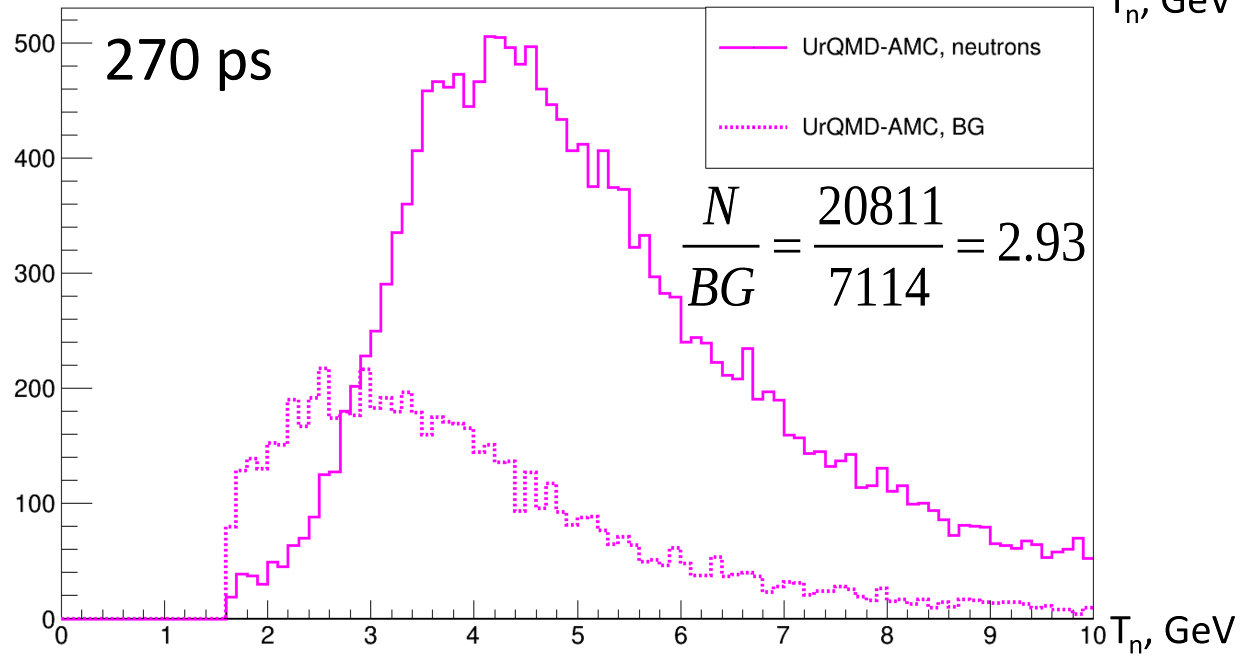


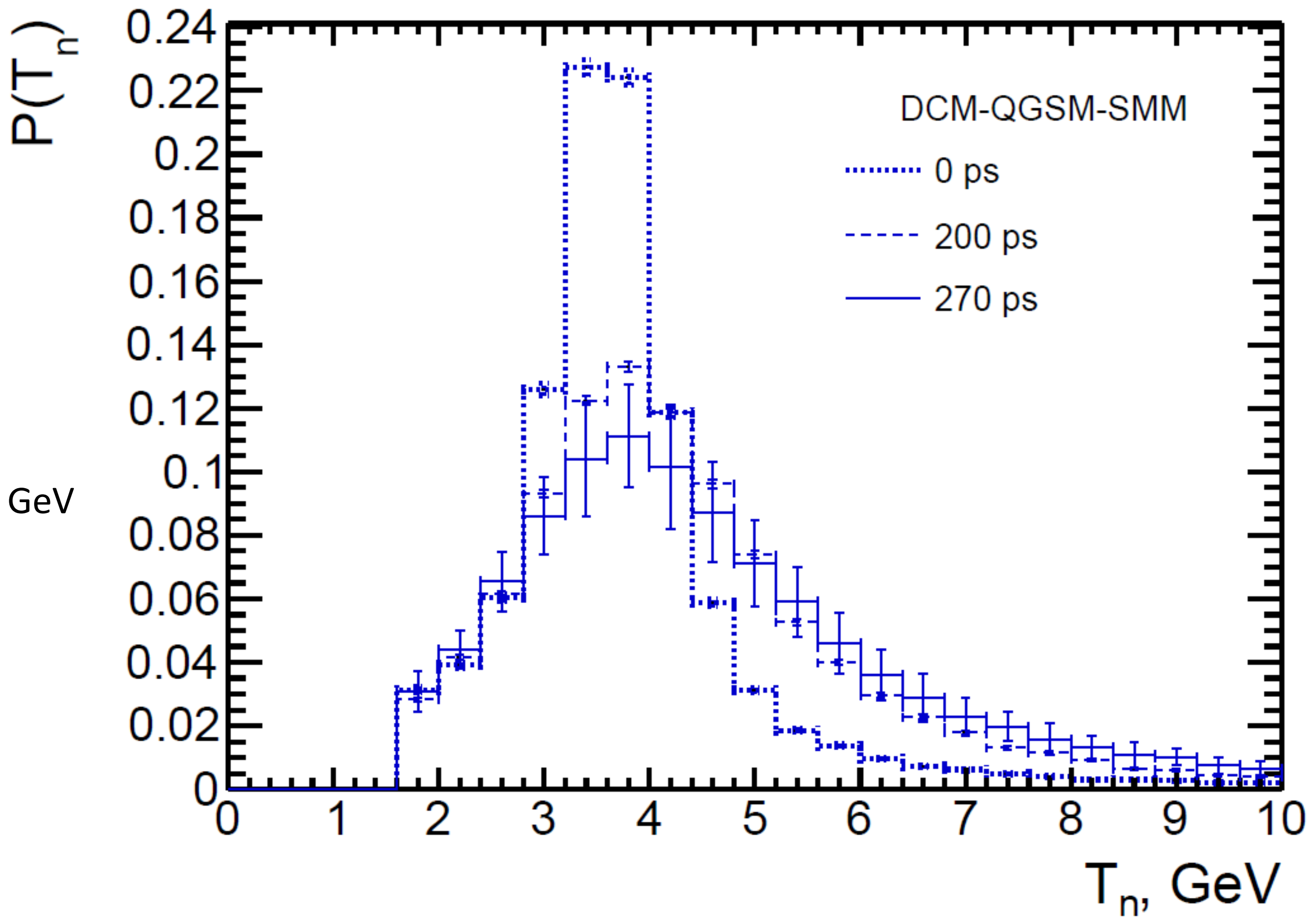

# Reconstructed neutron energy spectra for hadronic interactions

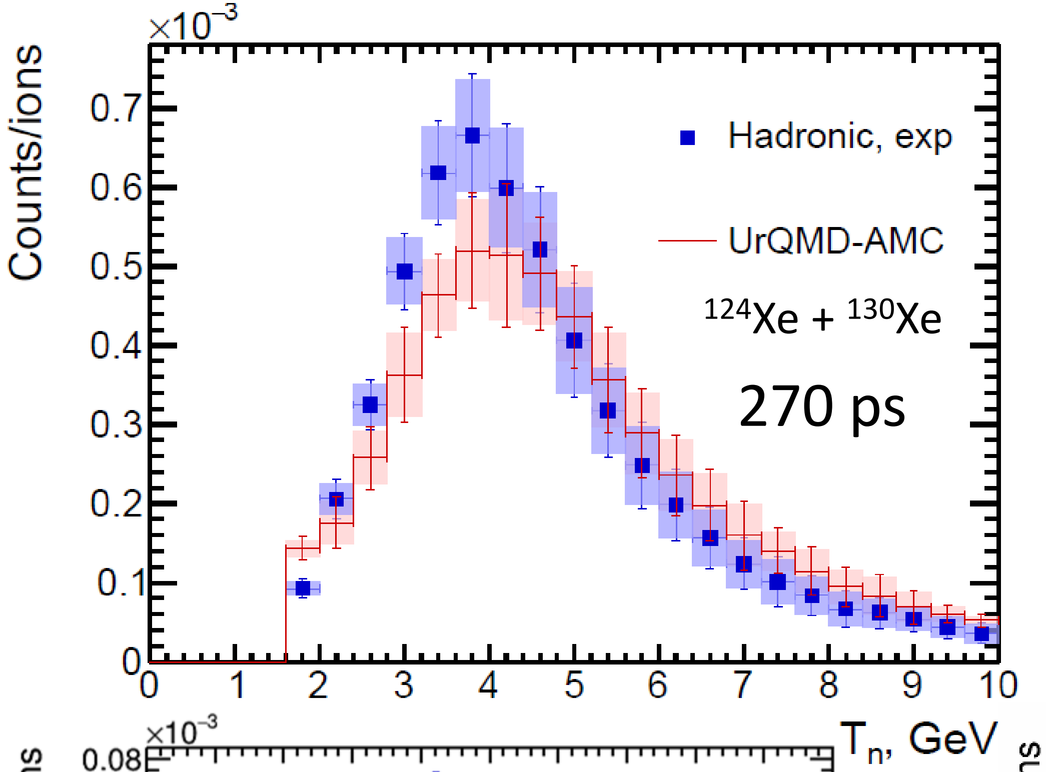


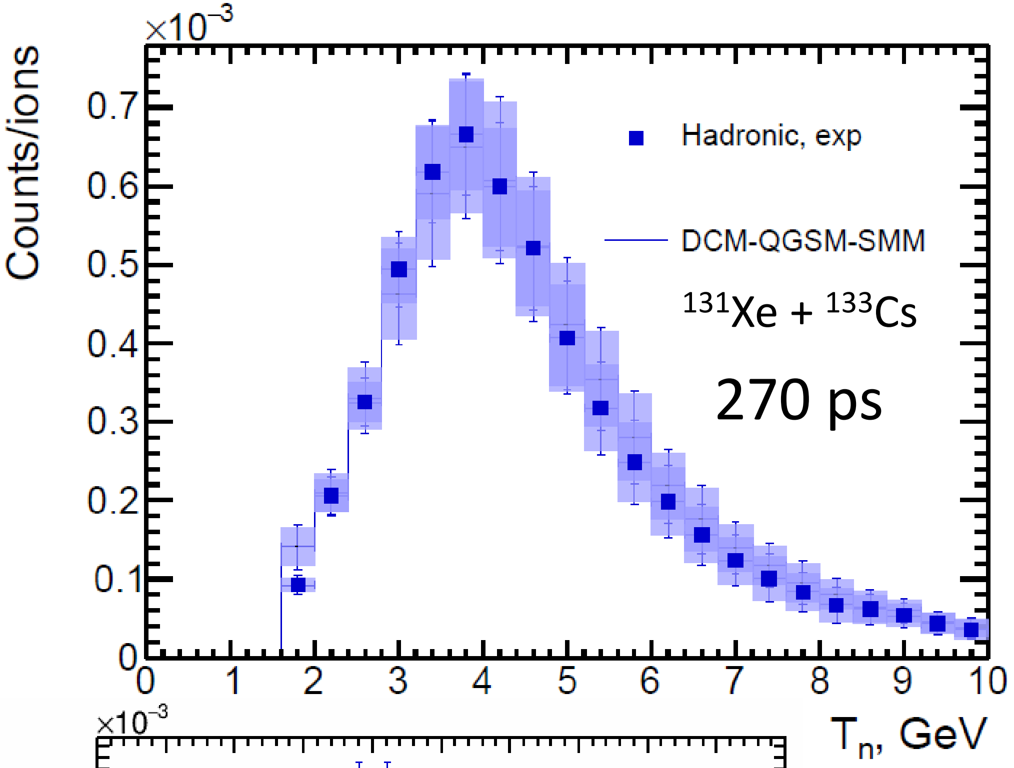


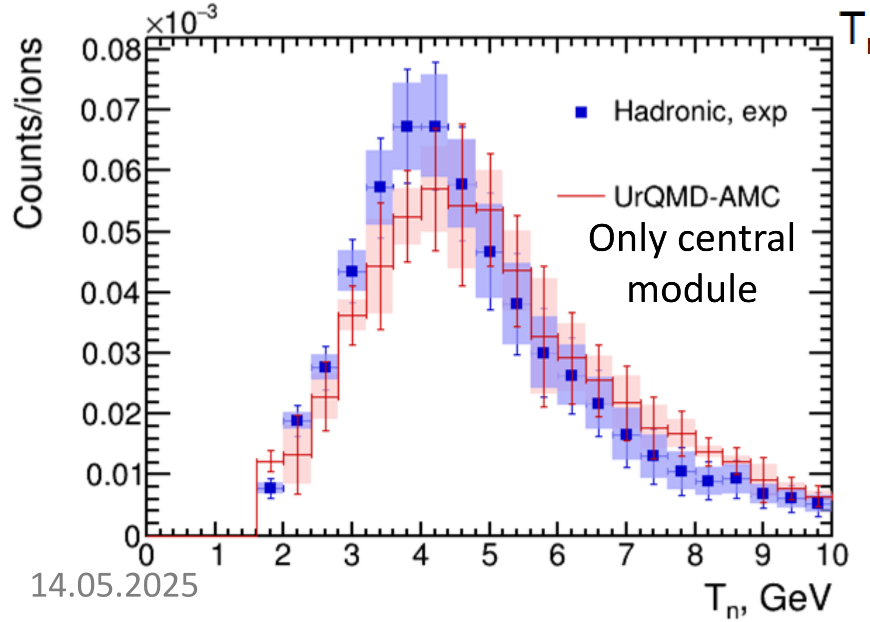


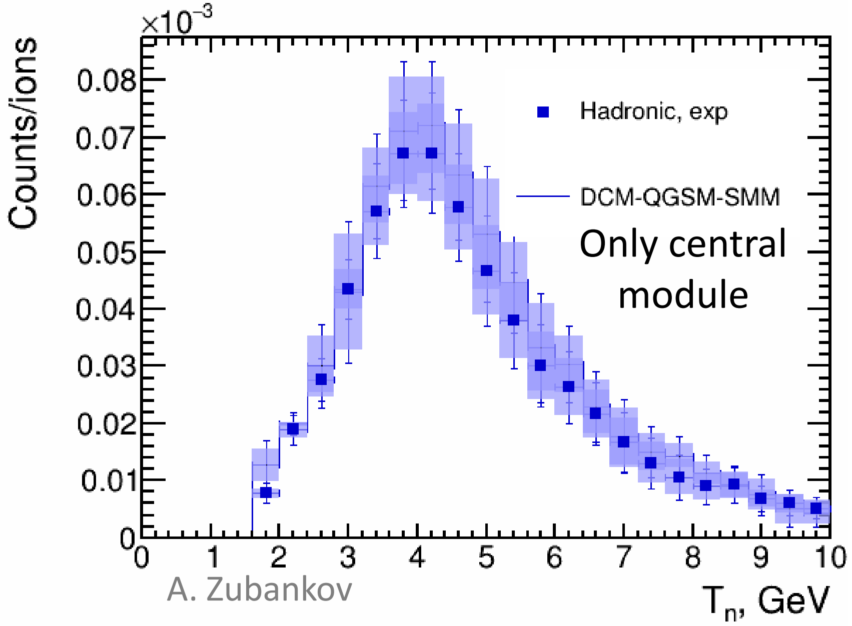


The difference in the shape and peak position of the reconstructed spectra of the models is noticeable, which is also due to the difference in the mean kinetic energy of neutrons and their multiplicity.

# HGND prototype efficiencies for hadronic interactions

$$acc = \frac{N_{hit}}{N_{gen}} \qquad \varepsilon = \frac{N_{rec}}{N_{hit}}$$

| Model | *acc*, % | *ε*, % | *acc* x *ε*, % |
|---|---|---|---|
| DCM-QGSM-SMM | 4.08 ± 0.02 | 36.23 ± 0.17 | 1.48 ± 0.01 |
| UrQMD-AMC | 2.87 ± 0.02 | 43.64 ± 0.24 | 1.25 ± 0.01 |
| DCM-QGSM-SMM (1 mod.) | 0.62 ± 0.01 | 27.81 ± 0.37 | 0.173 ± 0.002 |
| UrQMD-AMC (1 mod.) | 0.40 ± 0.01 | 35.73 ± 0.58 | 0.142 ± 0.002 |

The difference in ***acc*** and ***ε*** is explained by the differences in angular distribution of primary neutrons (17.70 vs 16.01) and in average multiplicity of neutrons hitting the detector (1.36 vs 1.51).

# Cross-section estimation

$$\sigma = \frac{N_{ev}}{N_{ions}} \cdot (acc \times \varepsilon) \cdot \langle N \rangle \cdot \frac{A}{d \cdot N_A \cdot \rho}$$

$d = 0.175\, cm$

$N_A = 6.02 \cdot 10^{23}\, mol^{-1}$

$\rho = 4.53\, g/cm^3$

| | RELDIS | DCM-QGSM-SMM | UrQMD-AMC |
|---|---|---|---|
| $N_{ev}/N_{ions}$ | $(1.51\pm0.14)\cdot10^{-3}$ | $(3.87\pm0.02)\cdot10^{-3}$ | |
| $N_{ev}/N_{ions} \cdot (acc \times \varepsilon) \cdot \langle N \rangle$ | $(7.21\pm0.72)\cdot10^{-3}$ | $(16.38\pm0.15)\cdot10^{-3}$ | $(17.47\pm0.18)\cdot10^{-3}$ |
| $\sigma^{\exp}$ | 1.96±0.20 b | 4.46±0.04 b | 4.76±0.05 b |
| $\sigma^{sim}$ | 1.89±0.02 b | 4.76±0.01 b | 4.89±0.01 b |

A detailed study of the systematics will be in the future.

$\sigma^{Glauber} = 5.28\, b$

# Neutron yields at 27°

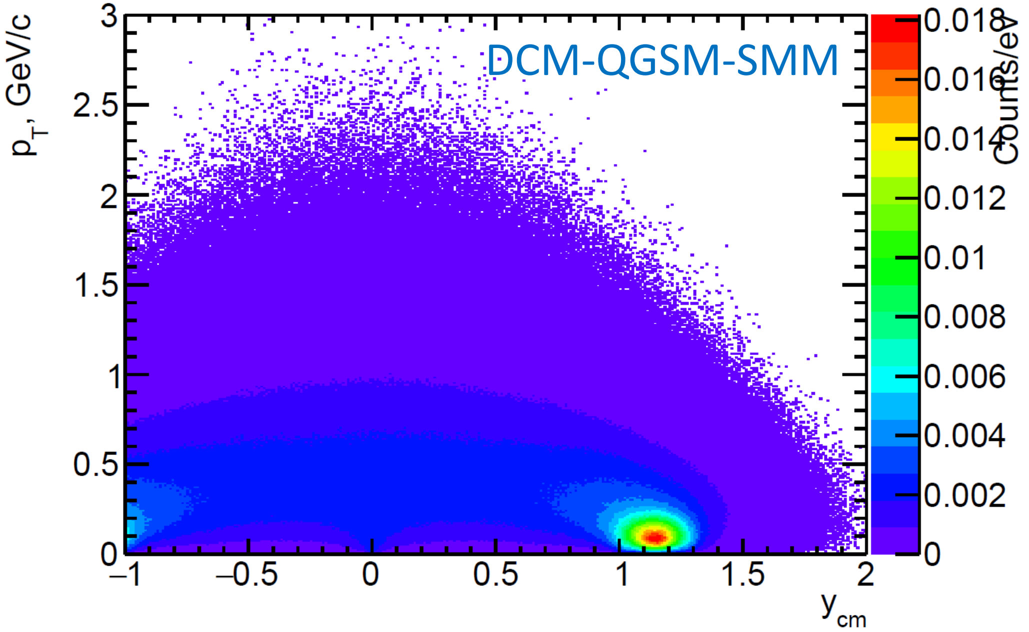


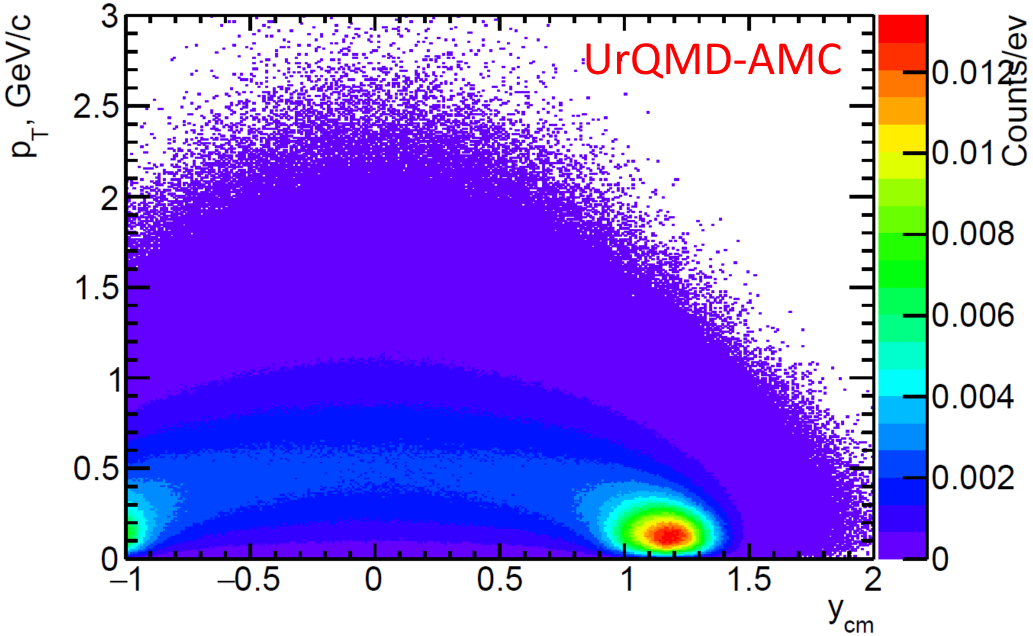


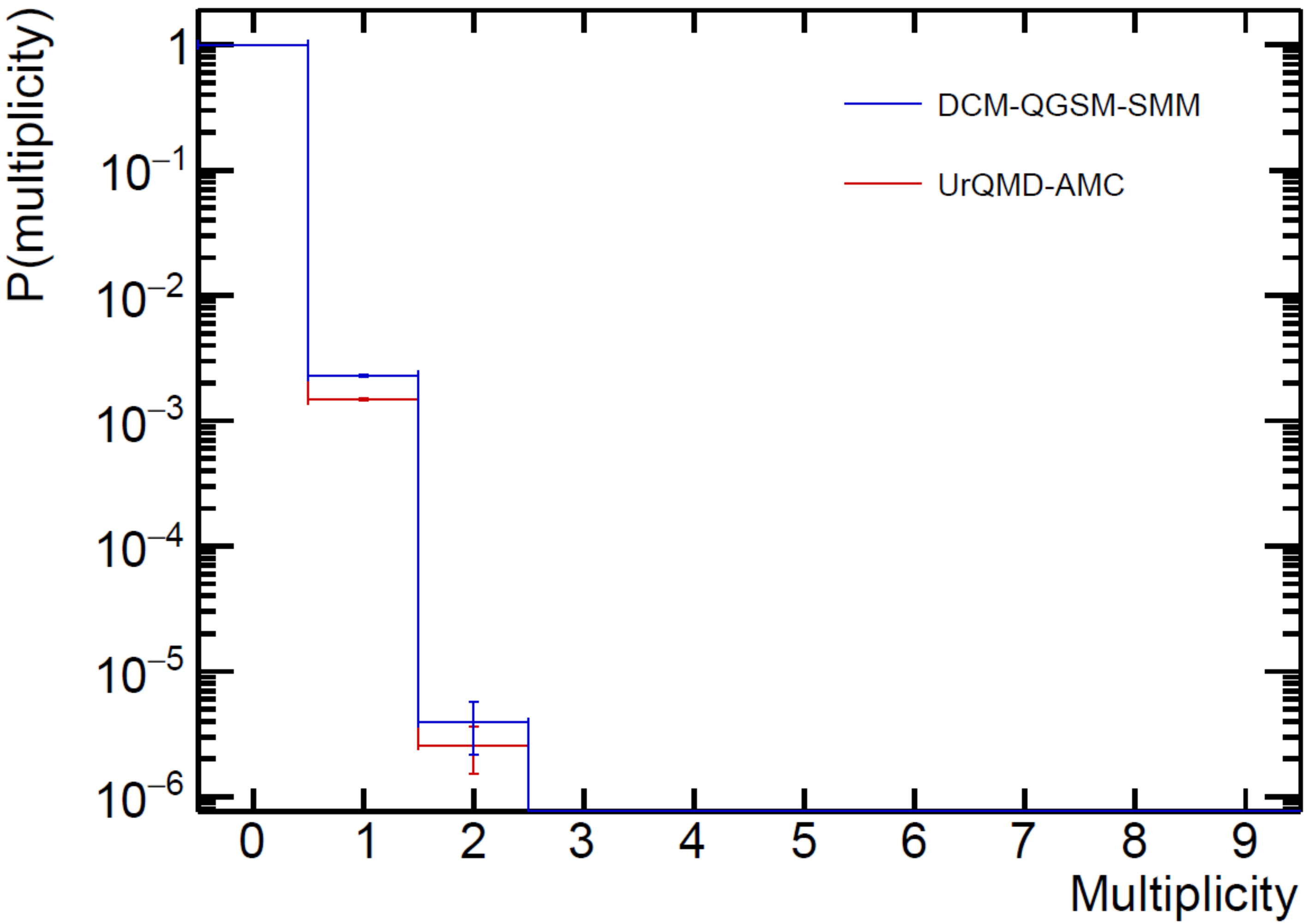

# Neutron yields at 27°

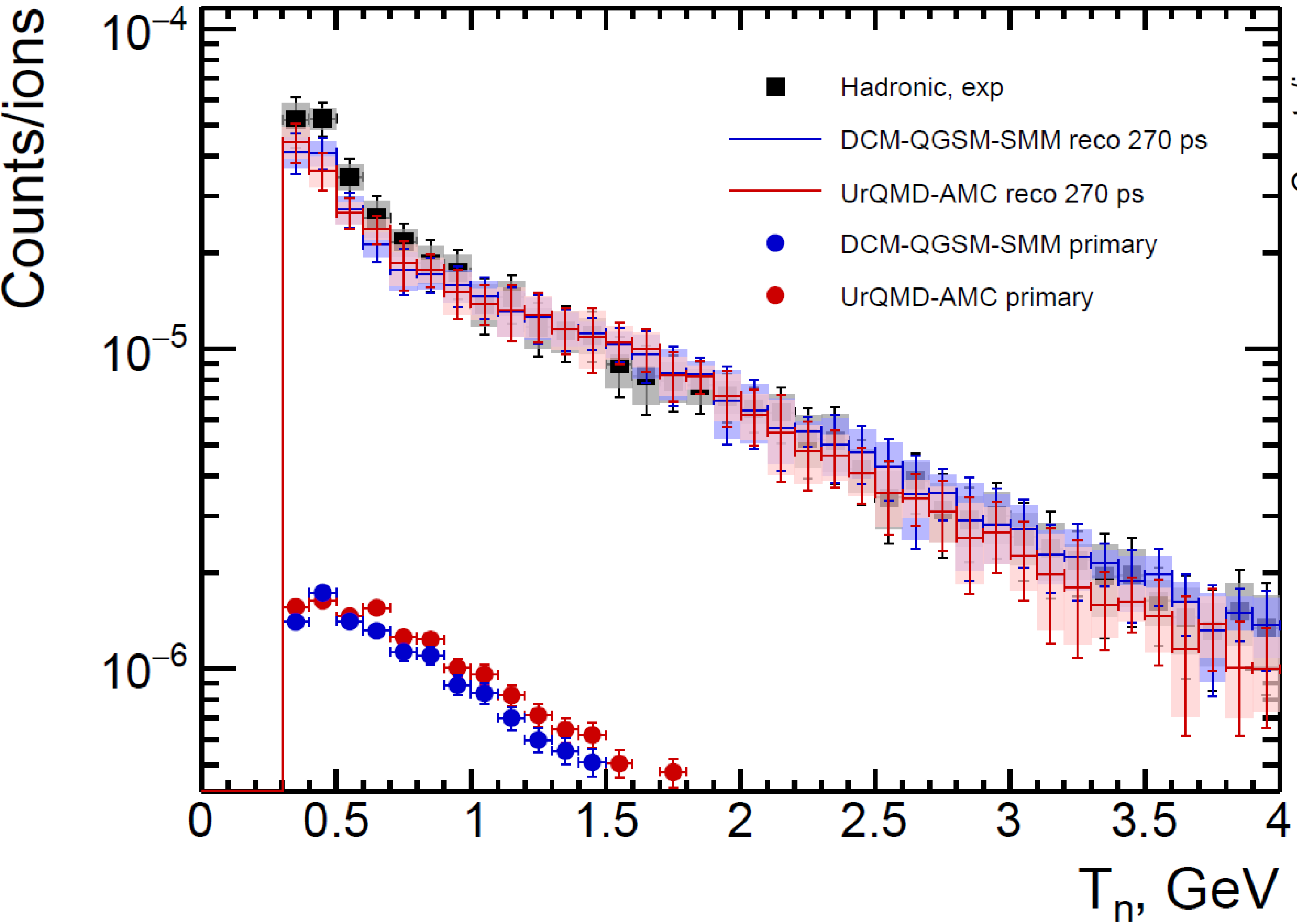


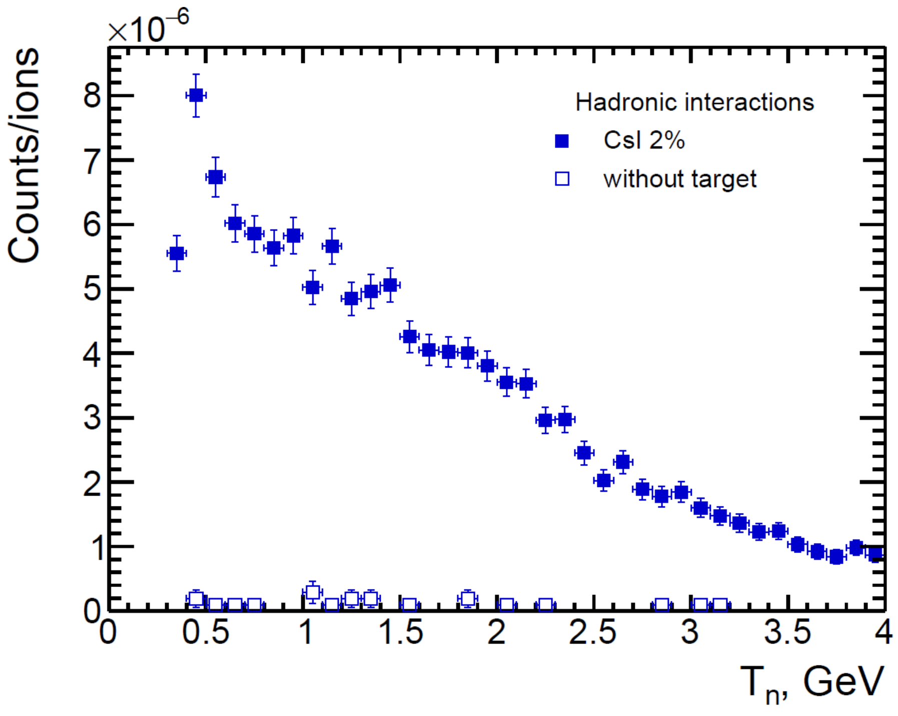

# Backgrounds DCM-QGSM-SMM

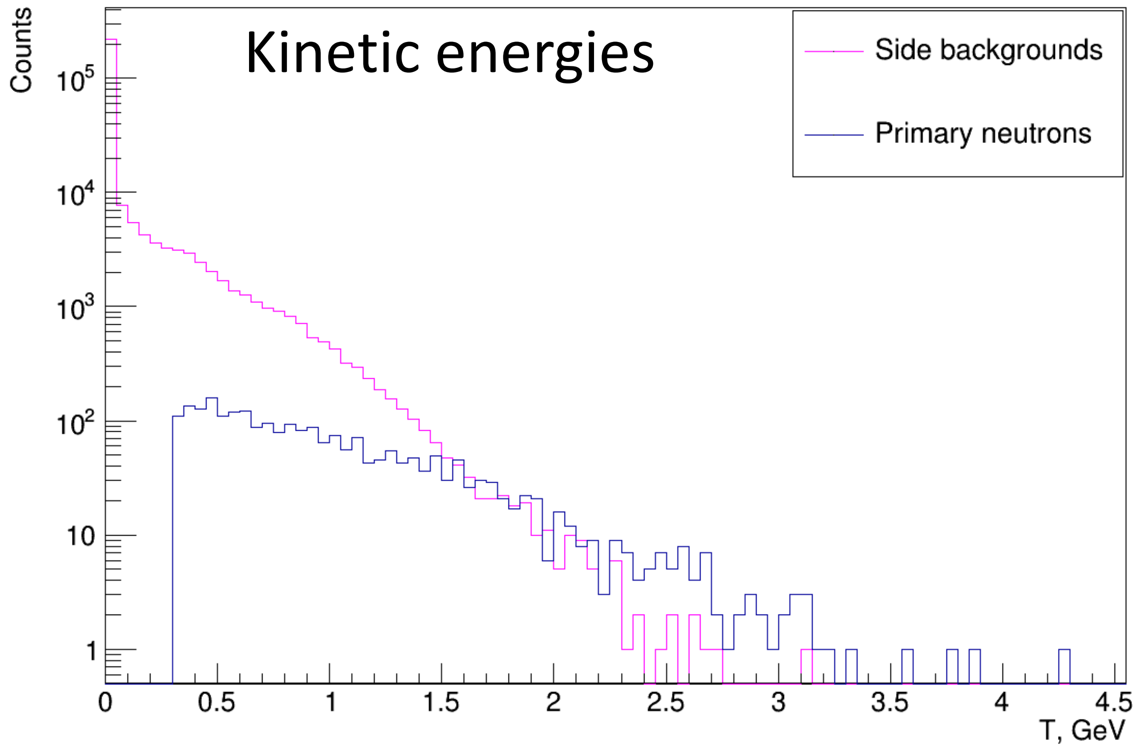


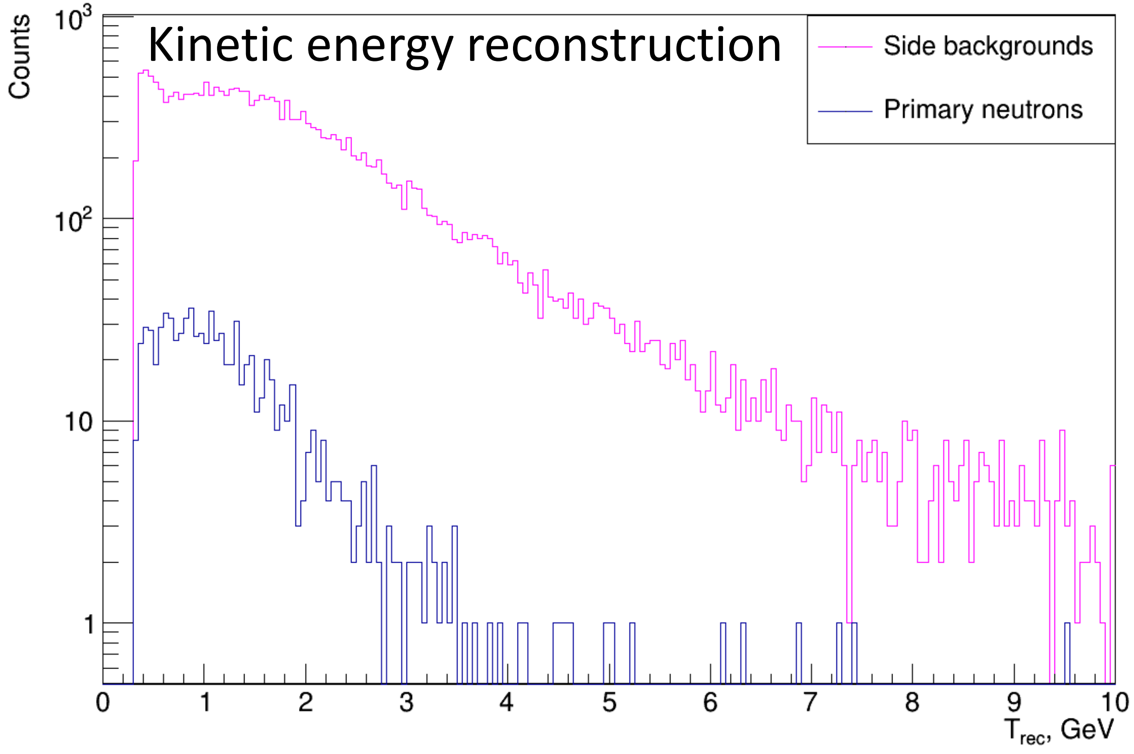


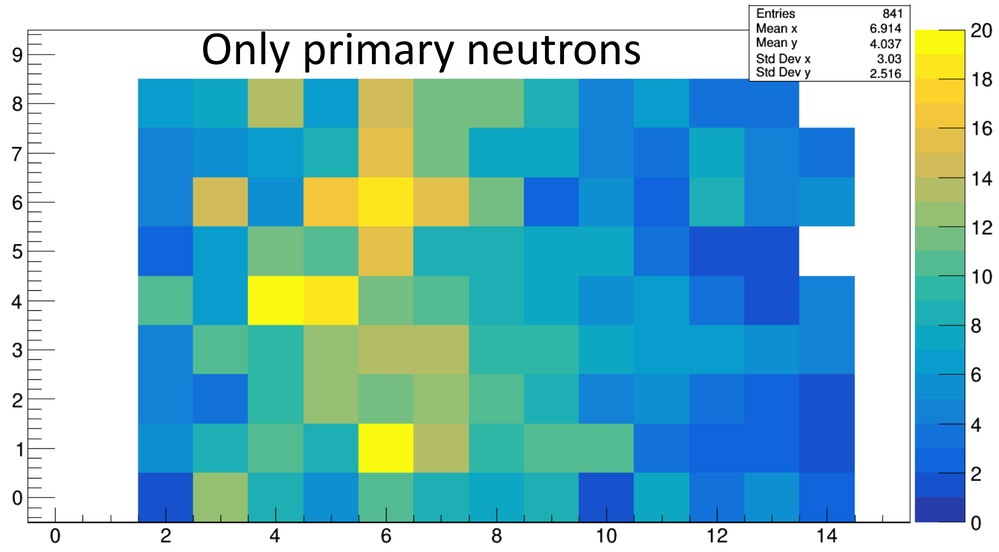


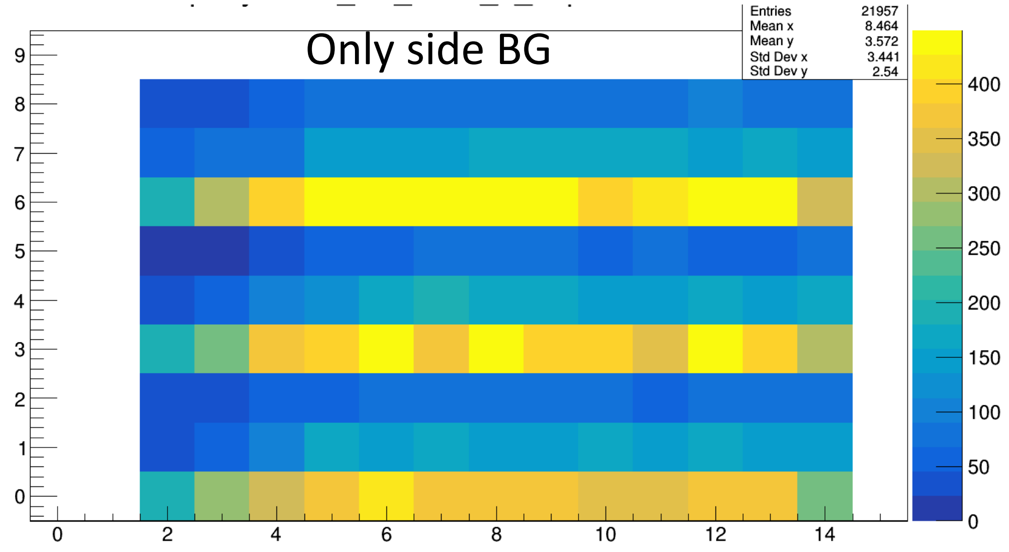


A. Zubankov

# Backgrounds

Experimental data
Kinetic energy reconstruction

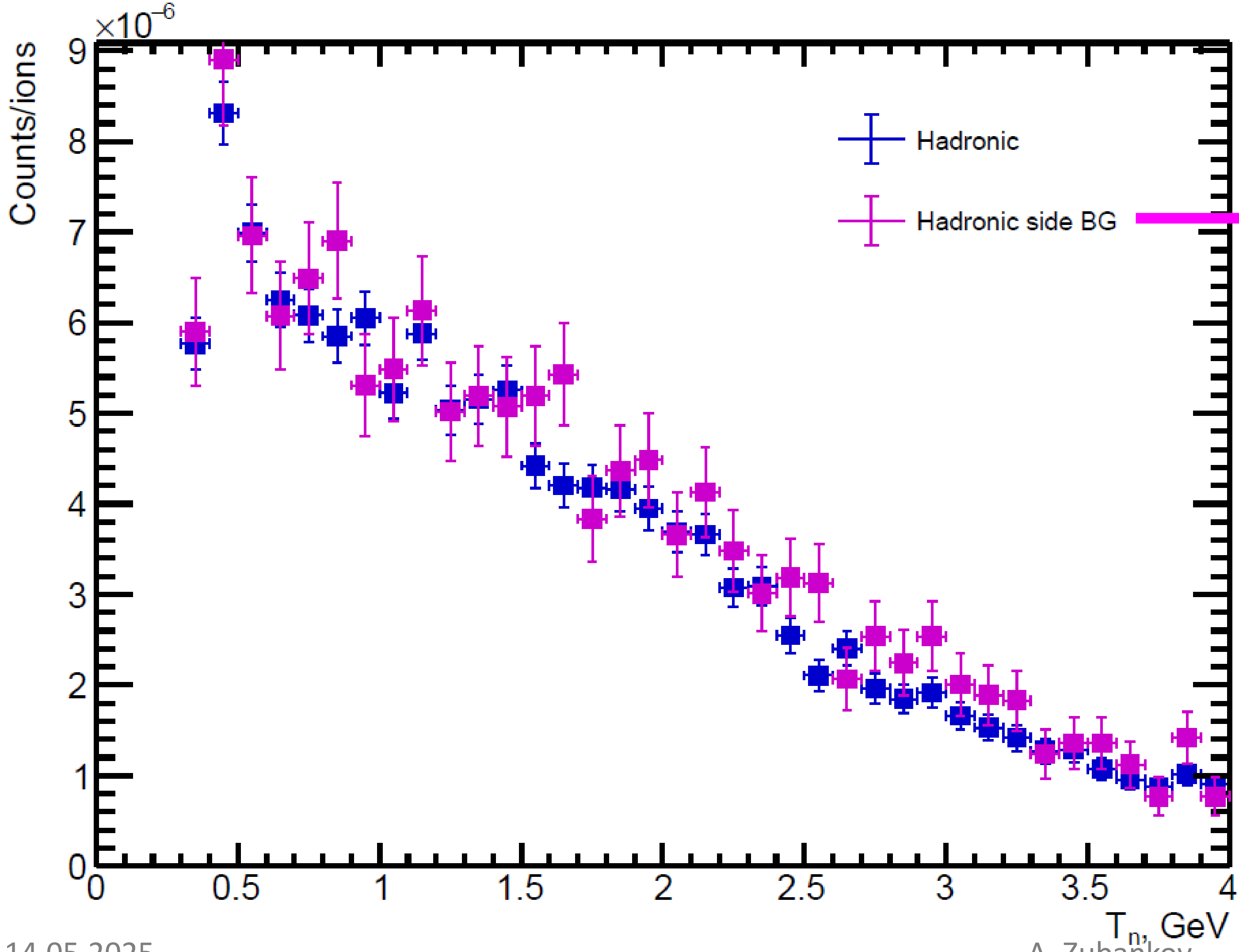


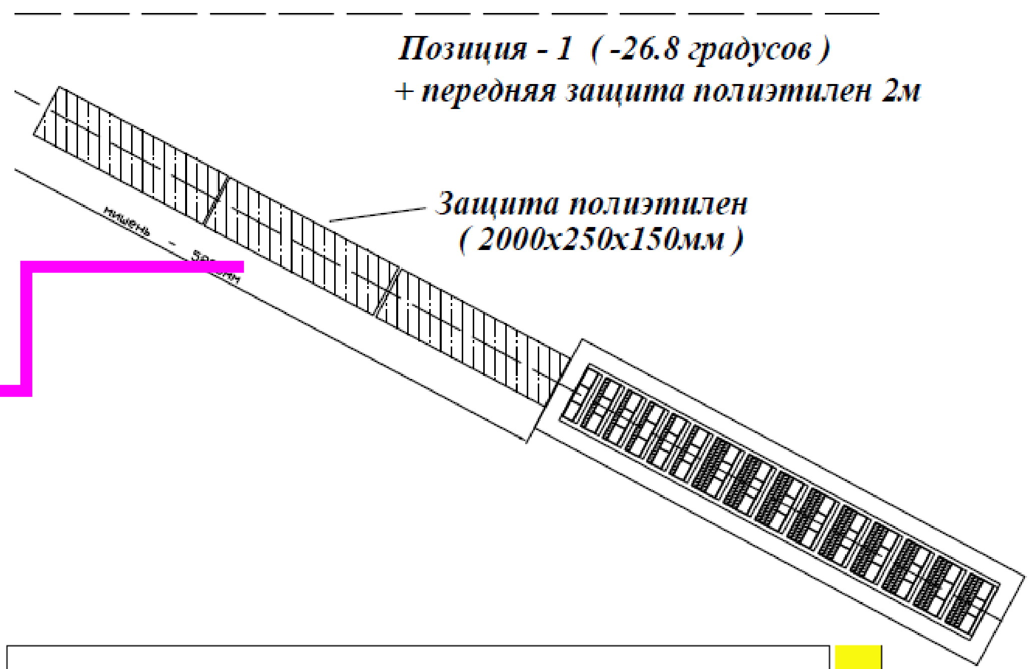


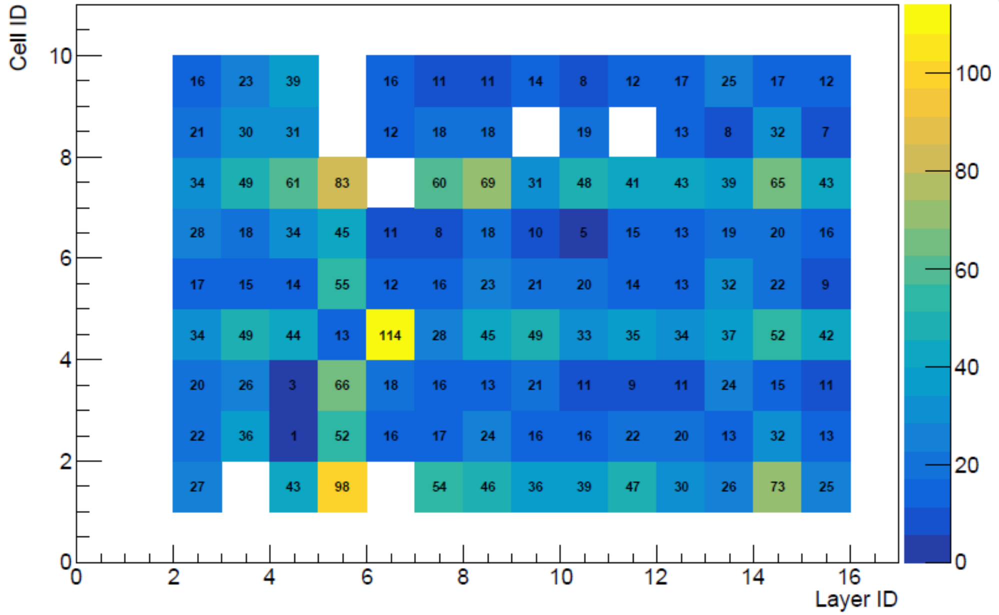

# Conclusions

- The acceptance and efficiency of the HGND prototype in detecting projectile spectator neutrons from hadronic interactions were studied using UrQMD-AMC and DCM-QGSM-SMM models to generate primary collisions.
- The models were validated with GSI data on neutron production in 600A MeV $^{124}$Sn + $^{124}$Sn reaction.
- Also, efficiency and acceptance have been investigated for neutrons from EMD using the RELDIS model.
- Preliminary estimates of neutron yields at the 0.7° position and cross sections have been made. A detailed study of the systematics will be in the future.
- Measurement of neutron yields by the HGND prototype at 27° position is not possible due to the large number of background-only events (more than a factor of 20).
- See A. Shabanov's report on methods of background control in full-scale HGND.

https://arxiv.org/abs/2503.12624

# Thank you for your attention!

# Backup

# HGND prototype

# Time resolution

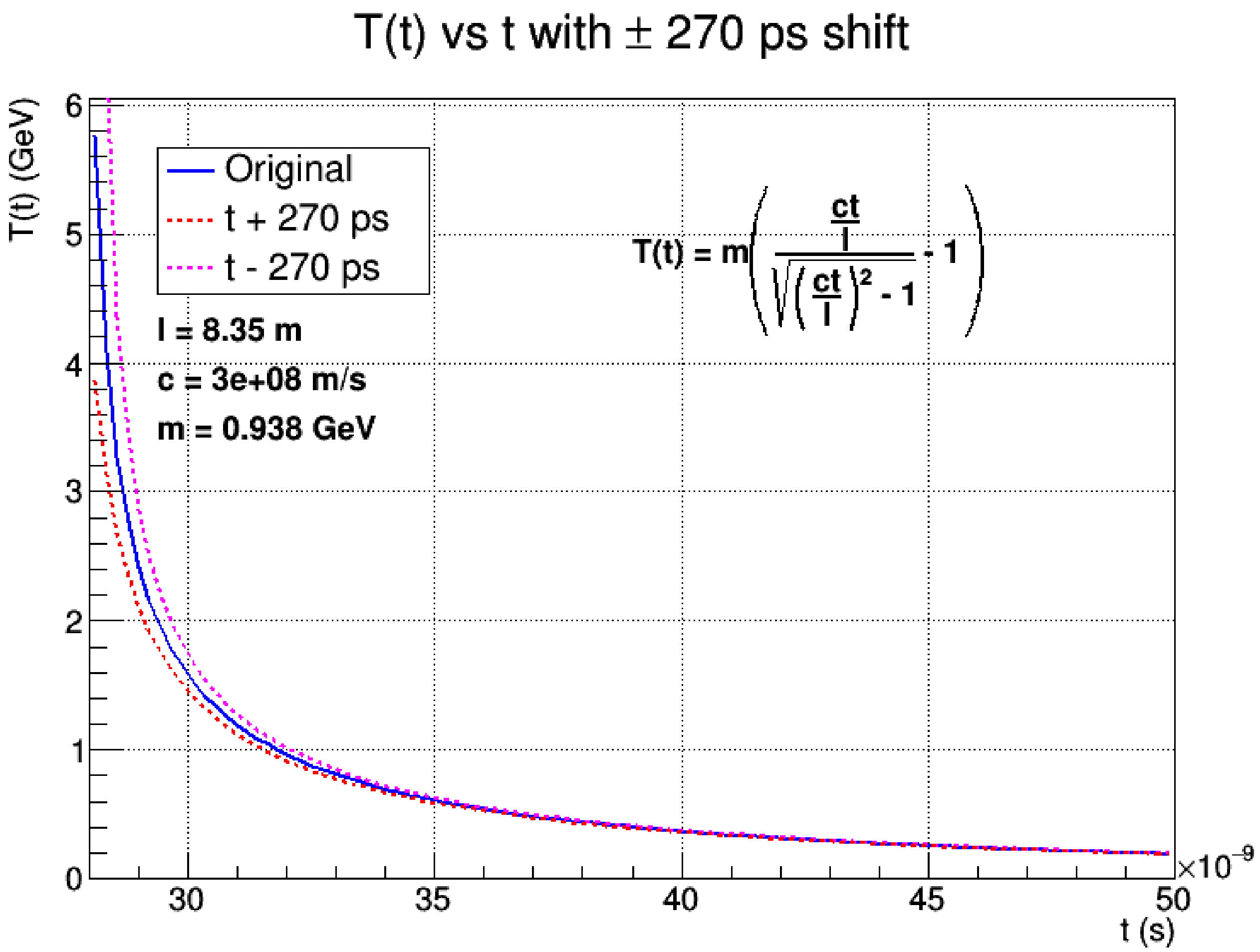


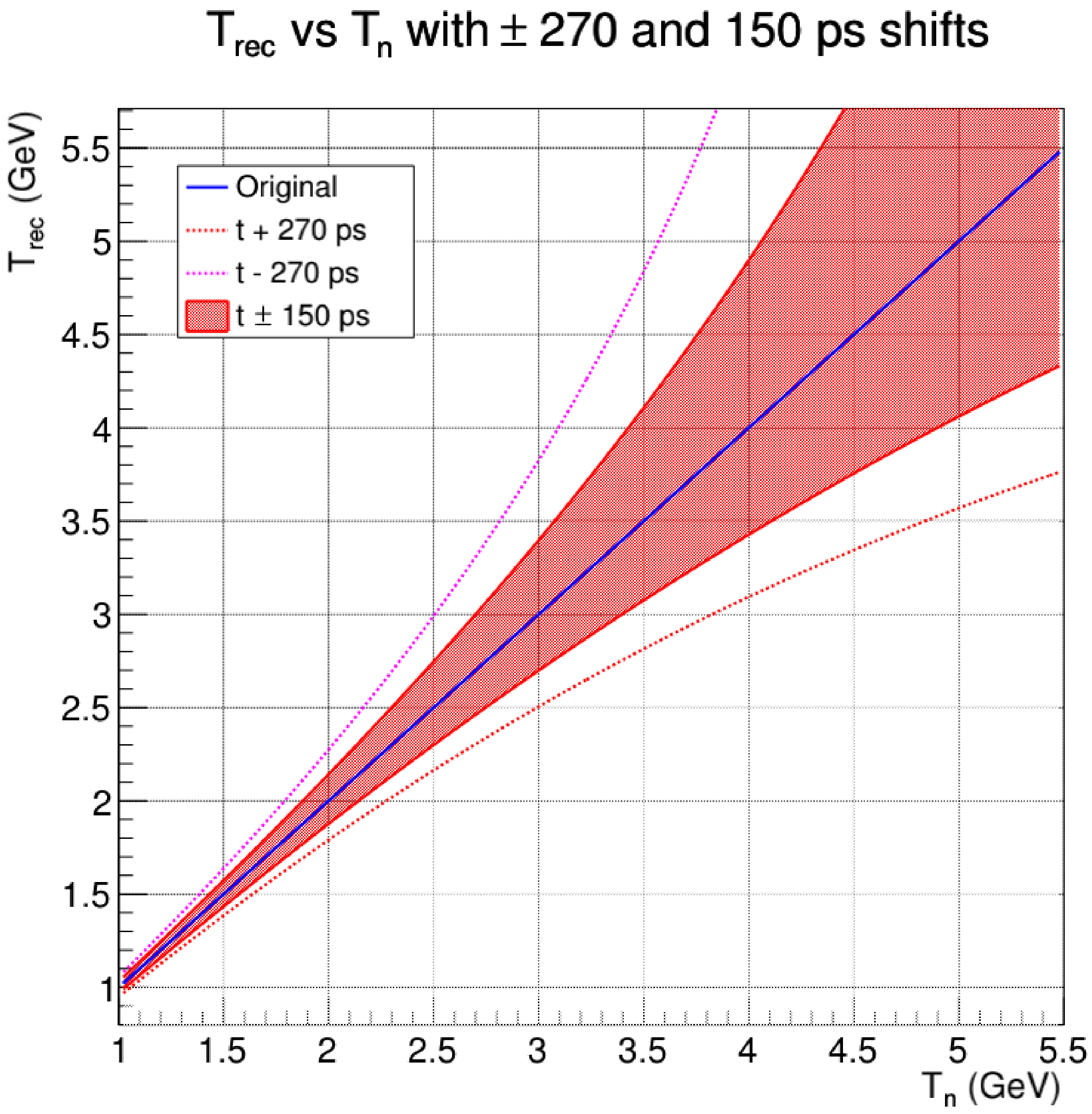

# HGND calibration

**Ideal case**

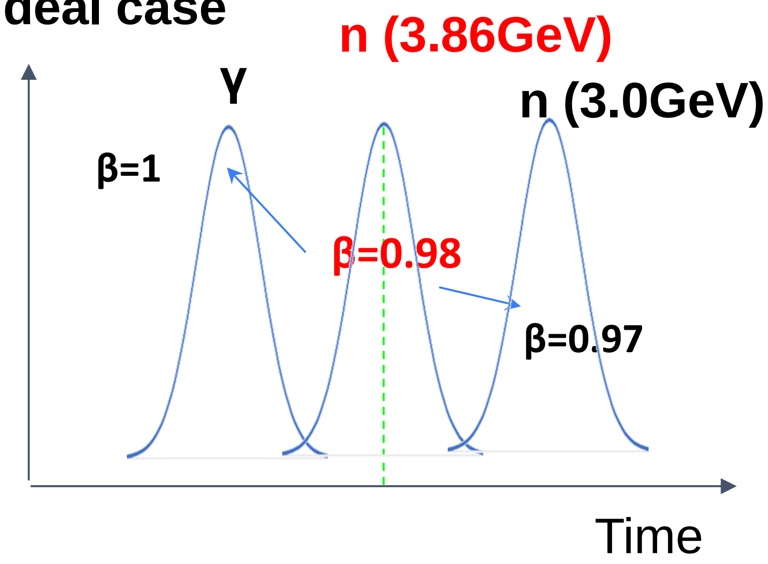


Calibration on neutrons

**Real data**

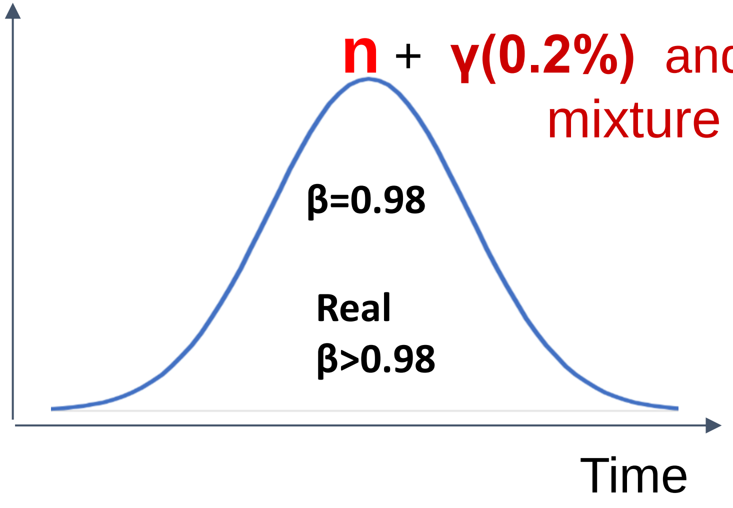


Calibration on neutrons

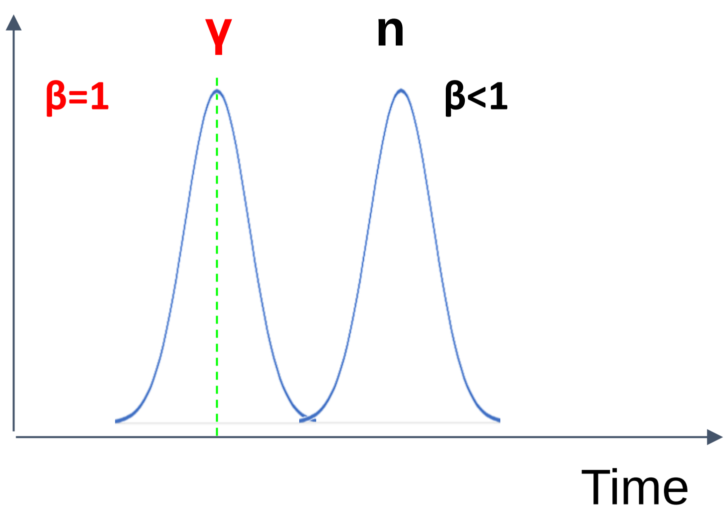


Calibration on photons

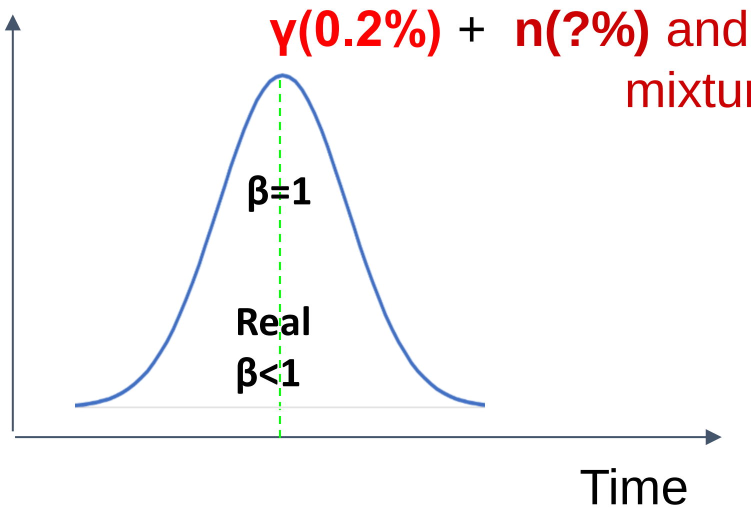


Calibration on photons is possible up to 8 layer

# HGND calibration

## 1. Amplitude normalization

$$Ampl = Ampl \cdot \frac{1}{MPV}$$

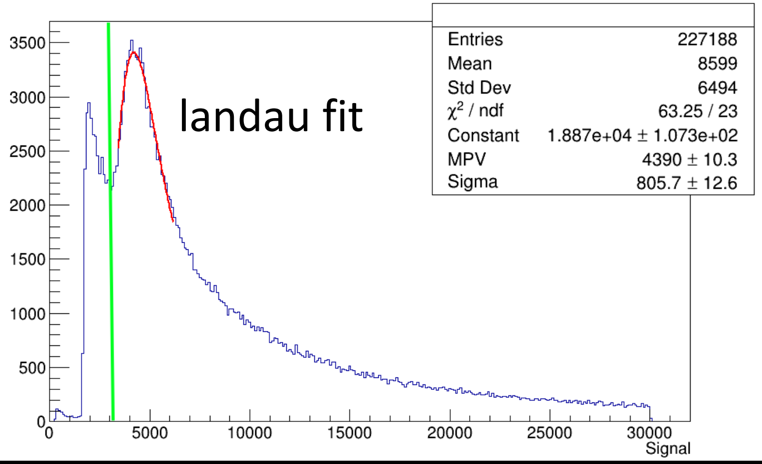


## 2. Time shift for all channels by the average fit value

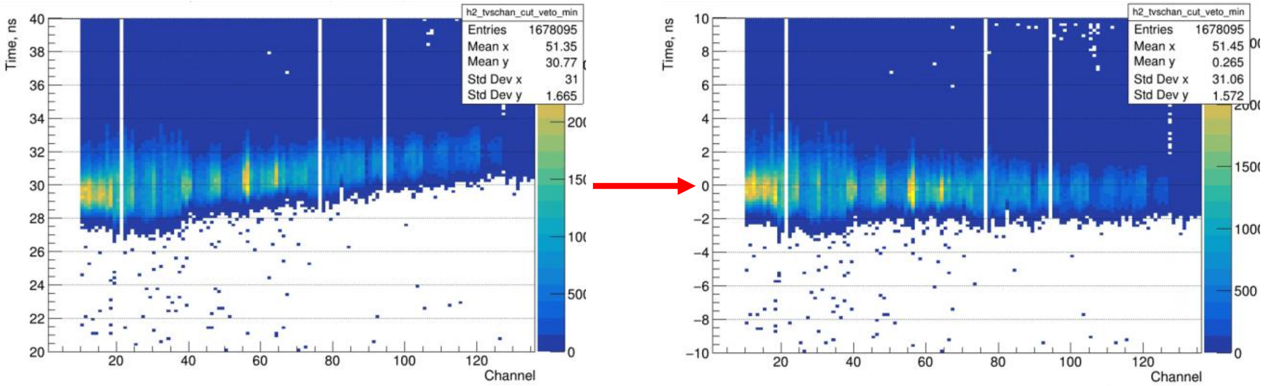


## 3. Determination of parameters of the approximating function for all channels & time limit

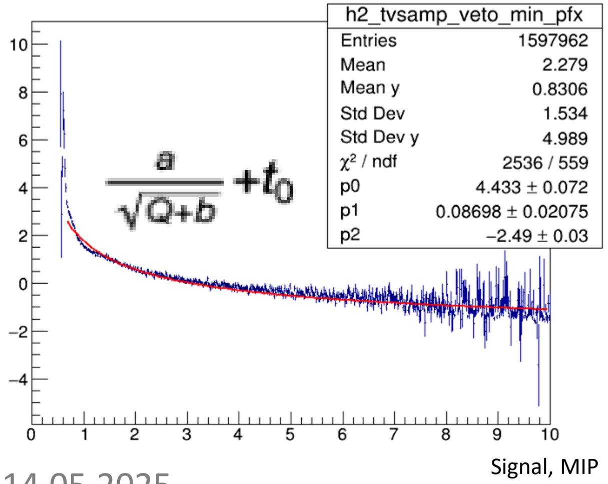


## 4. Time-amplitude correction

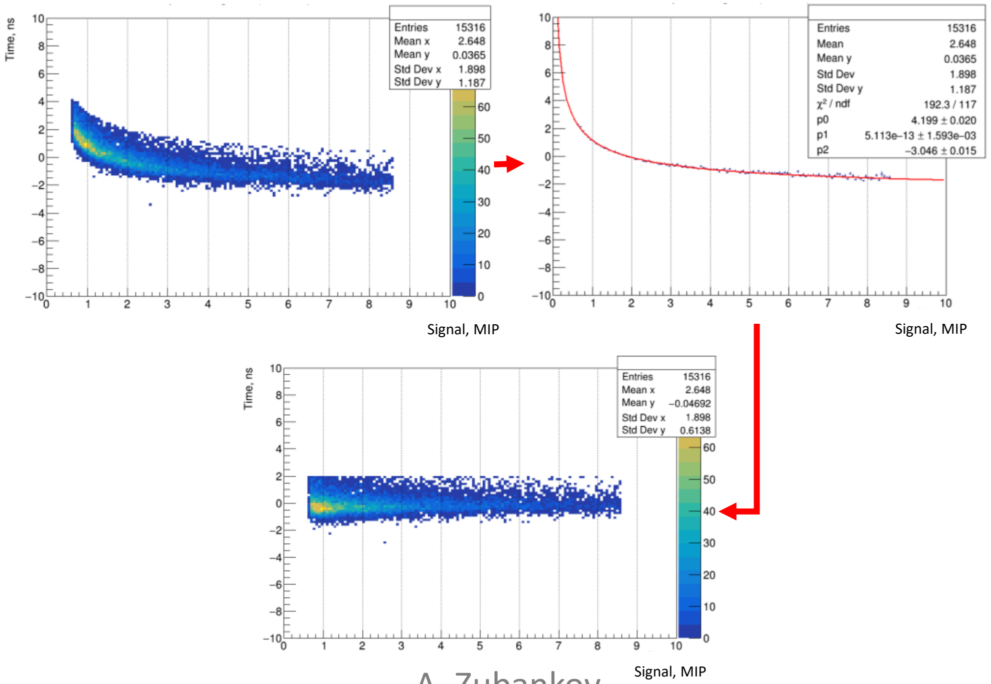


## 5. Time shift

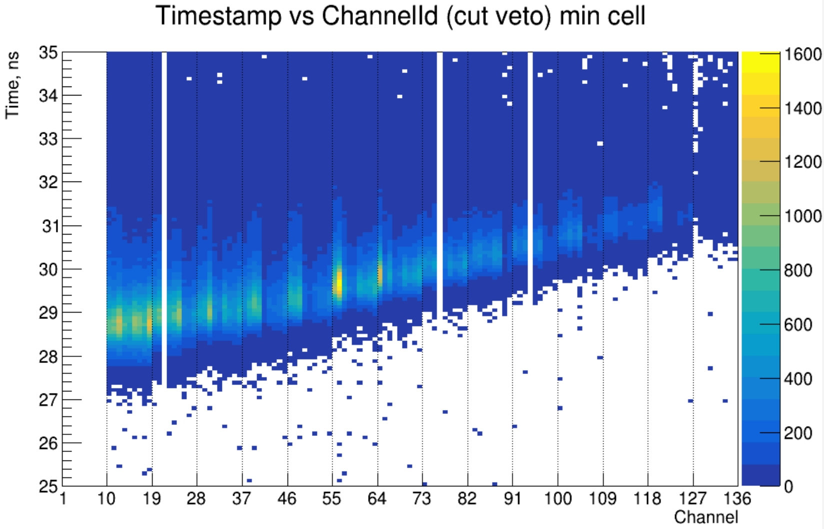

# HGND calibration

Time-amplitude correction of signals made it possible to get rid of the dependence of time on signal amplitude, which improved the time resolution by ~2.4 times.

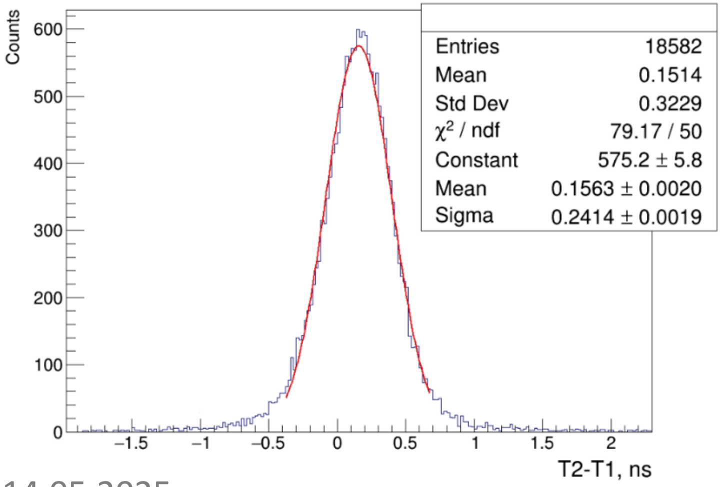


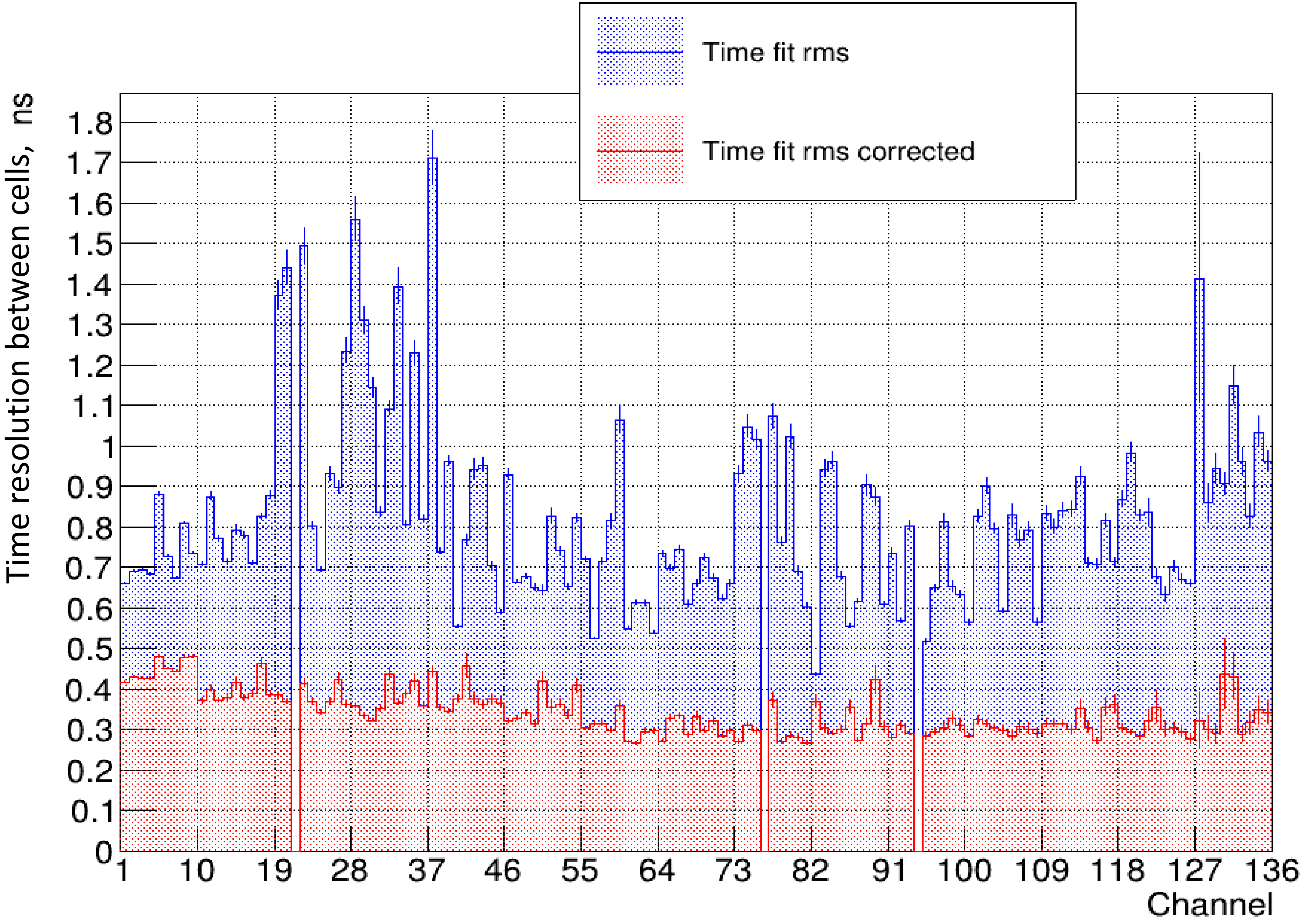

# Fastest cells for EMD vs hadronic interactions

Comparison of hadronic interactions (CCT2) with electromagnetic dissociation (BT)

**Run 8281 (BT) vs 8300 (CCT2)** 3.8 AGeV

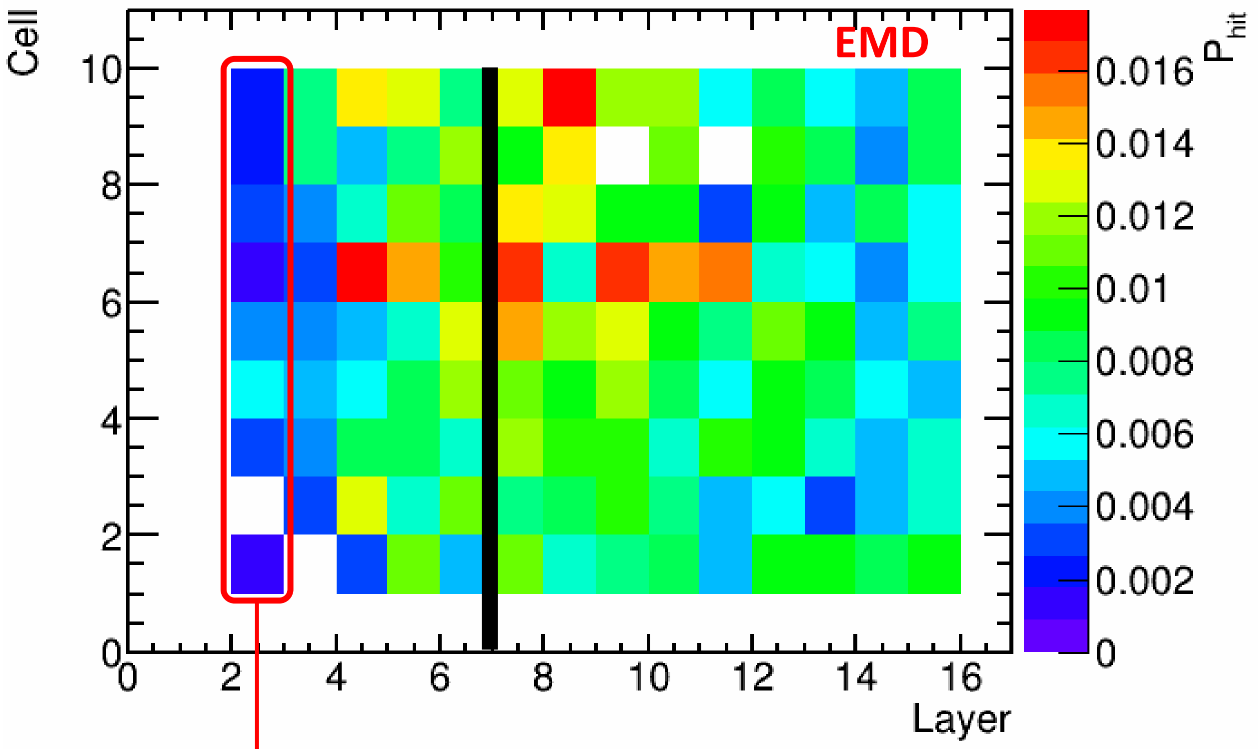


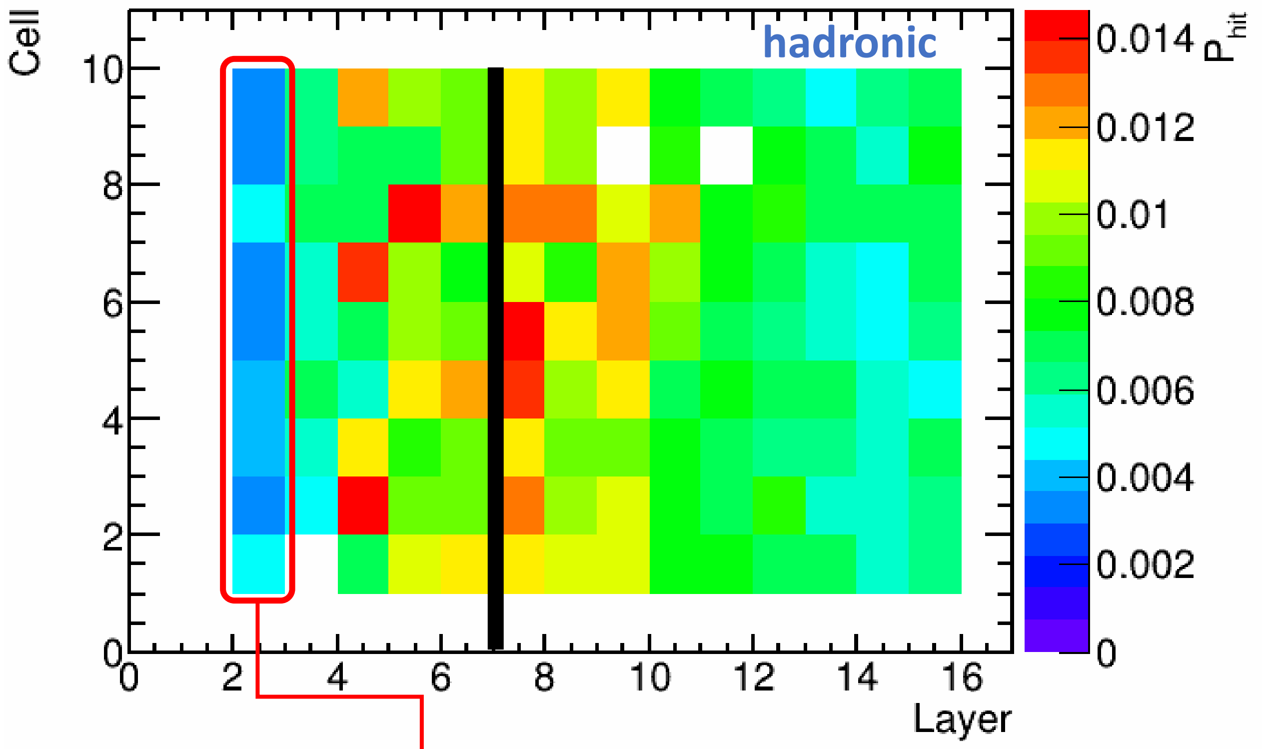


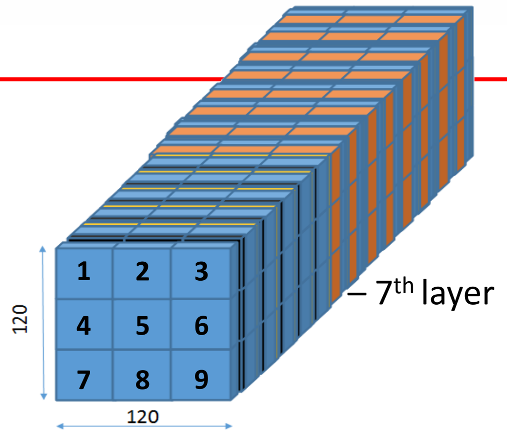


γ-quanta cut – no hits in 1-2 layers in module => 1.55 $X_0$ or 0.11 $\lambda_{int}$

Most of the neutrons are deposited after the 7th layer for both EMD and nuclear interaction

# Neutron yields at 27°

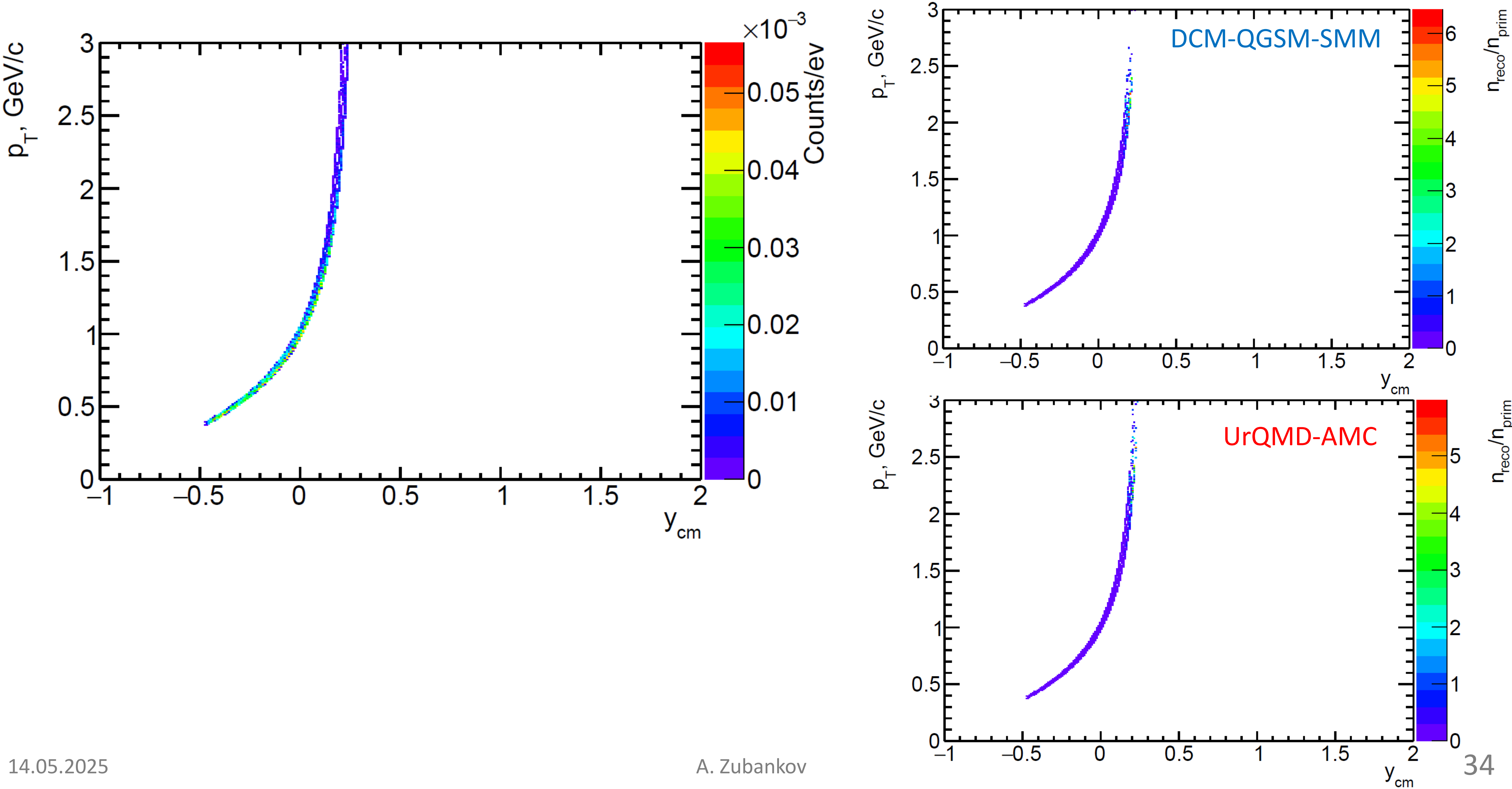

# Trigger efficiency

# Trigger efficiency by V. Plotnikov

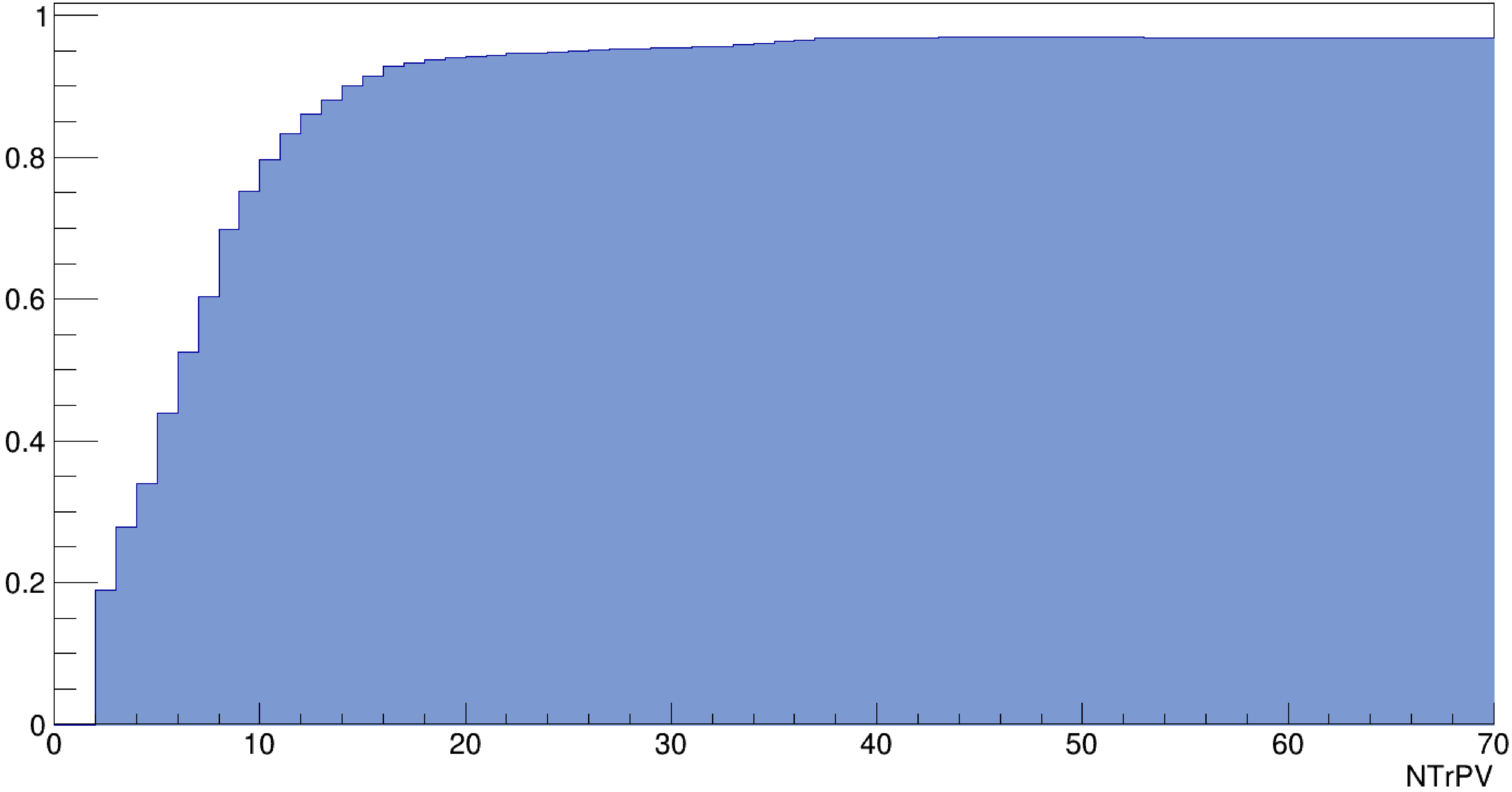

# Trigger efficiency by D. Idrisov

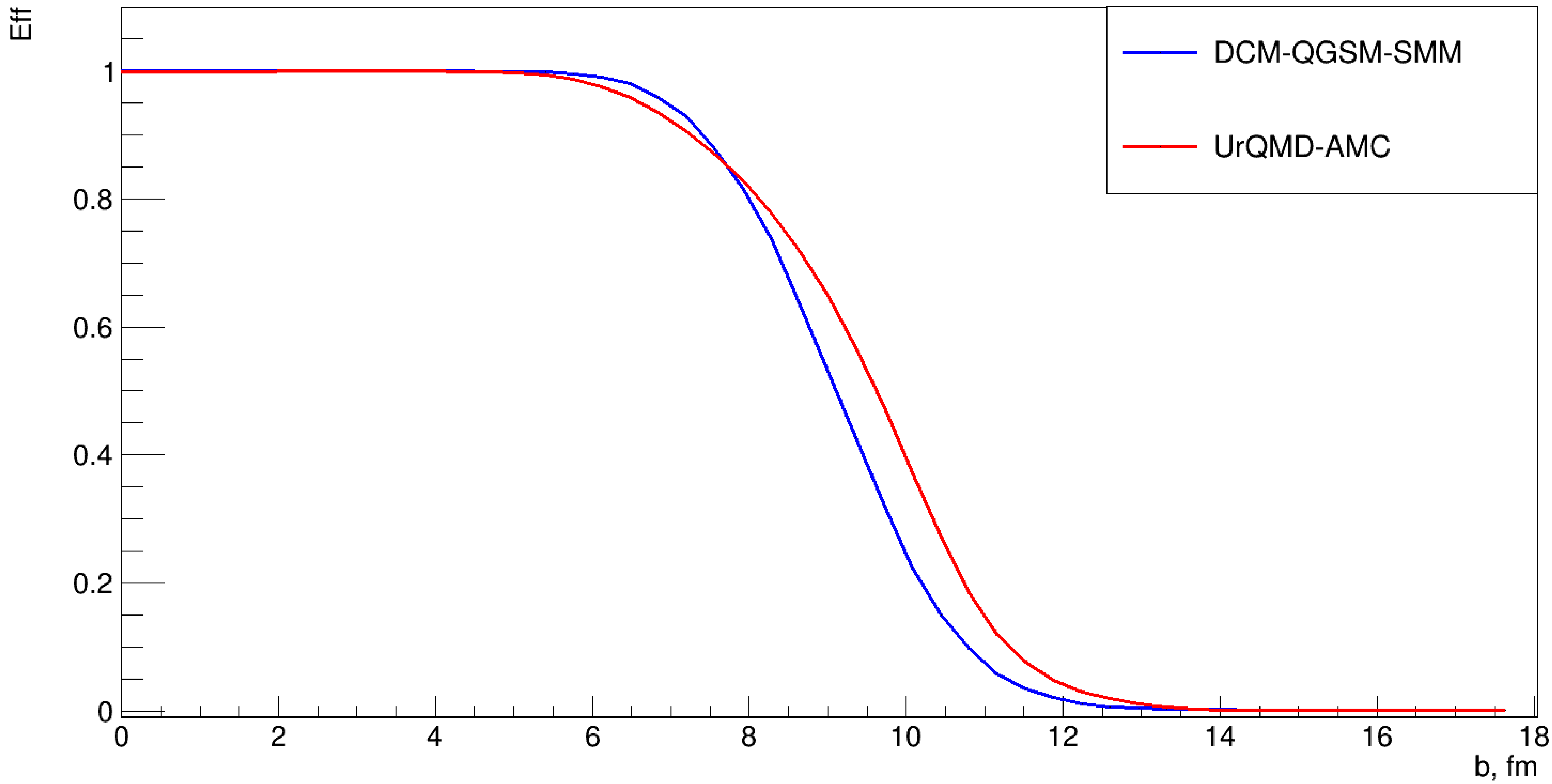

# Impact parameter distribution

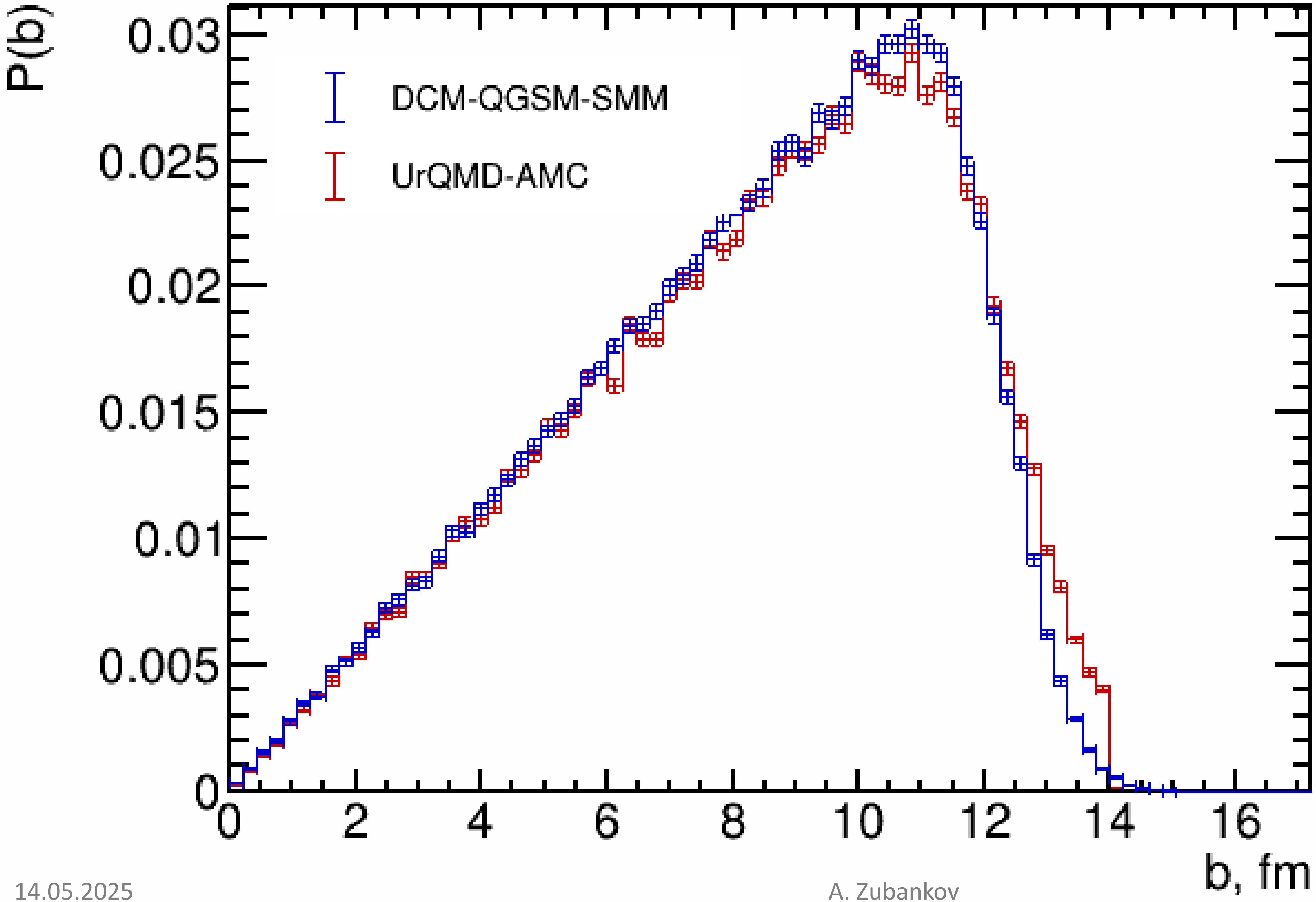

# Spectator neutrons on the surface of the HGND prototype

with trigger efficiency correction

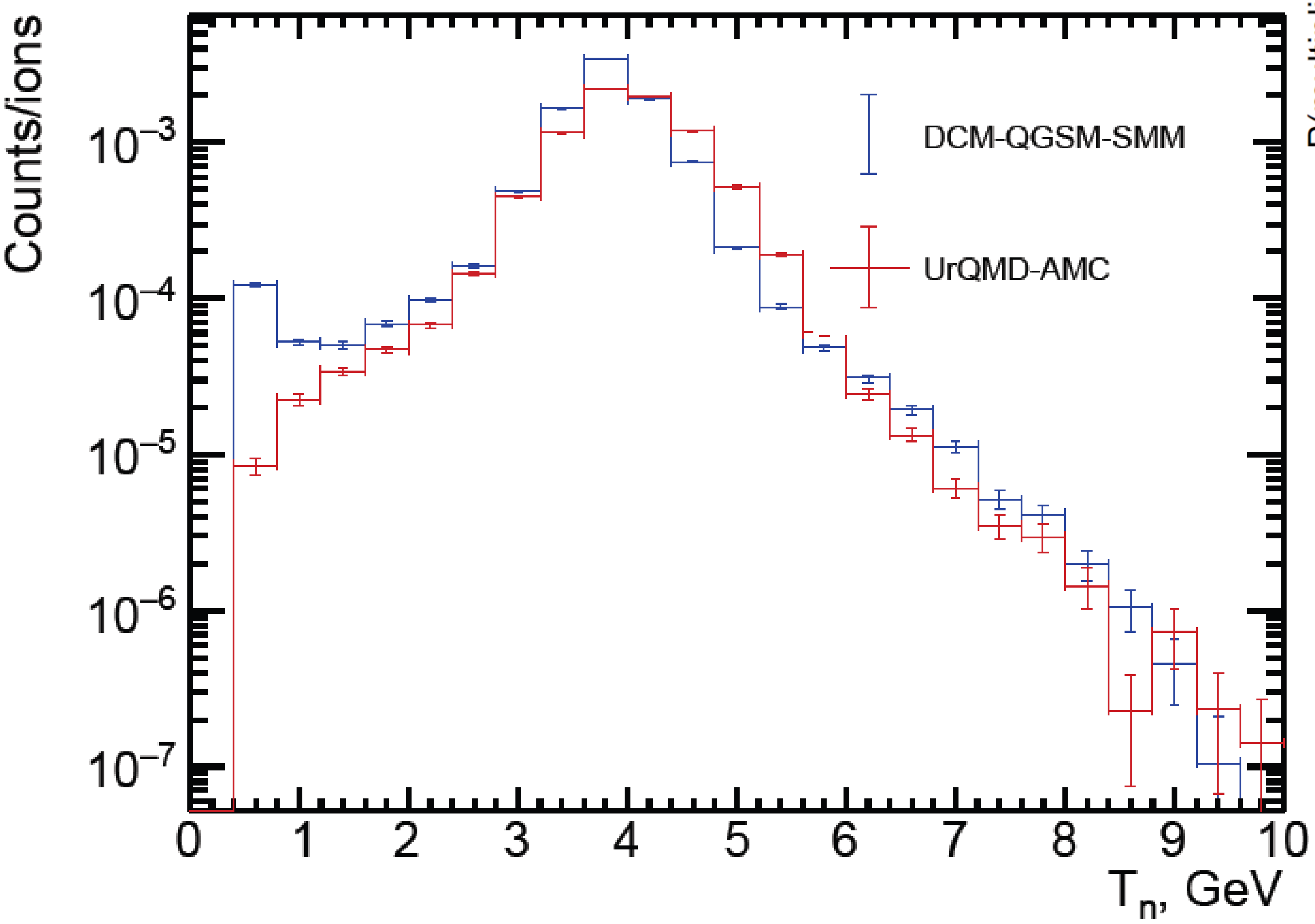


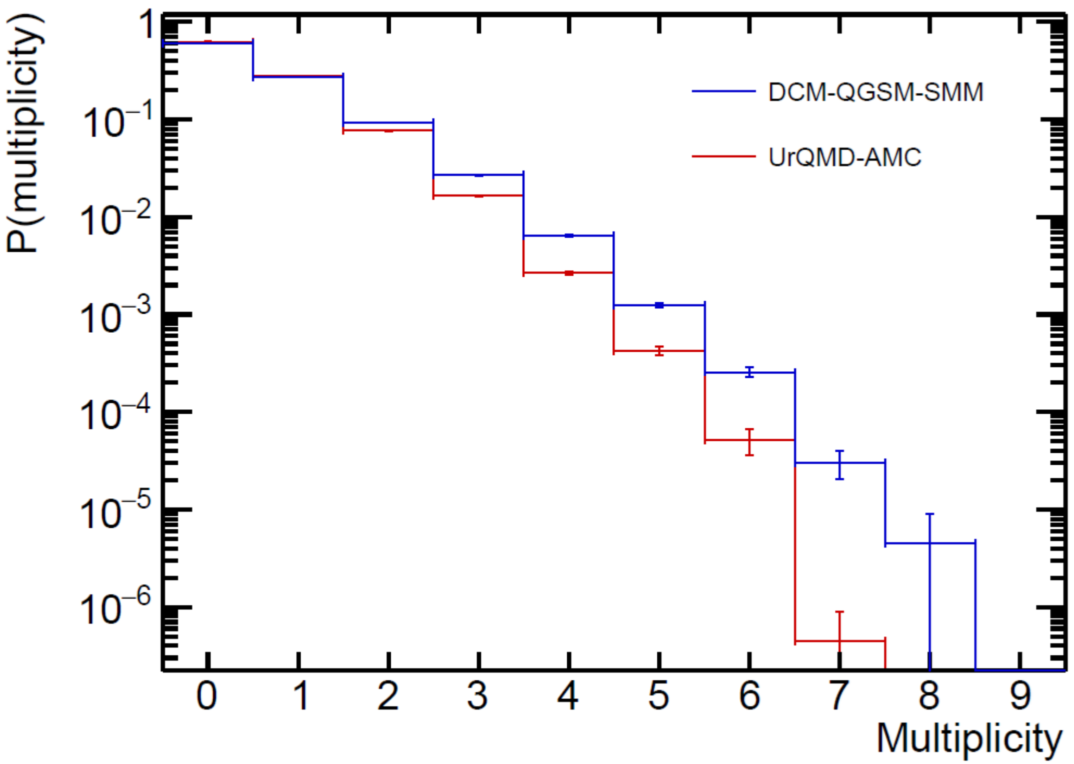


Neutron multiplicity on the surface of the HGND prototype
– **1.32** for **UrQMD-AMC**
– **1.43** for **DCM-QGSM-SMM**

# Backgrounds & time resolution

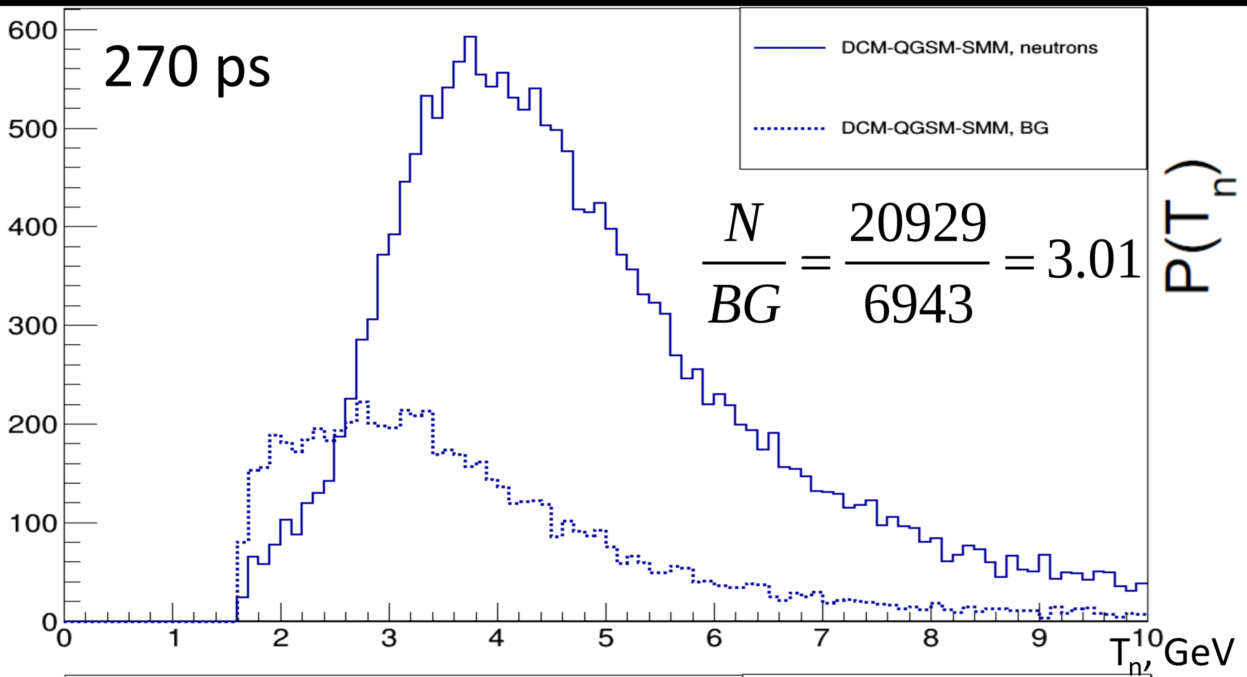


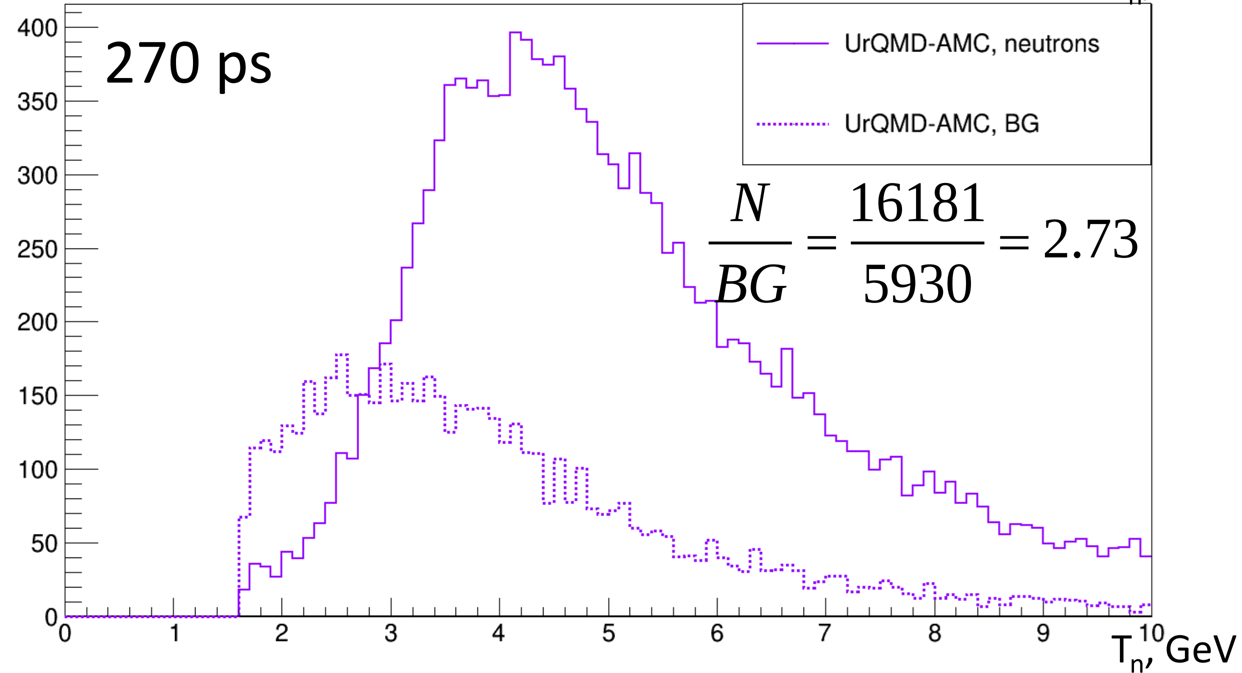


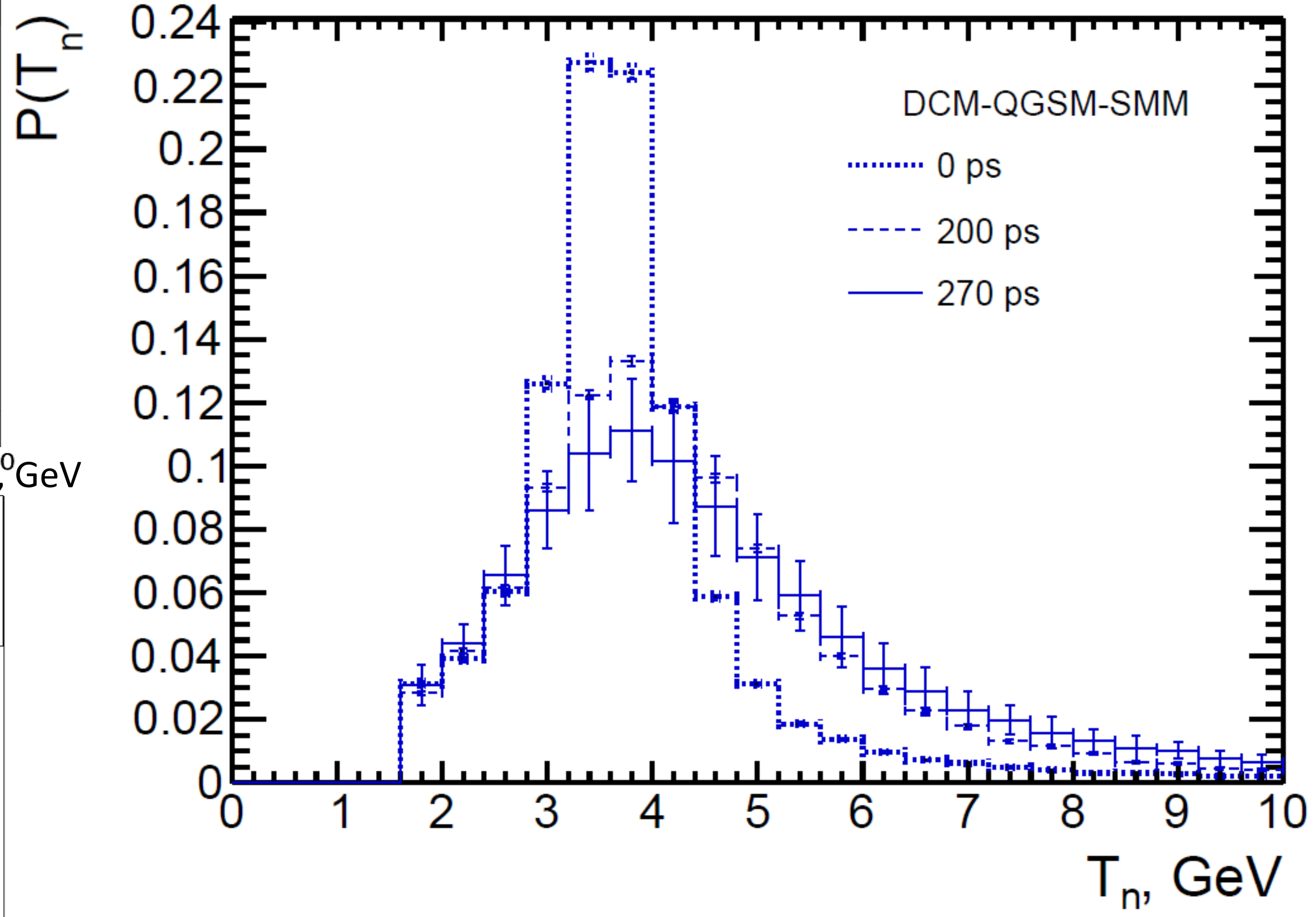

# Reconstructed neutron energy spectra for hadronic interactions

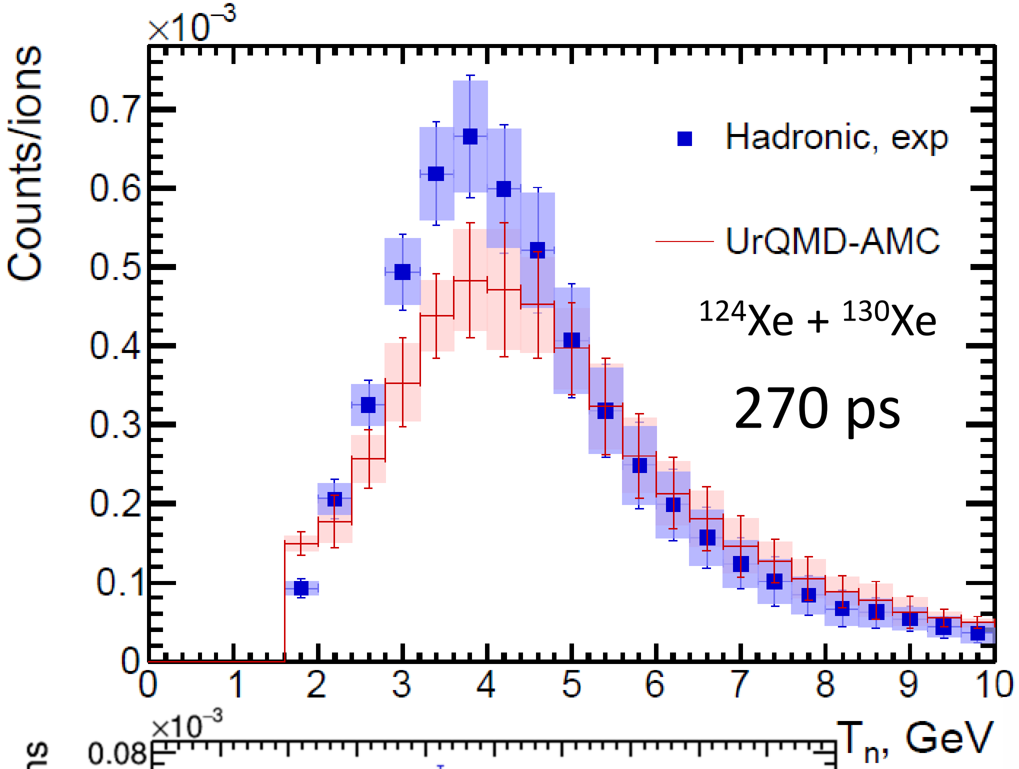


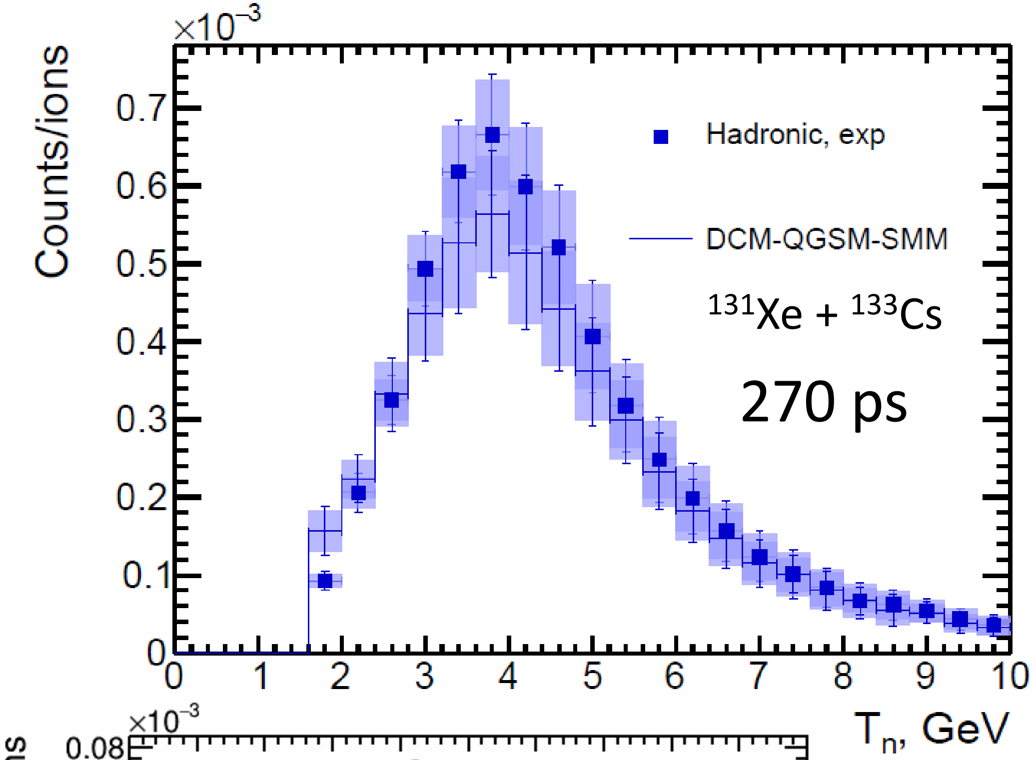


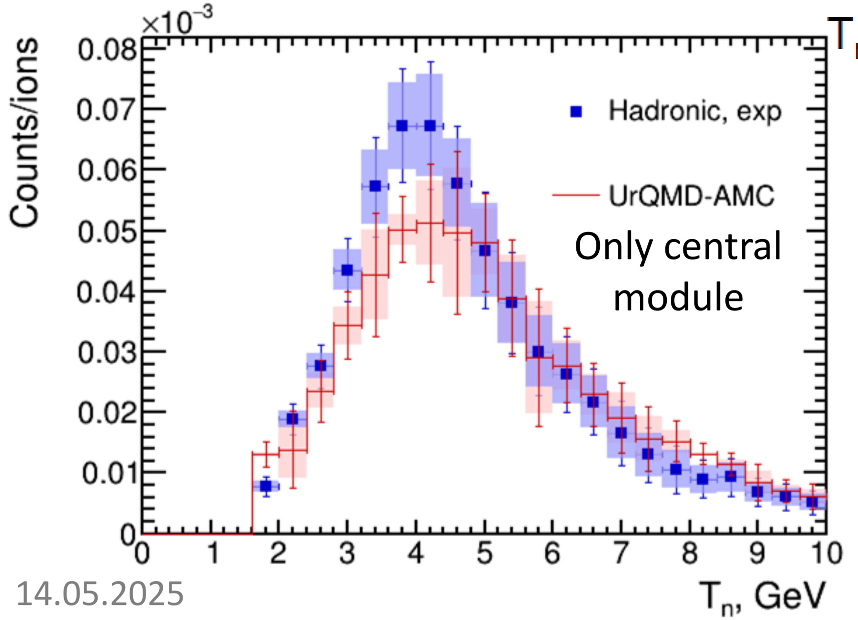


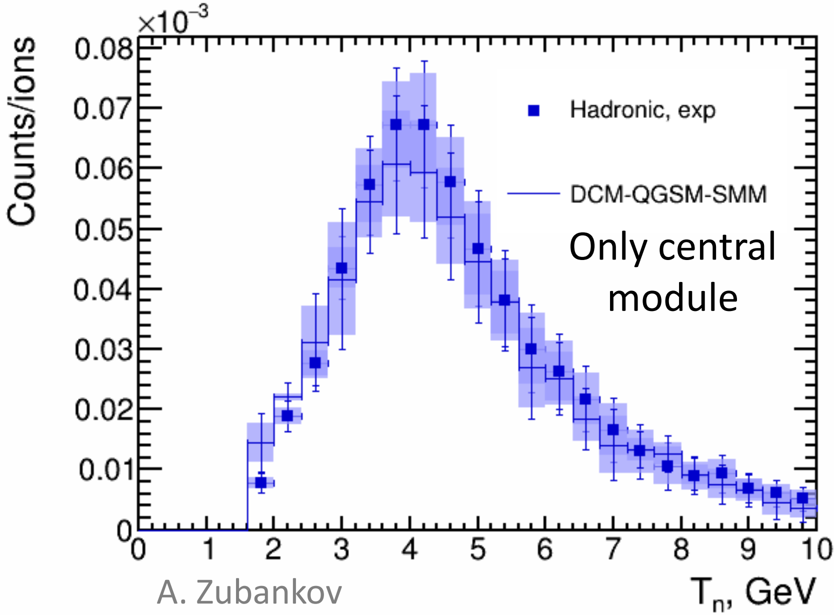


The difference in the shape and peak position of the reconstructed spectra of the models is noticeable, which is also due to the difference in the mean kinetic energy of neutrons and their multiplicity.

# HGND prototype efficiencies for hadronic interactions

$$acc = \frac{N_{hit}}{N_{gen}} \qquad \varepsilon = \frac{N_{rec}}{N_{hit}}$$

| Model | *acc*, % | *ε*, % | *acc* x *ε*, % |
|---|---|---|---|
| DCM-QGSM-SMM | 3.30 ± 0.02 | 39.36 ± 0.21 | 1.30 ± 0.01 |
| UrQMD-AMC | 2.57 ± 0.02 | 45.45 ± 0.28 | 1.17 ± 0.01 |
| DCM-QGSM-SMM (1 mod.) | 0.62 ± 0.01 | 24.02 ± 0.38 | 0.150 ± 0.002 |
| UrQMD-AMC (1 mod.) | 0.40 ± 0.01 | 33.11 ± 0.61 | 0.132 ± 0.002 |

The difference in ***acc*** and ***ε*** is explained by the differences in angular distribution of primary neutrons (17.70 vs 16.01) and in average multiplicity of neutrons hitting the detector (1.32 vs 1.43).

# Cross-section estimation

$$\sigma = \frac{N_{ev}}{N_{ions}} \cdot (acc \times \varepsilon) \cdot \langle N \rangle \cdot \frac{A}{d \cdot N_A \cdot \rho}$$

$d = 0.175\, cm$

$N_A = 6.02 \cdot 10^{23}\, mol^{-1}$

$\rho = 4.53\, g/cm^3$

| | RELDIS | DCM-QGSM-SMM | UrQMD-AMC |
|---|---|---|---|
| $N_{ev}/N_{ions}$ | (1.51±0.14)·10$^{-3}$ | (3.87±0.02)·10$^{-3}$ | |
| $N_{ev}/N_{ions} \cdot (acc \times \varepsilon) \cdot \langle N \rangle$ | (7.21±0.72)·10$^{-3}$ | (18.63±0.19)·10$^{-3}$ | (18.77±0.21)·10$^{-3}$ |
| $\sigma^{\exp}$ | 1.96±0.20 b | 5.07±0.05 b | 5.11±0.06 b |
| $\sigma^{sim}$ | 1.89±0.02 b | 4.76±0.01 b | 4.89±0.01 b |

A detailed study of the systematics will be in the future.

$\sigma^{Glauber} = 5.28\, b$

# Cross-section estimation

$$\begin{cases} P(d) = \dfrac{N_{ev}}{N_{ions}} \cdot (acc \times \varepsilon) \cdot \langle N \rangle \\ P(d) = 1 - \exp\left(-d/\lambda\right) \end{cases}$$

$d = 0.175\,cm$

$N_A = 6.02 \cdot 10^{23}\,mol^{-1}$

$\rho = 4.53\,g/cm^3$

$d \ll \lambda:$

$$P(d) = \frac{d}{\lambda} = \frac{d \cdot N_A \cdot \rho \cdot \sigma}{A}$$

$$\sigma = \frac{N_{ev}}{N_{ions}} \cdot (acc \times \varepsilon) \cdot \langle N \rangle \cdot \frac{A}{d \cdot N_A \cdot \rho}$$

# UrQMD-AMC

# Ablation Monte Carlo: decay code from AAMCC

- The excited nuclear fragments are formed by means of MST-clusterization algorithm after UrQMD
  - A few excited nuclear prefragments can be formed, in contrast with DCM-QGSM-SMM, where all the spectator nucleon remain bound in one prefragment.
- Excitation energy of prefragment is calculated by hybrid approximation: a combination of Ericson formula for peripheral collisions and ALADIN approximation otherwise[1)]
- Decays of prefragments are simulated as follows:
  - Fermi break-up model from Geant4 v9.2 [2)]
  - Statistical Multifragmentation Model (SMM) from Geant4 v10.4 [2)]
  - Weisskopf-Ewing evaporation model from Geant4 v10.4 [2)]
- They were validated and adjusted to describe the data[3)].

1) R. Nepeivoda, et al., Particles **5** (2022) 40
2) J. Alison et al. Nucl. Inst. A **835** (2016) 186
3) 55th Geant4 Techical Forum https://indico.cern.ch/event/1106118/contributions/4693132/



github.com/Spectator-matter-group-INR-RAS/AAMCC

# Combining UrQMD and AAMCC

- AMC is developed to simulate secondary decays of spectator fragments created in other models, in particular UrQMD.
- It is assumed that spectator matter is formed out of nucleons that do not undergo any collisions.

**UrQMD:**

- Version 3.4
- Cascade mode in this work
- Offset radius 5 fm
- Evolution time – 100 fm/c
- Other parameters are set to default values

→ **Unigen file**

**AMC:**

- Find spectator nucleons
- Define prefragments via MST-clustering
- Constant *d* = 2.7 fm
- Model prefragments decays
- All the participant data remain intact

→ **Unigen file**

# Knocking out some spectator nucleons by mesons

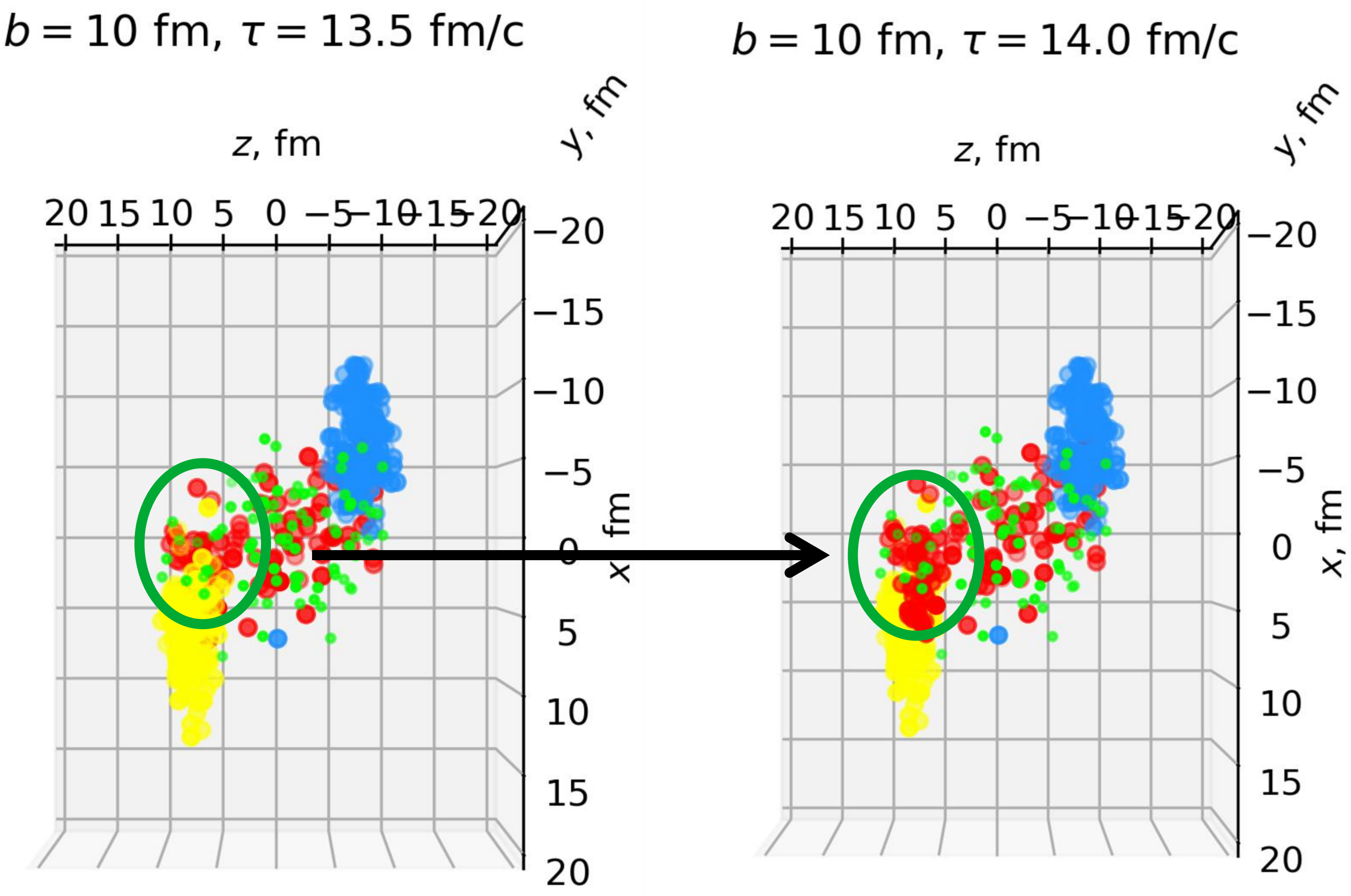


Blue and yellow – spectator nucleons, red – participant nucleons, green – produced mesons

# MST-clustering

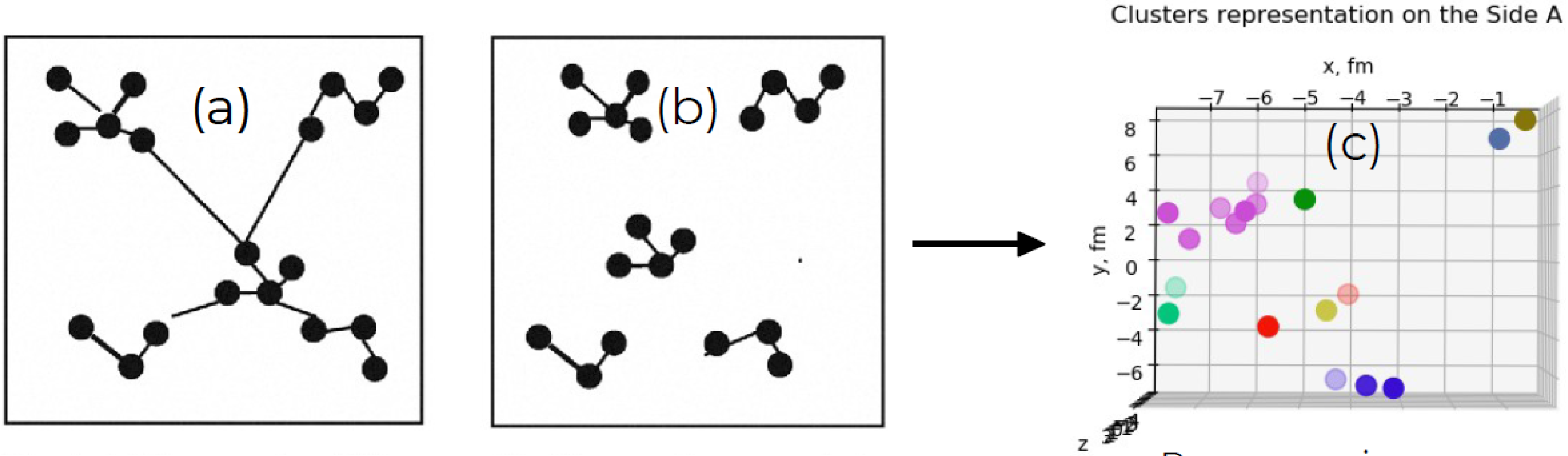


- Graph vertexes – nucleons, edges weights – Cartesian distances between them.
- **(a)** The minimum spanning tree is selected from the complete graph
- **(b)** All edges with a weight greater than $d$ are removed. $d$ is the clustering parameter depending on the excitation energy
- **(c)** Connectivity components are separate (pre-)fragments

Beam-eye view

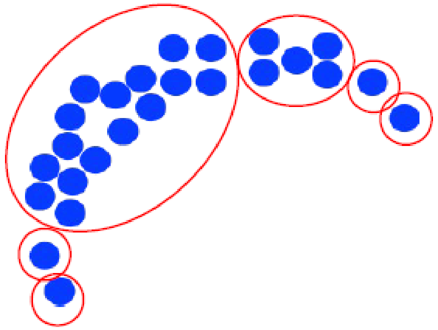

Prefragments in a central collision

The prefragment is dynamically divided into several prefragments until thermodynamic equilibrium is reached.

# $^{197}$Au fragmentation

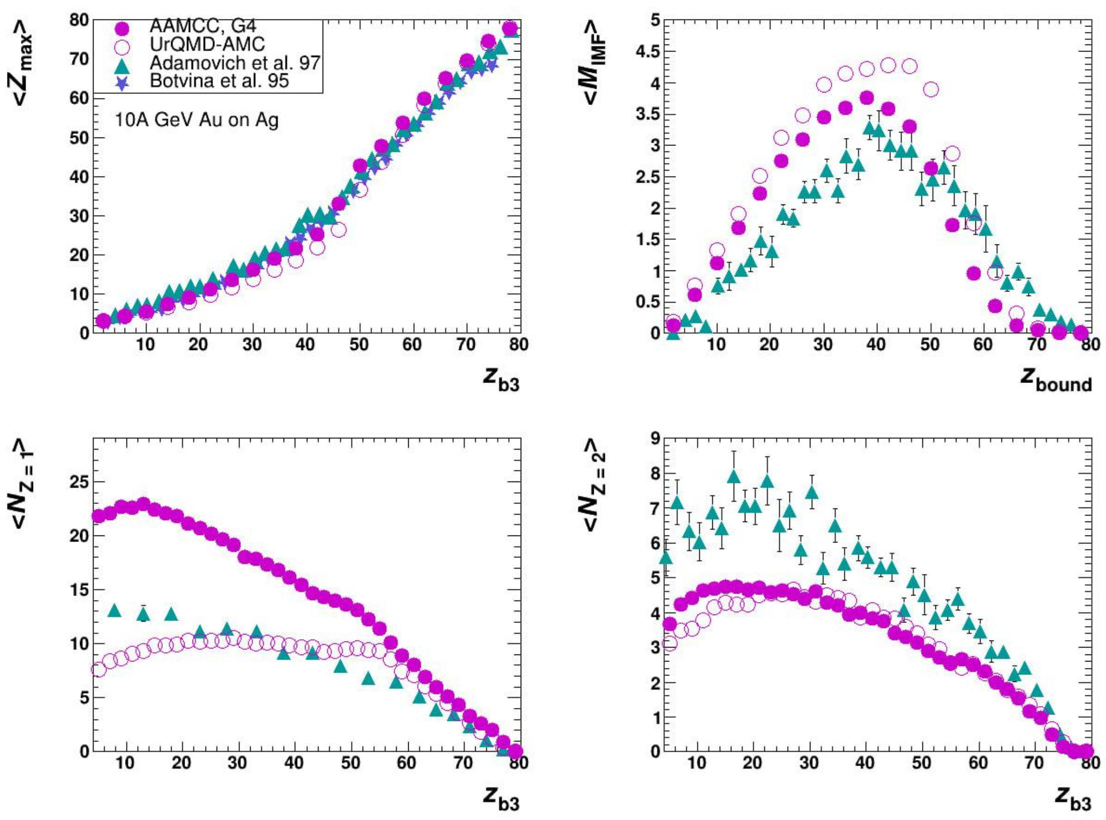


- UrQMD-AMC and AAMCC describe $Z_{max}$. Models give similar numbers of He
- UrQMD-AMC is systematically lower than AAMCC for $Z_{bound} < 50$. This is due to a smaller spectator volume in UrQMD.
- AAMCC is closer to data on $M_{IMF}$, while UrQMD-AMC overestimates $M_{IMF}$ in semi-central collisions. This is because of higher excitation energy of prefragments since more nucleons are removed.
- The difference in H fragments can be attributed to the different number of participants, because of a larger contribution of protons from MST-clustering

# Spectator matter volume as a function of impact parameter

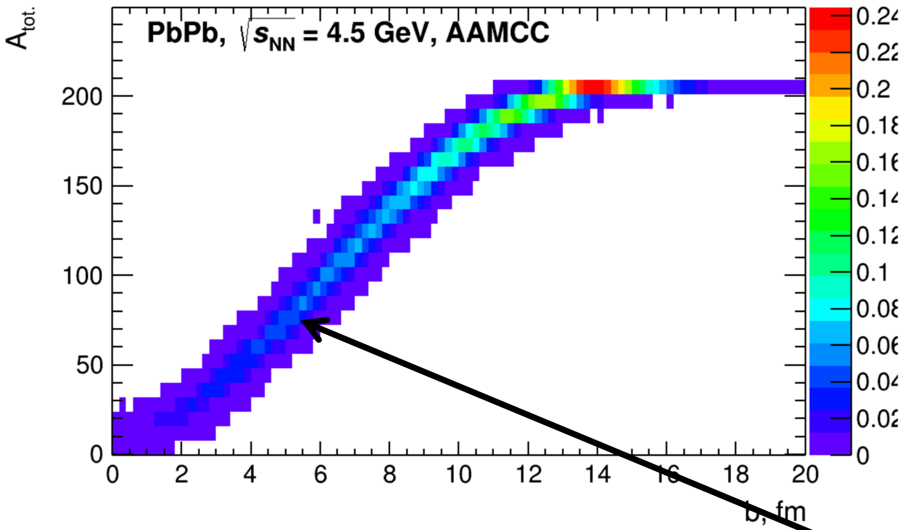


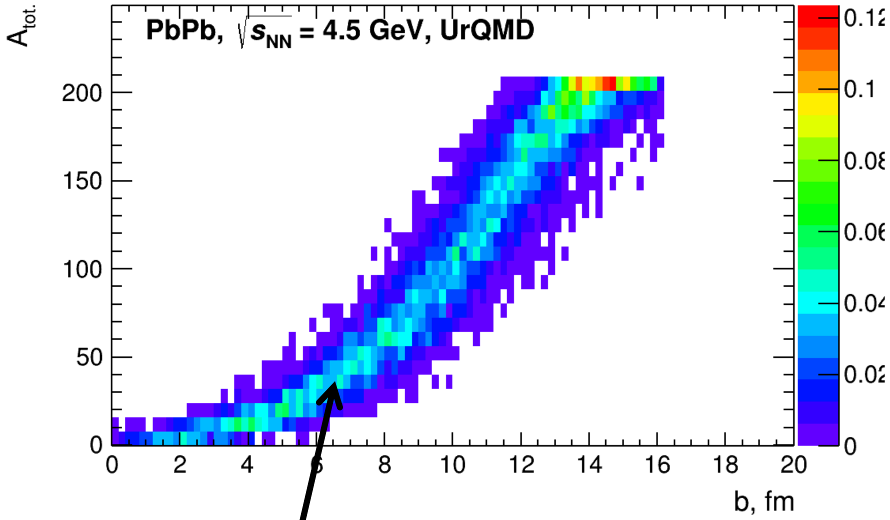


UrQMD gives less spectators than AAMCC for all b

# Nuclear interaction

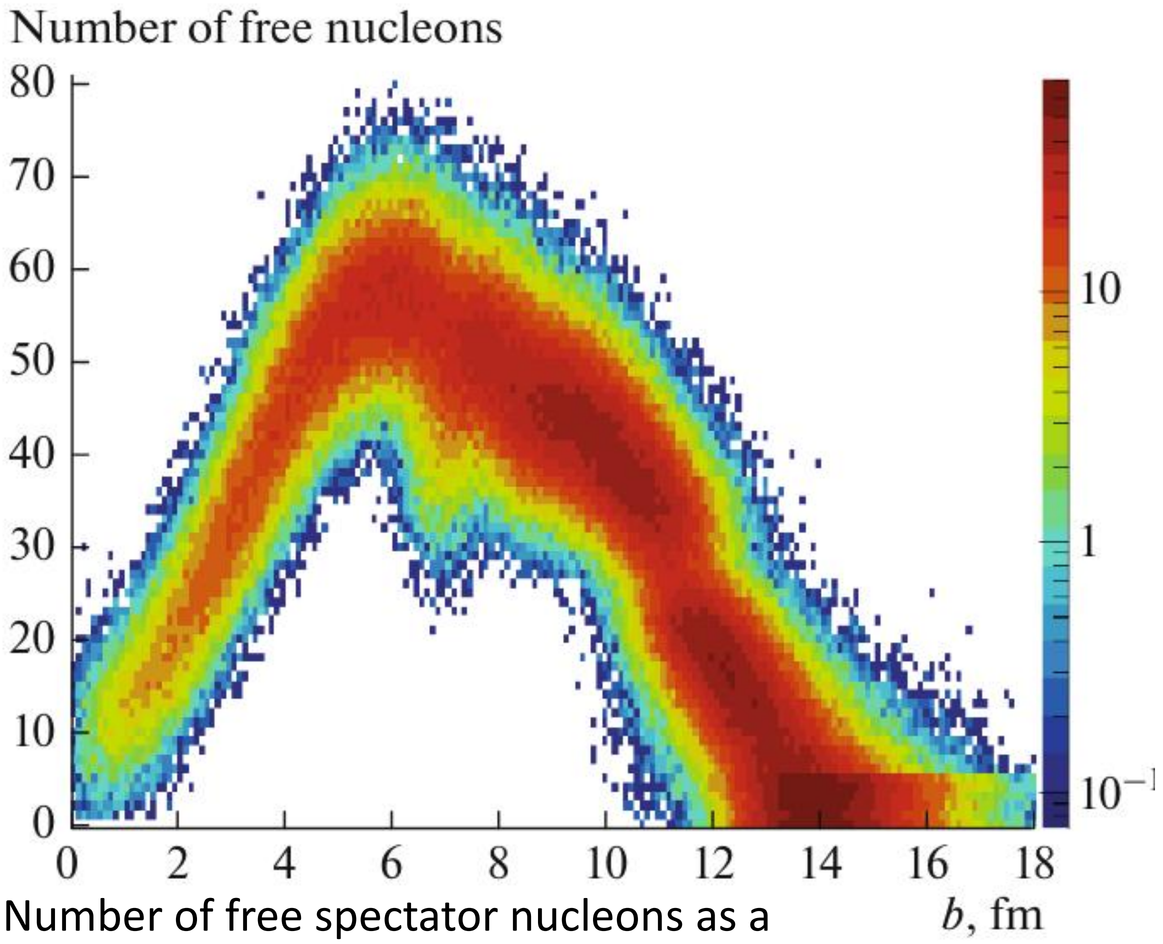


Number of free spectator nucleons as a function of the impact parameter in collisions between $^{197}$Au nuclei at NICA at $\sqrt{s_{NN}}$ = 5 GeV

A. Svetlichnyi & I. Pshenichnov, Formation of Free and Bound Spectator Nucleons in Hadronic Interactions between Relativistic Nuclei. *Bulletin of the Russian Academy of Sciences: Physics* **2020**, 84 (8), 911–916.

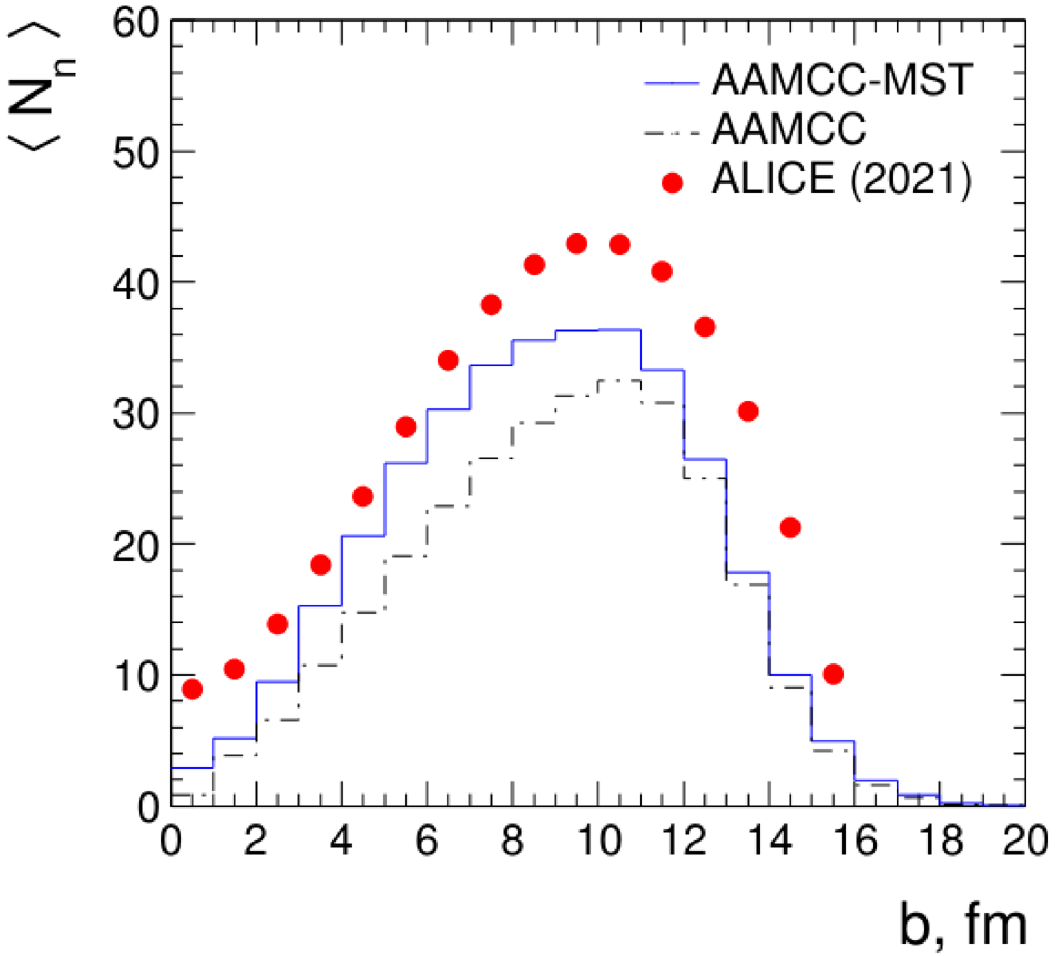


Average multiplicities of neutrons in $^{208}$Pb–$^{208}$Pb collisions at $\sqrt{s_{NN}}$ = 5.02 TeV as functions of the collision impact parameter

Nepeivoda, R. et al., Pre-Equilibrium Clustering in Production of Spectator Fragments in Collisions of Relativistic Nuclei. *Particles* **2022**, 5, 40–51.

# Nuclear interaction